The manoeuvrability of high-speed craft in the following sea

Bonci, Matteo

DOI
10.4233/uuid:843b41a4-fb9f-4211-8280-5767a03146eb

Publication date
2019

Document Version
Final published version

Citation (APA)
Bonci, M. (2019). *The manoeuvrability of high-speed craft in the following sea*. [Dissertation (TU Delft), Delft University of Technology]. https://doi.org/10.4233/uuid:843b41a4-fb9f-4211-8280-5767a03146eb

Important note
To cite this publication, please use the final published version (if applicable).
Please check the document version above.

The Manoeuvrability of High-Speed Craft in the Following Sea M. Bonci

The Manoeuvrability of High-Speed Craft in the Following Sea

Matteo Bonci

Invitation

for the public defense of
my Ph.D thesis:

The Manoeuvrability of High-Speed Craft in the Following Sea

by
Matteo Bonci

on Friday 15th November 2019 at 12:30
in the Senaatszaal, Aula of Delft University of Technology,
Mekelweg 5, Delft

Paranymphs
Federico Fanalista
Gunnar Jacobi

Before the defence at 12 o'clock I will give a brief summary of the research. A reception will follow in the Aula after the defense.

You are also invited to the dinner that will take place the same day at 19:00, at De Gist, Phoenixstraat 4C, Delft.

Matteo Bonci
m.bonci@marin.nl

Propositions

accompanying the dissertation

THE MANOEUVRABILITY OF HIGH-SPEED CRAFT IN THE FOLLOWING SEA

by

Matteo BONCI

1. The steering effectiveness together with a proper course keeping ability contribute to a large extent to enhance the vessel dynamic stability in following seas. (*This PhD thesis*)
2. The safety of high-speed, small craft is subordinate to their inherent manoeuvrability characteristics and to the master's skills when sailing in rough seas. (*This PhD thesis*)
3. The great progress in ship safety will never change the risk perception of mariners sailing on small boats. (*This PhD thesis*)
4. The choice of hard-chine, V-shape fast vessels in the research on broaching-to instability in following seas was unfortunate. (*This PhD thesis*)
5. RANSE solvers applied to fluid dynamics ship problems will become faster and more accurate in the future, but will never replace simpler numerical tools.
6. The uncertainty in the assessment of experimental uncertainty should be considered as a significant contributor of the total uncertainty.
7. The way scientists and academic researchers publish, share and finance their works must change, because knowledge should not be an object of competition.
8. The scientific method is not different from the methods employed in any other form of human artistic creation.
9. The democratic structure of our society is often faulty in the social-media era because politicians follow the people necessities, whereas the democracy is the representation and the participation of people's ideals.
10. The belief in bizarre conspiracy theories results from the natural human propensity to be freed from responsibilities.

These propositions are regarded as opposable and defendable, and have been approved as such by the promotor Prof. R. H. M. Huijsmans.

Stellingen

behorende bij het proefschrift

THE MANOEUVRABILITY OF HIGH-SPEED CRAFT IN THE FOLLOWING SEA

door

Matteo BONCI

1. In achterinkomende zeeën draagt de stuureffectiviteit in combinatie met goed koers kunnen houden ten zeerste bij aan het verbeteren van de dynamische stabiliteit van een schip.
2. De veiligheid van kleine hogesnelheidsvaartuigen is ondergeschikt aan hun inherente manoeuvreereigenschappen en aan de vaardigheden van de stuurman bij het varen op ruwe zee.
3. De grote vooruitgang op het gebied van scheepsveiligheid zal de risicoperceptie van zeelieden die op kleine boten varen, nooit veranderen.
4. De keuze voor V-vormige, snelle vaartuigen met knikspant in het onderzoek naar de instabiliteit in de achterinkomende zeeën was ongelukkig.
5. De RANSE-methoden die worden toegepast bij problemen met scheepshydrodynamica zullen in de toekomst sneller en nauwkeuriger worden, maar zullen nooit eenvoudige numerieke hulpmiddelen vervangen.
6. De onzekerheid in de beoordeling van experimentele onzekerheden moet worden beschouwd als een significante bijdrage aan de totale onzekerheid.
7. De manier waarop wetenschappers en academische onderzoekers hun werk publiceren, delen en financieren moet veranderen, omdat kennis niet concurrerend mag zijn.
8. De wetenschappelijke methode verschilt niet van de methoden die worden gebruikt in elke andere vorm van menselijke artistieke creatie.
9. De democratische structuur van onze samenleving is vaak defect in het tijdperk van sociale media, omdat politici de behoeften van de mensen volgen, terwijl de democratie de vertegenwoordiging van en een bijdrage aan de idealen van het volk is.
10. Het geloof in bizarre samenzweringstheorieën is het resultaat van de natuurlijke neiging van de mens om van verantwoordelijkheden te worden bevrijd.

Deze stellingen worden opponeerbaar en verdedigbaar geacht en zijn als zodanig goedgekeurd door de promotor Prof. R. H. M. Huijsmans.

THE MANOEUVRABILITY OF HIGH-SPEED CRAFT IN THE FOLLOWING SEA

THE MANOEUVRABILITY OF HIGH-SPEED CRAFT IN THE FOLLOWING SEA

Dissertation

for the purpose of obtaining the degree of doctor
at Delft University of Technology,
by the authority of the Rector Magnificus prof. dr. ir. T.H.J.J. Van Der Hagen,
Chair of the Board for Doctorates,
to be defended publicly on Friday 15 November 2019 at 12:30 p.m.

by

Matteo BONCI

Master of Science in Naval Architecture and Marine Engineering,
University of Genoa, Italy
born in Genoa, Italy.

This dissertation has been approved by the promotors.

Composition of the doctoral committee:

Rector Magnificus,	chairperson
Prof. dr. ir. R. H. M. Huijsmans,	Delft University of Technology, *promotor*
Dr. ir. I. Akkerman,	Delft University of Technology, *copromotor*

Indipendent members:

Prof. dr. M. R. Renilson,	Australian Maritime College, University of Tasmania
Prof. dr. G. Thomas,	University College London
Prof. dr. ir. H. W. M. Hoeijmakers,	University of Twente
Prof. ir. H. Hopman,	Delft University of Technology

Reserve members:

Prof. dr. ir. M. Kaminski,	Delft University of Technology

Other member:

Dr. ir. P. De Jong,	Maritime Research Institute of the Netherlands

Keywords: Manoeuvrability-in-waves; high-speed craft; broaching-to; following sea; captive model tests; panel method.

Printed by: Gildeprint Drukkerijen, Enschede, The Netherlands

Cover: Giuseppe Bonci
`https://www.facebook.com/BeppebonciPittore/`

ISBN 978-94-6366-212-3

An electronic version of this dissertation is available at
`http://repository.tudelft.nl/`.

CONTENTS

SUMMARY

Broaching-to is a highly complex, non-linear dynamic instability event that several vessels might face when sailing in the same direction of the waves, for example when returning to port during a storm. This condition is referred to as following sea. Vessels such high-speed craft but also patrol and rescue boats, fishing trawlers or small frigates are the most subjected to the severity of the sea, and therefore also the most vulnerable to the broaching. A broach occurs when the ship is captured by the incoming stern waves (surf-riding), and is turned beam-to-sea by the large wave yawing moment. This yaw-turning motion is so sudden and the acceleration is so high that even the most skilled mariners are not able to avoid it, losing dangerously the control of the vessel. In extreme cases, a broach can cause the capsize of the vessel.

The first apparitions of the term broaching-to date back to the 18th century. Sailors have always been frightened by the potentially devastating consequences of sailing windward, but this phenomenon has been consistently studied starting from the 1950s only. Several naval architects put in evidence the main characteristics of the physical phenomenon of the broaching-to in following sea, developed useful and accurate techniques meant to predict the behaviour of the vessel sailing in those scenarios. Although the great efforts spent in the research on this subject, there is still some uncertainty about the causes of a broaching-to event, and about the characteristics of the vessel that might lead to an unsafe behaviour in following waves. This thesis aims to investigate these aspects, with the final desirable result of providing guidelines for safer vessels to designers and shipbuilders.

This study takes as main assumption that the ability of a vessel in manoeuvring-in-waves play a crucial role in a broach inception. However, the controllability of the vessel is highly dependent on the wave conditions: for this reason, broaching-to is a typical coupled seakeeping-manoeuvrability problem. The most direct and straightforward way to investigate the broaching behaviour of a ship is by experiments on self-steered ship models. The direct observation of the model in following waves is helpful to assess the safety of a vessel, but unfortunately does not provide any information on the dynamics of the system, and therefore neither insights into the causes of the unstable behaviour of a ship. In order to understand the mechanism behind the broaching-to, it is necessary to know the forces acting on the vessel in following and stern-quartering waves. A large part of this thesis focuses on the determination of the forces acting on a fast rescue vessel, the KNRM SAR NH-1816, when manoeuvring in following waves. This has been achieved by means of experimental captive model tests: force transducers connecting the ship model and the towing carriage measured the hydrodynamic loads acting on the vessel. The experimental campaigns were carried out at the towing tank of TU Delft and at the Seakeeping and Manoeuvring Basin of MARIN.

The information collected during these experiments helped to understand many aspects of the ship hydromechanics in the following sea. As main result of this investiga-

tion, it was ascertained that the dynamics of the ship in waves differs significantly from the calm water case; moreover, the manoeuvrability loads in following seas highly depend on where the vessel is located in the wave. The ship location in the wave can determine the inception of a broaching dynamic instability. But the experimental results were also useful to validate and tune a time domain, potential flow boundary element (panel) method. Thanks to an extensive use in seakeeping and manoeuvrability applications, panel methods had proved to be a reliable tool in the prediction of the ship motions in waves; however, due to lacks in the computation of the hydrodynamic pressures on the horizontal plane, these models require still some semi-empirical tuning to provide reliable results for manoeuvrability problems. This can be especially important during broaching-to inception, that is a result of a weak equilibrium of wave, hull and steering forces. After the validation and the correction of some manoeuvring loads computed by the panel method, the numerical prediction of the ship loads were satisfactory. This mathematical tool was then employed in the numerical simulation of the behaviour of the free sailing vessel in following seas.

The last investigation of this thesis concerns two main aspects of the high-speed vessels manoeuvrability: the ability to change the heading, the turning ability, denoted by the effectiveness of the ship steering system; the intrinsic capability of a vessel of keeping the course, the course-keeping ability, denoted by the hull directional stability. These two characteristics of a ship can play a crucial role into the inception of a broaching instability. In the last part of this thesis, the steering effectiveness and the directional stability of the rescue boat NH-1816 were modified in order to estimate the sensitivity of the vessel to broaching with respect to these manoeuvrability properties. The most common solution for designers to improve the dynamic stability of a vessel in following seas is to increase the steering force (for example enlarging the rudder). The effectiveness of this option was confirmed by the analysis of this thesis: the number of broaching events of the rescue vessel with enhanced steering dropped compared to the original ship configuration. However, when a greater steering force is coupled with a better course-keeping, the dynamic stability of the vessel is enhanced even further, significantly decreasing the likelihood of a broach.

The findings of this thesis must still find a wider validation in realistic sea states, not only in the regular wave case object of this work. The deterministic characterisation of the manoeuvrability loads and the broaching-to dynamics in an irregular sea state will be the most challenging task. However, the information collected by this thesis can be of help during the design of a ship when this shows a dangerous inclination towards a broaching-to behaviour.

SAMENVATTING

Broaching is een zeer complexe, niet-lineaire dynamische instabiliteit waar veel schepen mee te maken krijgen wanneer ze in dezelfde richting als de golven varen, bijvoorbeeld wanneer ze tijdens een storm terugkomen naar de haven. Deze toestand wordt achterinkomende zee genoemd. Schepen zoals hogesnelheidsvaartuigen, maar ook patrouille- en reddingsboten, trawlers en kleine fregatten zijn het meest onderworpen aan de ernst van de zee en daarom ook het meest kwetsbaar voor broaching. Er is sprake van een broach wanneer het schip wordt gevangen door de achterinkomende golven (surf-riding) en door het hoge giermoment dwars op de golven wordt gezet. Deze beweging is zo plotseling en de versnelling is zo hoog, dat zelfs de meest bekwame zeelieden het niet kunnen vermijden en de controle over het schip verliezen. In extreme gevallen kan een broach een kapseis veroorzaken. .

De eerste beschrijvingen van de term broaching dateren uit de 18e eeuw. Zeelieden zijn altijd al bang geweest voor de potentieel verwoestende gevolgen van windwaarts zeilen, maar dit fenomeen is alleen vanaf de jaren 1950 bestudeerd. Verschillende scheepsbouwkundigen hebben de belangrijkste kenmerken van het natuurkundige broachingfenomeen bij achterinkomende golven aangetoond en nuttige en nauwkeurige technieken ontwikkeld om het gedrag van het vaartuig in die scenario's te voorspellen. Ondanks de grote inspanningen die in het onderzoek naar dit fenomeen al zijn verricht, bestaat er nog steeds enige onzekerheid over de oorzaken van een broach en over de kenmerken van het schip die kunnen leiden tot onveilig gedrag bij achterinkomende golven. Dit proefschrift beoogt deze aspecten te onderzoeken teneinde ontwerpers en scheepsbouwers richtlijnen voor veiligere schepen te kunnen bieden.

In deze studie wordt als belangrijkste veronderstelling aangenomen dat het vermogen van een hogesnelheidsvaartuig voor het manoeuvreren-in-golven een cruciale rol speelt bij het ontstaan van een broach. De bestuurbaarheid van het vaartuig is echter afhankelijk van de golfcondities: om die reden houdt broaching standaard verband met een manoeuvreerbaarheids- en zeewaardigheidsprobleem. De meest directe en eenvoudige manier om een broach van een schip te onderzoeken, is door middel van experimenten met zelfsturende scheepsmodellen. De directe observatie van het model in de achterinkomende golven is nuttig om de veiligheid van een schip te beoordelen, maar biedt helaas geen informatie over de dynamiek van het systeem en dus ook geen inzicht in de oorzaken van de instabiliteit van een schip. Om het mechanisme achter broaching te begrijpen, is het noodzakelijk om de krachten te kennen die in deze situaties op het schip inwerken. Een groot deel van dit proefschrift richt zich op de bepaling van de krachten die optreden op een snel reddingsschip (SAR NH-1816) bij het varen in achterinkomende golven. Dit is bereikt door middel van experimentele proeven met een vastgezet model: krachtopnemers die het scheepsmodel en de sleepwagen met elkaar verbonden, maten de hydrodynamische krachten die op de romp optraden. Het experimentele programma werd uitgevoerd in de sleeptank van de TU Delft en op het

Seakeeping and Manoeuvrability Basin van MARIN.

De informatie die tijdens dit experimentele programma werd verzameld, hielp om veel aspecten van de scheepshydromechanica bij achterinkomende zee te begrijpen. Als belangrijkste resultaat van dit onderzoek werd vastgesteld dat de dynamiek van het schip in golven significant verschilt van de situatie in vlak water; bovendien hangen de manoeuvreerkrachten in de golven sterk af van waar het schip zich in de golf bevindt. De locatie van het schip in de golf kan het ontstaan van een dynamische instabiliteit veroorzaken. Maar de experimentele resultaten waren ook nuttig om een tijdspanne en potentiële stroom randwaarde (paneel) methode te valideren en af te stemmen. Dankzij een uitgebreid gebruik van zeegang- en manoeuvreertoepassingen, waren paneelmethoden een betrouwbaar hulpmiddel bij het voorspellen van de scheepsbewegingen in golven; door een gebrek aan berekeningen van de manoeuvreerkrachten, vereist dit model echter nog enige semi-empirische correcties om betrouwbare resultaten te kunnen bieden. Dit kan vooral belangrijk zijn bij het ontstaan van een broach ten gevolge van een labiel evenwicht van golf-, romp- en stuurkrachten. Na de validatie en de correctie van de manoeuvreerkrachten berekend met behulp van de paneelmethode, was de numerieke voorspelling van de scheepskrachten bevredigend. Dit wiskundige model werd vervolgens gebruikt bij de numerieke simulatie van het gedrag van de scheepsbewegingen in achterinkomende zeeën.

Het laatste onderzoek van dit proefschrift betreft twee hoofdaspecten van de manoeuvreerbaarheid van hogesnelheidsschepen: enerzijds het vermogen om van koers te veranderen dat wordt bepaald door de effectiviteit van het stuursysteem, en anderzijds het intrinsieke vermogen van een vaartuig om koers te houden dat wordt bepaald door de richtingsstabiliteit van de romp. Deze twee eigenschappen van een schip zijn belangrijk bij een broaching-instabiliteit. In het laatste deel van dit proefschrift werden de stuureffectiviteit en de richtingsstabiliteit van de reddingsboot NH-1816 aangepast om de gevoeligheid van het schip voor broaching met betrekking tot deze kenmerken te schatten. De meest gebruikelijke oplossing voor ontwerpers om de dynamische stabiliteit van een schip in de volgende zeeën te verbeteren, is het vergroten van de stuurkracht (bijvoorbeeld door het vergroten van het roer). De effectiviteit van deze optie werd bevestigd door de analyse in dit proefschrift: het aantal broaches van het reddingsschip met verbeterd stuurvermogen daalde ten opzichte van de oorspronkelijke scheepsconfiguratie. Wanneer echter een grotere stuurkracht wordt gekoppeld aan een betere richtingsstabiliteit, wordt de dynamische stabiliteit van het schip nog verder verbeterd, waardoor de waarschijnlijkheid van een broach aanzienlijk wordt verkleind.

De bevindingen van dit proefschrift moeten nog steeds breder worden bevestigd in realistische golfcondities, niet alleen in de reguliere golfanalyse die in dit werk is ontwikkeld. De deterministische karakterisering van de manoeuvreerkrachten en de broachingdynamiek in onregelmatige golven zal de meest uitdagende taak zijn. De informatie die in dit proefschrift is verzameld, kan echter helpen bij het ontwerpen van een schip wanneer dit een neiging tot broaching vertoont.

Riding for the feeling
is the fastest way to reach the shore

1

INTRODUCTION

This Introduction gives a historical and scientific review of the problem of fast vessels sailing in following seas. The main developments of the research done on this subject so far are presented and discussed. Starting from the state-of-art of the research on the field, the thesis objectives are defined, along with the outline that explains how the problem is tackled. The high-speed small craft are chosen as subject of the investigation in this thesis. The assessment of the behaviour at sea of these vessels is a fascinating and challenging task.

1.1. THE FOLLOWING SEA

THE behaviour of the ship sailing at sea has been investigated by designers and researchers mostly in conditions of head and bow-quartering waves. This is the condition in which the vessel sails against the incoming waves. In rough seas, the peaks of the vertical accelerations caused by the violent slamming of the hull on the water surface are extreme: an acceleration impulse at the bow can reach 5 to 10 g on fast vessels. During the design, the vertical accelerations at the bow and at the bridge are the main limiting factors to ensure a safe operability of the ship and to guarantee her structural integrity.

A less known and investigated condition for ships sailing at sea is the following and stern-quartering sea. Differently from the head sea state case, in the following sea the capabilities of the ship to manoeuvre play a crucial role. It is not rare that the crews on board experience serious difficulties in steering when sailing downwind (i.e. along the same direction of propagation of the waves), with the risk to lose the control of the ship. Conolly in 1972 [1] reported a statement of the *Admiralty Manual of Seamanship*: *"All ships will find that steering is difficult downwind, and some may be quite unmanageable"*.

"Difficulty in steering" appears as a quite vague terminology to understand what actually happens in these scenarios. Sailing downwind can lead to devastating consequences due to the instability of the ship. One of the most catastrophic events experienced in a following sea is the broaching-to. Often referred to as simply broaching or

broach, a broaching-to is the sudden and unforeseen movement of the ship that veers or yaws dangerously so as to lie broadside to the waves [2]. This phenomenon can threaten the life of the crew on board, and it can end up, in extreme cases, in a capsize when the vessel turns beam-to-sea. The broaching can be regarded as a dynamic instability that usually builds-up in few seconds, often causing frightening heeling angles and high turning velocities. It is almost impossible, even for the most skilled mariners, to avoid such a sudden and involuntary circumstance. Masters recognize the following sea as one of the most dangerous situations in which a vessel could operate, and in many cases sailing downwind is deliberately avoided. However, the growing strictness of the ship operability requirements forces the masters to face these dangerous situations. The safety assessment of the ship manoeuvring-in-waves becomes then a vital necessity.

The controllability problems of the vessels sailing in the following sea were well known and dreaded since a long time before the current days. In 1762, the celebrated Scottish poet and sailor William Falconer, inspired by the hazardous life at sea, wrote the poem *"The Shipwreck"* [3]. At Canto II:

"While shoreward now the bounding vessel flies,
Full in her van St. George's cliffs arise; [...]
High o'er the rest a pointed crag is seen,
That hung projecting o'er a moffy green.
Nearer and nearer now the danger grows,
And all their skill relentless fates oppose.
For, while more eastward they direct the prow,
Enormous waves the quiv'ring deck o'erflow.
While, as she wheels, unable to subdue
Her sallies, still they dread her broaching-to." [1]

The poem *"The Shipwreck"* contains a few appearances of the term broaching-to, along with the use of many other nautical terms. As an experienced sailor, William Falconer knew very well the attributes of the navigation; but the context of a poem does not allow a clear understanding of the events cited. The first detailed and less poetic description of the phenomenon of broaching-to can be found very few years later, in 1792. In his review of the works of British poets [5], Robert Anderson wrote in a footnote of Falconer's poem a surprisingly precise definition of broaching-to: *"Broaching-to is a sudden and involuntary movement in navigation, wherein a ship, whilst scudding or sailing before the wind, unexpectedly turns her side to windward. It is generally occasioned by the difficulty of steering her, or by some disaster happening to the machinery of the helm."* [1].

The scientific research on the problem of the ships sailing in the following and stern-quartering waves started consistently after World War II. The PhD dissertation of Renilson [6] contains a detailed overview of the research done on this subject prior to the 1980s. Many numerical and experimental research studies [7–14] highlighted some important aspects of the ship manoeuvring-in-waves and the controllability in following seas. In 1972 Conolly [1] documented the disaster happened in 1968 to the ferry *Wahine*, caught in a storm while returning to port and sank in shallow water due to broaching.

[1] This text is taken from the historical review of broaching-to of Spyrou [4], published in *Contemporary Ideas On Ship Stability and Capsizing in Waves (2011), Springer, p. 399-411*

Conolly also provided a detailed review of the circumstances in which such events might occur, the important factors that could be important for instabilities and the countermeasures to put into action to avoid them.

In the beginning of the research on this subject, model experiments were usually favoured over numerical techniques because it was possible to assess more accurately the capability of a vessel in following seas. In 1974 Nicholson [15], together with Lloyd's Register, carried out systematic experiments on auto-steered and auto-propelled vessels able to sail freely in sea state scenarios reproduced in a large tank. The experiments were carried out at several speeds and wave conditions in order to highlight the most likely situations where a ship could experience a broach: this is one of the pioneering works that inspired the modern probabilistic characterisation of ship instability in a seaway. In 1982 Renilson ([6, 16]) carried out captive model experiments on ship models, in order to measure the forces and moment acting on the hull in waves. The main aim of this work was to estimate the stability index of the ship when sailing in following sea, and its influence to the inception of broaching. In more recent years, in the 1990s and beginning of 2000s, experimental research works in Japan were carried out by means of free sailing and captive model tests [17–21]. These studies started the modern research on the topic of manoeuvrability-in-waves.

Interest grew also in the development of numerical methods able to accurately describe such phenomena. De Kat [22], Ayaz et al. [23], Van Walree and De Jong [24], developed and validated mathematical models meant to describe the dynamics of broaching-to and to predict the likelihood of its occurrence. The problem of the ship manoeuvring-in-waves is very complex, and often the mathematical simulations need empirical corrections to reach an acceptable level of accuracy. Ruttgerson and Ottoson [25] underlined that the coupling between experimental and numerical techniques is highly beneficial in the study of the ship manoeuvrability-in-waves. De Jong et al. in [26] and Umeda et al. in [27] corrected the computed loads acting on the vessel through empirical data from experiments on ship models.

The most recent developments in the study of the ship sailing in following and stern-quartering waves regard the computation of the probability of dynamic instabilities occurrence in realistic sea states. Interest in the statistical assessment of stability failures in waves arose with the necessity to update the Intact Stability Code (IS 2008) [28]. The International Maritime Organization (IMO), with the Second Generation Intact Stability Criteria, has started to develop criteria and regulations that quantify the vulnerability of a ship to the loss of stability in rough sea, filling the gap between a static transverse stability assessment and the more dynamic conditions in a sea state. Namely the loss of transverse stability in waves, the condition of dead ship, the parametric rolling and the broaching-to are the phenomena taken into account. Belenky and Spyrou [29] proposed a method to quantify the probability of rare events such as capsize and broaching-to. Umeda et al. [27] developed a method to estimate the probability of broaching that connects the deterministic dynamics in regular waves to the probabilistic one in a realistic irregular sea state. The high complexity of the dynamic instability phenomena in following seas makes this connection non-trivial, especially for fast vessels [30]; in practical applications, free sailing model tests are an obligated fall-back in the direct assessment of broaching-to vulnerability.

1

The main characteristics of the phenomenon of broaching-to are well known [17, 19, 31, 32]. According to the definition by Cohen and Blount [33], broaching-to is a non-oscillatory, combined yaw-roll dynamic instability. It can be considered as a single wave event [27]. The occurrence of a broach is more common at Froude number higher than 0.3, and at wave lengths within 1 and 3 ship lengths. The ships that are more vulnerable to the broaching instability are thus relatively small vessels (up to 70m in length) that operate at medium-high pre-planing speed ($Fr < 0.9$): high-speed craft, fishing vessels, patrol boats, small frigates and destroyers. In very extreme scenarios, a broach might occur also to larger ships: this was the case of the *Wahine* [1], 150 meter in length sailing at 17 knots. A broach occurs typically at rather high steepness. It is in fact more likely when the ship sails shore-ward in shallow water where the waves are steeper and breaking. De Jong et al. [34] showed that the likelihood of broaching increases with the wave steepness. Usually a broaching-to event is preceded by another known and more accurately studied phenomenon, the surf-riding [26, 34–36]: the vessel is captured by the incoming wave surfing on it and accelerating to the wave celerity. The vessel then spends a considerable time in the same location in a wave: the destabilizing wave yawing moment grows larger at the point that the turning movement of the ship cannot be compensated by the counter-action of the steering devices. The equilibrium location of the vessel in the wave depends on a series of factor: wave length, steepness, thrust of the propulsion devices. In most cases, a broaching occurs in the front of the wave between the incoming crest and the wave trough [32]. The destabilizing yawing moment increases with the wave incidence angle, but as shown in [34] this does not necessarily increase the likelihood of a broach. The reason is that at higher wave incidence angle a surf-ride is less likely, since the larger difference in relative speed between the ship and the wave. The surf-riding and the broaching-to are therefore tightly connected phenomena. A broach builds-up in few seconds during a surf-ride on the wave: without a surf-ride the ship would experience only a periodic motion. A rendering of the main steps leading to a dynamic instability in following seas is shown in Figure 1.1.

Thanks to past research done on the subject, the characteristics of a broaching-to are well known. Designers and researchers are aware of the circumstances in which a broach could occur, as well as of the kinematics that characterises it. What is still not clear it is the reason why certain ships suffer more than others from broaching-to, and which aspects determine the inclination of a vessel to be dynamically unstable in following seas. The solution of this debate must be sought in the capabilities of a vessel to manoeuvre at sea, and this is a problematic task.

The ship manoeuvring-in-waves is extremely complex and it is scarcely investigated during the design process. As Conolly explained in [1] referring to following sea scenarios, *"mariners tend to be philosophical on this subject, and to accept the problems of following seas as a natural environmental hazard. They rely heavily on individual experiences and would not necessarily all follow the same course of action when confronted by a given set of circumstances"*. The work presented in this thesis will focus on the manoeuvrability characteristics of the ship when sailing in following waves, and their influence to the inception of broaching-to. Designers do not have sufficient certainty yet to judge the behaviour of a vessel sailing in the following sea, and therefore to conceive solutions meant to prevent or at least mitigate the vessel vulnerability to dynamic instabilities. The

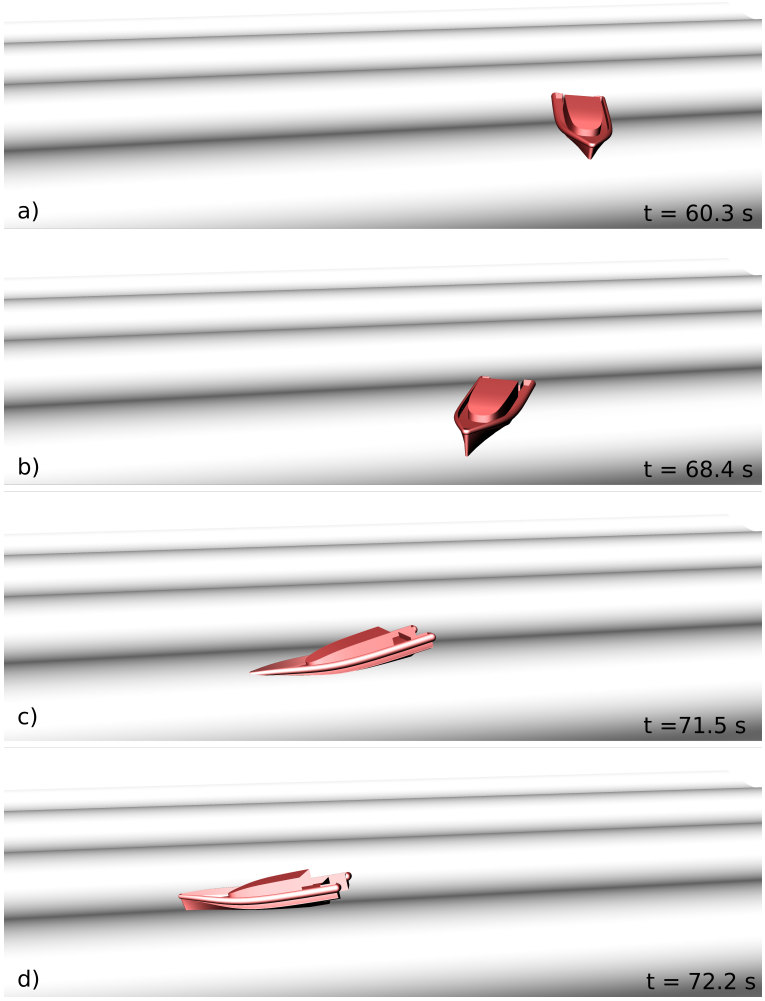

Figure 1.1: Rendering of four different instants of the phenomena of surf-riding and broaching-to. a) The vessel is captured on the wave front and accelerated to the wave celerity. b) The vessel starts rotating because of the large wave yawing moment, and the broach is starting. c) The forward speed drops because of the high turning rate, and the vessel yaws dangerously beam-to-sea. d) The vessel has irreparably lost its course, and the wave overtakes it, dreading the eventuality of a capsize. It is important to notice that the dynamic instability is extremely quick, developing in about 4 seconds since the initial turning.

accomplishment of these objectives is of vital importance for a reliable safety assessment of vessels sailing in rough sea.

A hard-chine, V-shape high-speed craft will be taken into account in this research (see Section 1.2). The choice of the high-speed craft as subject of the study is motivated by the fact that the manoeuvrability of small and fast vessels, both in calm water and waves, is marginally considered during the design process, and thus it is a rather unknown subject. As consequence, the controllability of small high-speed craft is entrusted to the masters and the helmsmen who operate the vessel: as a great relative propulsive power is available on board of high-speed craft, masters have the possibility to steer or accelerate quickly evading dangerous situations. However, small vessel can be more vulnerable to the severity of the sea, and the risk of instability is a real threat. These events, as in the case of broaching, can develop in few seconds making the counter-actions of the crew worthless. Moreover, these phenomena are extremely complex and governed by a large number of factors and their study is difficult: more research is still needed to ensure an acceptable level of safety for small fast boats.

1.2. THE HIGH-SPEED CRAFT

HARD-CHINE high-speed craft are the vessels taken as subject of this study in the manoeuvrability in following seas. Whereas the seakeeping qualities of the fast craft have been thoroughly investigated by several past works [37–40], the manoeuvrability of fast craft in waves is still a rather obscure topic. Most of the research on the fast vessel controllability have been carried out in calm water, as in [41, 42].

When compared to bigger ships, high-speed small craft are designed to have outstanding controllability and seakeeping characteristics. However, they also experience larger relative motions and accelerations in a seaway. In the mildest cases, this can cause discomfort; in other rougher conditions, operating these vessels can be dangerous and threaten the life of the people on board. The achievement of a design that can pair performance and safety is not a task.

The controllability, the seakeeping and the stability of small and fast craft are very interesting features: their response in calm water and waves is highly non-linear and dependent on the forward speed. Moreover, they are continuously subjected to ferocious wave impacts and relatively large motions when sailing in a seaway. These features play a crucial role in the conditions of following waves: in those situations, small vessels are subjected to great fluctuations of forward speed and to dangerous difficulties in steering. Studies of manoeuvring-in-waves for these craft are rarely undertaken during the design: large scale research on high-speed craft moving at sea is greatly needed to guarantee the safety of the crew during the operational phases.

The Dutch rescue boat SAR NH-1816 operated by the Royal Netherlands Sea Rescue Institution (KNRM) was chosen as the test-case of this research. The NH-1816 is the result of an innovative and versatile design project [43] aimed to provide improved manoeuvrability and seakeeping performance. The vessel design originates from the upgrade of the rescue vessel Arie Visser converted to the Axe-Bow concept [44], meant to improve the response of the ship in head waves. Figure 1.2 shows the two designs, the Arie Visser and the NH-1816, close to each other during full scale trials. The craft is equipped with two waterjets, that facilitate the rescue operations and ensure good ma-

Figure 1.2: Photograph taken from the full scale trials of the original rescue vessel Arie Visser (top) and the new Axe-Bow NH-1816 (bottom). Courtesy of DAMEN Shipyards.

Quantity	Symbol	Value
Length between the perpendicular	L_{PP}	18.37 m
Reference length	L	18.37 m
Length over all	L_{OA}	19.5 m
Breadth	B	5.60 m
Draught	D	1.10 m
Weight	W	34.4 t
Longitudinal centre of gravity	LCG	6.00 m
Height of the centre of gravity	KG	1.60 m
Metacentric height at zero speed	GM_T	1.91 m
Wetted surface at zero speed	S_W	78.2 m^2
Maximum speed	U_M	35 kts
Deadrise angle	β_D	24 deg
Steering rotation velocity	$\dot{\delta}$	10 deg/s
Maximum steering angle	δ_M	23 deg

Table 1.1: Main characteristics of the SAR NH-1816 craft.

noeuvrability, and with two retractable skegs meant to improve the course stability in the seaway. Visch and Keuning in [45–47] and De Jong et al. [26] investigated the capabilities of this vessel both in calm water and in waves; several data were then already available as a starting point for this study. The hull lines of the vessel, along with the main experimental results of these studies [47] are shown in Figure 1.3. The main characteristics of the SAR NH-1816 are summarised in Table 1.1.

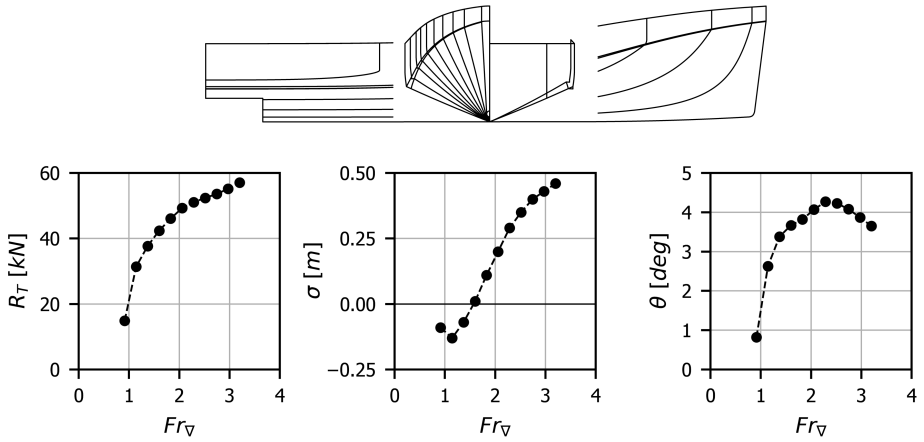

Figure 1.3: Top: longitudinal and transversal hull lines of the SAR NH-1816 craft; bottom: measured experimental total resistance, sink/rise and trim (positive bow-up) as functions of the volumetric Froude number [47]. No uncertainty data were available for these experiments.

1.3. RESEARCH QUESTIONS

The research study of this thesis is structured on two different subsequent phases.

First, the accuracy of the mathematical methods required to predict the behaviour of a vessel sailing in following seas must be assessed. Use will be made of experimental techniques focused on the measurement of the forces and moments acting on the vessel in waves. This will be of help in the understanding of such complex scenarios and in the implementation and validation of the numerical computations.

Second, these mathematical methods must be applied in the design process, aiming to develop effective counter-measures to ensure safer ships with better performance. A direct assessment of the vulnerability of a vessel to dynamic instability events, for example using free sailing, self-propelled ship models, is not always a viable option. Mathematical tools have the advantage to be more flexible; moreover, studies on the dynamic stability in waves during the design are rarely carried out, seen the high-complexity that characterises the following sea.

The first phase is motivated by the substantial lack of manoeuvrability studies on high-speed craft. An extensive study involving both model experiments and numerical computations is an occasion to improve the knowledge of this problem. The second phase tries to answer a debate that was already mentioned in this Introduction: although the kinematics of a dynamic instability event in the following sea is well known, there are still questions about the causes and the characteristics of a ship that lead to it. This work aims to move a step forward towards the solution of this debate.

These concepts are summarised by two research questions, formulated below.

- *How to predict the dynamics of the high-speed craft manoeuvrability and seakeeping in following and stern-quartering waves?*

- *Which are the most important factors that lead to the inception of dynamic instabilities in following seas?*

An answer to the first question will provide insightful information on the manoeuvrability characteristics of the high-speed craft. The objective is to being able to predict their behaviour in following waves by means of numerical methods. But the numerical simulations still need some tuning to reproduce the motions of the vessel in such complex scenarios accurately: experimental methods are therefore indispensable to investigate the fast craft manoeuvring features. Mathematical methods and experimental techniques are the tools used in the early design phase: the coupled use of these tools will allow to outline the best practices suited for the study in this field and the most relevant factors in following seas.

The second question is linked to the design of the vessel. Knowing and understanding the most important variables causing the inception of broaching-to could let designers to enact the right choices to improve the ship response in potentially dangerous situations as in following seas. This objective cannot be achieved without giving a satisfactory answer to the first question. The manoeuvrability of high-speed craft in a seaway is based on a thin equilibrium of wave loads, steering force, hull inertia, hydrodynamic and hydrostatic response. The physics of the vessel then can be investigated only through accurate and reliable numerical and experimental techniques.

1.4. CONCLUDING REMARKS

THIS thesis investigates the manoeuvrability characteristics of high-speed craft in following and stern-quartering waves. The focus is directed to the understanding of the manoeuvring-in-waves characteristics of the fast craft sailing in such conditions. The objective is twofold: a description of the loads acting on the vessel in waves, and the understanding of the effects that dominate the inception of a broaching instability. This research work can be divided into two parts: the first one consists of the experimental data acquisition, both in calm water and regular waves; the second one will utilise these empirical data to implement and validate a numerical simulation tool meant to predict the behaviour of fast vessels at sea.

Chapter 2 will present the backgrounds of the research on the fast vessels sailing in the following sea. The main methods used in this work, both experimental and numerical, will be briefly presented and discussed with respect to the state-of-art of fast vessels manoeuvrability-in-waves. The use of the most common numerical and experimental techniques employed in naval architecture will be shown, in relation with the problem of the high-speed craft sailing in following waves.

Chapter 3 summarises the findings of the experimental campaign in calm water carried at the Ship Hydromechanics Laboratory of Delft University of Technology. The analysis of the manoeuvrability characteristics of the vessel in calm water is the first necessary step for the research of the ship controllability in waves. Often in the design of a ship, only its manoeuvrability characteristics in calm water are taken into considerations. A comparison between calm water and sea scenarios allows a clearer understanding of the dynamic stability problem in waves.

Chapter 4 contains the description of the methods and the results of two subsequent

experimental campaigns in following and stern-quartering regular waves. Model tests were carried out at TU Delft and at the Seakeeping and Manoeuvring Basin of MARIN in Wageningen, in order to estimate the main manoeuvrability characteristics of the craft sailing in following and stern-quartering waves.

Chapter 5 will make use of the data collected in the two previous chapters to implement and validate a 3D boundary element method chosen as the preferred tool to simulate numerically the behaviour of the fast craft at sea. The mathematical tool is described in Chapter 2. An empirical description of the ship loads in waves is presented. The idea is to express the force and moments acting on the ship in waves as function of the forward speed, wave characteristics and position in the wave.

In Chapter 6 the numerical tool will be used to analyse the inception of dynamic instability events in the following sea in relation to the controllability characteristics of the high-speed craft. In particular, the capability of the vessel to maintain a straight course despite external wave disturbances, and to change its course turning to other directions are considered. These are assumed to be the most important qualities of the ship manoeuvring in following seas. This last chapter outlines the main findings of this thesis.

2

BACKGROUND OF THE MANOEUVRABILITY OF HIGH-SPEED CRAFT IN WAVES

In naval architecture, the areas of study of stability, seakeeping, manoeuvrability, propulsion and resistance have been always marked by rather sharp divisions: different approaches, different mathematical models, even different notations. Due to the great complexity of the ship dynamics problem, the development of those fields went in different directions. Such separations can no longer exist for ships manoeuvring-in-waves. The response to the waves and the controllability of the vessel must be considered as a whole in these particular situations. The motion equations of the fast craft manoeuvrability-in-waves are described. The approaches introduced at this stage will be used throughout the entire research of this thesis. The main experimental and numerical tools used in this field are discussed in relation to their application in the following sea problem. A potential flow boundary element method will be used in this thesis to simulate the motions of the high-speed craft in the following sea. A brief insight into the mathematical foundation of this simulation tool is given.

2.1. THE MOTION EQUATIONS

In many applications, the manoeuvrability of a ship is studied considering the motions of advance, sway and yaw. The heave, roll and pitch are neglected. The same cannot be done for small craft sailing in a seaway: the vertical and transversal position of the vessel in waves change also the submerged geometry and then the hydrodynamic forces in the horizontal plane. High-speed craft are often said to *contour* the waves.

Therefore, the motion equations of the vessel in waves must be expressed in 6 degrees of freedom (DOF), as from Equations 2.1 to 2.6:

$$(m+m_X)\dot{u}+m(vr-wq)=X_H+X_W+X_A \tag{2.1}$$
$$(m+m_Y)\dot{v}+m(wp-ur)+m_Y\alpha_X\dot{r}=Y_H+Y_W+Y_A \tag{2.2}$$
$$(m+m_Z)\dot{w}+m(uq-vp)=Z_H+Z_W+Z_A \tag{2.3}$$
$$(I_X+J_X)\dot{p}+(I_Y-I_Z)qr-m_Y\alpha_Z\dot{v}=K_H+K_W+K_A \tag{2.4}$$
$$(I_Y+J_Y)\dot{q}+(I_Z-I_X)rp=M_H+M_W+M_A \tag{2.5}$$
$$(I_Y+J_Y)\dot{r}+(I_Z-I_X)pq+m_Y\alpha_X\dot{v}=N_H+N_W+N_A \tag{2.6}$$

The motion equations are expressed in dimensional form. The equations are solved in the time domain due to the great non-linearity of the problem: the motions of the ship manoeuvring-in-waves is non-oscillatory and the forward speed is not constant. As it is common in the ship manoeuvrability research, the forces and moments are denoted with the letter X, Y, Z for surge, sway and heave forces, and K, M, N for roll, pitch and yaw moments. The equations are derived in the ship-fixed moving reference frame, shown in Figure 2.1.

On the left-hand side of the equations, m is the mass of the ship, and m_X, m_Y and m_Z are the added masses in the x, y, z directions respectively. I_X, I_Y and I_Z represent the inertia of the ship in roll, pitch and yaw, together to the respective added inertia J_X, J_Y and J_Z. The inertial forces and moments are represented: the first terms are caused by the accelerations of the body in the water; the second ones are virtual loads that arise when the motion equations are expressed in a system frame moving together with the ship body. The cross inertia I_{XY}, I_{XZ} and I_{YZ} evaluated in a system frame centred in the centre of gravity of the vessel are small and thus neglected.

On the right-hand side, the terms denoted with the subscript H represent the forces and moments, both hydrostatic and hydrodynamic, that the water exerts on the ship hull; they are due to the ship body velocity and position (radiation). The wave loads, sum of the Froude-Krylov and diffraction components, are denoted with the subscript W. The Froude-Krylov forces are calculated by the integration of the undisturbed wave pressure normal to the hull surface. The contribution from the steering and propulsive devices and appendages are denoted with the subscript A. The appendage and control device contributions are given typically by semi-empirical formulations.

In the field of ship manoeuvrability, the hydrodynamic forces and moments acting on the hull are often expressed by polynomials as function of the vessel motions and velocities; the coefficients of the polynomials are commonly known as hydrodynamic coefficients or manoeuvrability coefficients. The knowledge of these parameters is very helpful to separate the effects and to quantify their contribution into the behaviour in a manoeuvre. The hull loads due to surge, sway, roll and yaw are expressed by Equations 2.7 to 2.10:

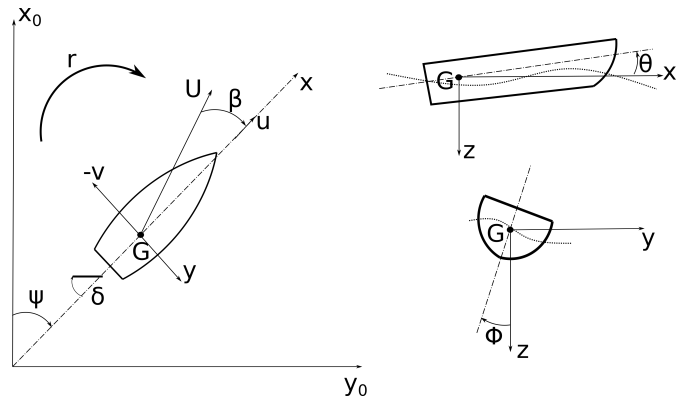

Figure 2.1: Earth-fixed $E^e = (x_0, y_0, z_0)$ and ship-fixed $E^b = (x, y, z)$ reference coordinate systems. The origin of the ship-fixed coordinate system is located in the centre of gravity G of the vessel. The ship-fixed is a yawed-only frame: axis y, pointing starboard, and axis x, pointing ship forward, lay on the horizontal plane; axis z points constantly downwards. The hydrostatic and gravity forces do not contribute to the manoeuvring loads acting on the horizontal plane.

$$X'_H = R'_T + X'_{NL} \tag{2.7}$$
$$Y'_H = Y'_v v' + (Y'_r - m')r' + Y'_{\phi'}\phi' + Y'_{NL} \tag{2.8}$$
$$K'_H = K'^*_\phi \phi - \Delta' GM'_T \phi' + K'_v v' + K'_r r' + K'_{NL} \tag{2.9}$$
$$N'_H = N'_v v' + N'_r r' + N'_{\phi'}\phi' + N'_{NL} \tag{2.10}$$

The first-order terms (linear) of the polynomials are expressed explicitly; higher-order terms (non-linear) are denoted with the subscript NL. The Equations are written in non-dimensional form. Each non-dimensional term, denoted with the subscript $'$, is obtained by dividing the dimensional quantity with the correct combination of the water density ρ, ship reference length L and total speed U, according to the ship manoeuvrability convention [48]:

$$F' = \frac{F}{0.5\rho L^2 U^2}; \quad M' = \frac{M}{0.5\rho L^3 U^2};$$

$$u' = \frac{u}{U}; \quad v' = \frac{v}{U}; \quad r' = r\frac{L}{U}; \quad m' = \frac{m}{0.5\rho L^3}; \quad GM'_T = \frac{GM_T}{L};$$

$$Y'_v = \frac{Y_v}{0.5\rho L^2 U}; \quad K'_v = \frac{K_v}{0.5\rho L^3 U}; \quad N'_v = \frac{N_v}{0.5\rho L^3 U};$$

$$Y'_\phi = \frac{Y_\phi}{0.5\rho L^2 U^2}; \quad K'^*_\phi = \frac{K^*_\phi}{0.5\rho L^3 U^2}; \quad N'_\phi = \frac{N_\phi}{0.5\rho L^3 U^2};$$

$$Y'_r = \frac{Y_r}{0.5\rho L^3 U}; \quad K'_r = \frac{K_r}{0.5\rho L^4 U}; \quad N'_r = \frac{N_r}{0.5\rho L^4 U};$$

where F and M are the generic force and moment. The terms Y'_v, N'_v, Y'_r and N'_r

are the dominant linear parameters over the estimation of the main manoeuvrability characteristics of a vessel. Y'_v and Y'_r represent a measure of the force developed on the hull when the vessel has a sway or yaw component of total speed. N'_r represents the resistance moment to the turning yaw velocity. N'_v represents the yaw moment due to the distribution of hydrodynamic pressure along the length of the ship when the vessel has a sway velocity component. In a turn, the moment $N'_v v'$ has a destabilizing effect: the sway velocity leads to an increase of the turning rate of the ship.

The terms Y'_ϕ and N'_ϕ are the heel-sway and heel-yaw hydrodynamic coupling coefficients. They represent the sway force and yaw moment induced by the static heel of the ship, that change the submerged geometry of the ship and then the lateral pressure distribution. These terms are often neglected in manoeuvrability studies [49]. Their importance on big and slow ships is uncertain; however, recent studies showed that the heel induced loads change significantly the controllability of small vessels in following waves [21, 50, 51]. The induced sway force and yaw moment by the heel and the roll motion are not marginal for the high-speed craft, not even in calm water [52–55]. The roll moment of the high-speed craft due to heel in the seaway is determined by a hydrodynamic component K'^*_ϕ originating from the hull lift, and by the restoring hydrostatic moment evaluated at zero speed. Also the sway speed v and the yaw rate r contributes to the total roll moment through the terms K'_v and K'_r.

In the instability problem studies, the radiation hull loads due to the vessel velocities are usually linearised around the initial position of stable equilibrium. In the case of the ship manoeuvrability, this is the situation where the vessel sails with a stationary straightforward speed, thus being the other components of motion and velocity very small. High-order terms are not taken into account. For this reason, only the linear coefficients are analysed in this work, because the focus is toward the dynamic loss of stability. The non-linear terms due to viscous phenomena such as the flow separation influence the dynamic behaviour of the vessel at sea; however, their effect is not directly linked to the onsets of loss of stability.

The relative angle between ship heading and wave direction depends on the vessel turn. Therefore, similarly to what was defined for the hull hydrodynamic coefficients, also the wave loads can be conveniently written using their derivatives with respect to the wave incidence angle μ, as in Equations 2.11 to 2.13:

$$Y'_W = Y'_\mu \mu' \tag{2.11}$$

$$K'_W = K'_\mu \mu' \tag{2.12}$$

$$N'_W = N'_\mu \mu' \tag{2.13}$$

The physical characteristics of the loads acting on the vessel hull depend on a high number of variables. The hydrodynamic coefficients for high-speed vessels depend on the forward speed: this is different from the more common displacement ship manoeuvrability, in which the coefficients are constant, for $Fr < 0.3$. In a seaway, the hydrodynamic coefficients depend also on the wave characteristics (wave length and wave steepness). Since in the following sea the encounter frequency is low, the controllability of the vessel is studied in a quasi-steady fashion [6], assuming that the ship is “frozen”

in a wave location. This approximates well the situation were a surf-riding occurs. The manoeuvrability loads depend also on the longitudinal location of the vessel in the wave, denoted as ξ_G, distance between the ship *LCG* and the first approaching wave crest. The parameter ξ_G is shown in Figure 2.2. Therefore, the generic force f can be written as a function of forward speed, wave incidence angle, wave length, wave steepness and location in the wave, as in Equation 2.14:

$$f = f(u, \mu, \lambda/L, H/\lambda, \xi_G/\lambda) \tag{2.14}$$

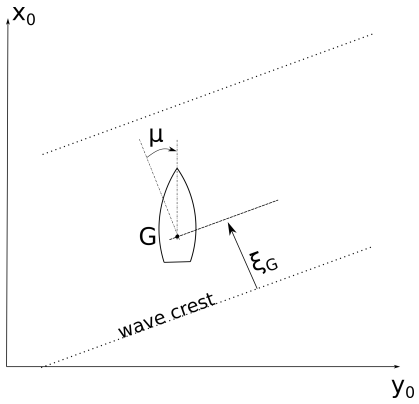

Figure 2.2: Location of the vessel in the wave, with respect to the centre of gravity *G*. $\xi_G/\lambda = 0$ or 1 means that the vessel is located close to the wave crest; $0 < \xi_G/\lambda < 0.5$ wave front; $\xi_G/\lambda = 0.5$ wave trough, $0.5 < \xi_G/\lambda < 1$ wave back.

In the description of the hull loads, the terms in heave and pitch are intentionally omitted. The hull forces depend also on the vertical position that the vessel assumes in waves, namely the heave and pitch. Therefore, the hydrodynamic loads acting on the hull must be estimated at the vertical running attitude that the vessel assumes naturally under the action of the waves. Hereby, all the force and moment terms are measured or calculated considering the vessel to be in its vertical equilibrium position at each location of the vessel in the wave.

2.2. EXPERIMENTAL METHODS

EXPERIMENTAL techniques are useful when studying the physics of the phenomenon investigated is highly complex. This is the case of the ship sailing in following waves: this problem involves a great number of effects interconnected with each other. Model testing can provide insightful details of the vessel behaviour. Sometimes they are the only viable tools to obtain reliable results when numerical models are not sufficiently accurate.

Free sailing tests with self-propelled and radio controlled ship models are frequently used to estimate directly the vessel vulnerability to dangerous dynamic instabilities. Free sailing models are also employed in calm water applications: ship manoeuvres are sim-

ulated and the controllability of the vessel is predicted. In common seakeeping applications, sea state scenarios are reproduced in large towing tanks and the motions of the model in waves are measured.

Many examples of experimental tests on auto-steered and auto-propelled models in following waves are reported in literature [18, 20, 21, 56]. However, free sailing tests are very expensive, and do not give any insights into the dynamics of the problem: forces and moments acting on the model can not be measured when freely sailing in the basin. Moreover, free-running model testing cannot be employed in the very wide range of ships and wave conditions necessary to assess the safety in a real sea state case.

Common techniques of manoeuvrability experiments in calm water, such as Planar Motion Mechanism (PMM), Rotating Arm, Oblique Tests [48] are widely used to measure the forces and moments acting on the vessel and then to obtain the hydrodynamic derivatives. However, these tests are complicated in following waves, and they are not usually carried out. The difficulty arises from the separation of the different force components acting on the model: the contribution of the waves from the loads due to the motions (radiation). For high-speed craft the problem is even more difficult, because the model must be oriented in such way to guarantee its natural position in the wave. The loads on the hull of small craft are highly dependent on the vessel orientation and thus on the highly variable submerged geometry.

Renilson [6, 16] measured the hydrodynamic loads on a ship in following seas at different locations in the wave, in order to quantify the manoeuvrability coefficients. The waves were generated by a dozer travelling with the carriage, then producing a constant wave profile around the vessel. The model could be easily positioned in any fixed longitudinal location in the wave, and oscillating PMM tests were performed. Matsuda and Umeda [57] proposed a new experimental procedure for the identification of the manoeuvrability coefficients separating those effects from the wave action. Hashimoto [50] evaluated the loads on a fully captive model in steep following waves, and then correct the measured values keeping into account the correct vertical running attitude of the model in the waves. Other examples of loads measurements in waves can be found in [27, 58]. Manoeuvrability captive tests should be preferably performed in large basin, rather than in rectilinear towing tank. This allows a clearer separation between the two effects due to the incoming wave angle and the vessel motions.

Although of more complex set-up, carrying out captive model tests is advantageous in view of a simulation of the vessel manoeuvring-in-waves by means of numerical tools. The measurements of the forces acting on the vessel in waves can be useful to implement and validate numerical methods that can be utilised over a wider field of application. Moreover, they also provide helpful insights into the dynamics of the problem. As this thesis aims to understand the dynamics of the craft in the following waves, captive model tests are preferred. Accurately knowing the forces and moments acting on the ship during a broach would help the designers to understand this phenomenon better and then to improve the safety of new designs, instead of simply assess the vulnerability of a ship to dynamic instability events.

2.3. MATHEMATICAL METHODS

SIMULATIONS of ship motion in waves can be simulated in the frequency and time domain. The behaviour of the vessel in following waves is highly non-linear and non-oscillatory, therefore the frequency domain approach is excluded in the study of these phenomena, and time-stepping discretization is preferred. The loads acting on the ship are computed at each time step. Time domain models are commonly used to assess the dynamic stability of the vessel in waves.

The problem of the high-speed craft sailing in the seaway is very complex: an accurate prediction of the ship behaviour demands a significant computational effort. This complexity excludes advanced numerical tools, such as CFD solvers, from a wide utilization in the problem. It would be very unpractical to statistically describe the vulnerability of a vessel to dynamic instability in a seaway by means of CFD simulations. A more preferable choice is to use easier, handier and faster mathematical methods to express the vessel behaviour at different sea conditions. Examples are tools based on slender body strip theory, or boundary element methods (BEM). Although less accurate, these tools are still used for practical design purposes and not yet completely substituted by the advent of the powerful "brute-force" CFD simulations.

The mathematical models used in the field of the ship manoeuvrability are often parametric, i.e. the forces and moments acting on the ship are approximated by polynomials. The coefficients of the polynomials can be estimated by means of empirical tests, semi-empirical formulations, CFD simulations. This is particularly beneficial since the controllability is governed by a large number of factors. In common manoeuvrability-in-waves applications, the Froude -Krylov and buoyancy forces are evaluated on the actual wavy submerged geometry. Instead, the damping loads due to the velocity components of the vessel in the horizontal plane are estimated by polynomials; the terms of these polynomials, the manoeuvrability coefficients, are estimated in calm water. This is a feasible approach for medium-large vessels: the waves are smaller than the vessel size and do not significantly influence the characteristics of the submerged geometry, thus neither the manoeuvrability loads. This is not applicable for small, fast craft: the waves are comparable with the vessel size, therefore the submerged geometry and the hydrodynamic loads change with respect to the position in the waves.

The hydrodynamic coefficients are typically obtained by means of captive model tests, such as towing tank Oblique Tests, Rotating Arm or PMM. These techniques are well-known and normally applied to calm water applications; the use of such experimental methods in the case of the vessel sailing in a seaway is not straightforward, and they must be carefully arranged. The experiments are difficult, time consuming and often related to only one or few wave conditions and model speeds. An alternative to the experimental tests is the use of less demanding CFD computations on captive ships. There are few examples of advanced numerical applications of loads calculation in waves [58, 59]. Accurate CFD solvers are substituting the experimental model tests in the computation of the hydrodynamic coefficients especially in calm water [60, 61], but not yet in waves.

Bailey [62], Fossen [63], Skeijc and Faltinsen [64] proposed unified seakeeping - manoeuvrability mathematical models for the description of the vessel motions in a seaway. These models differentiate the two time scales of the problem for high-frequency vertical

motions and low-frequency manoeuvring motions in waves.

Commonly, seakeeping - manoeuvrability tools are based on the slender body assumption, reasonable for slim, fast vessel, and on the division of the ship hull in transverse 2-dimensional sections: body-exact, non-linear strip theory methods have been widely used to predict the high-speed craft behaviour in waves. Zarnick [65], Keuning [37], Van Deyzen [39] and Rijkens [40] used these mathematical tools to calculate the vertical motions of fast vessels in head waves. In principle, a similar mathematical approach is also applicable to the horizontal loads when manoeuvring [66]. The practical and reliable use of these methods is unfortunately limited by the necessity of empirical formulations to express viscous phenomena and the sectional added mass characteristics [67], that have a significant impact in the result of the computations.

Potential flow boundary element methods (BEM) are based on a more sophisticated mathematical model [68], that keeps into account the memory effects and the surface dynamics around the ship body. In general, BEMs are more accurate than strip theory models. In his review of the state-of-art of the numerical methodologies used in the problem of the manoeuvrability-in-waves, Reed [69] confirms that potential blended flow methods represent the best compromise between accuracy and versatility of application. However, work must be still carried out for a reliable validation of these tools, especially for the manoeuvring loads.

2.4. NUMERICAL SIMULATIONS

ALL numerical simulations in this work are carried out using a 3D BEM. This tool has been developed during the past years as a reliable and relatively fast tool for the characterization of ship behaviour at sea. Originally conceived for high-speed hydrofoil craft applications [70], the code has been employed to simulate the fast vessel seakeeping in head waves. The exhaustive description of the code is out of the scope of this work; details of the mathematical model can be found in [38, 71–74]. The tool was recently applied to following sea conditions; a validation of the code in following and stern-quartering wave can be found in [24, 26, 34].

In principle, BEMs can predict the ship motions in waves within a reasonable computational time and with good accuracy, without the need of empirical data corrections. The most challenging task for these models is the prediction of the manoeuvrability loads. A BEM tool was chosen in this research because its use allowed a detailed understanding of its capability in the broaching problem. This is advantageous in view of future applications of the simulation tool, for other sea conditions and different vessels.

The hull surface discretization is made up of planar quadrilateral panels, as shown in Figure 2.3. A Green function [75] is specified on a fixed submerged geometry obtained by cutting the hull surface with a flat waterline given by the equilibrium orientation of the model at speed. The use of the Green Function allows to keep into account the memory effects and to avoid the discretization of the free surface.

The dynamic pressures due to radiation and diffraction potentials are evaluated only on the fixed below water geometry, where the Green function is defined, without considering the variations in wetted hull area due to the motions of the vessel. This linearisation allows less demanding computations, at the cost of lower accuracy if the motions of the vessel are large when sailing in high waves. The computational time can be an issue

in following waves simulations: the encounter frequency is low, and simulating enough wave encounters demands a large numerical effort. With BEMs, a high number of wave encounters and different sea conditions can be tested in a reasonable time on a normal desktop computer. This can not be achieved with more powerful and accurate tools.

The static loads (buoyancy) and Froude-Krylov wave loads are specified on the actual submerged geometry, i.e. on the instantaneous wavy free surface. The viscous effects, the propulsive and steering devices loads are calculated through semi-empirical formulations.

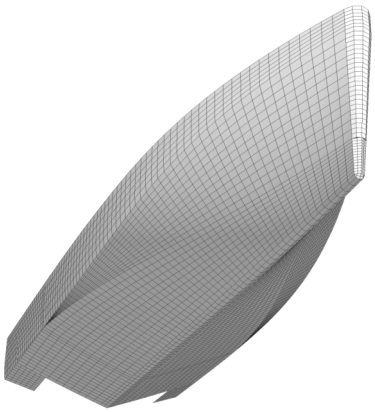

Figure 2.3: Example of discretization of the SAR NH-1816 for the above and below water hull surface by means of quadrilateral panels. In this picture the calm water linearisation corresponds to the running attitude of the vessel at $Fr = 0.48$.

The main difficulty in the use of this method in manoeuvrability problems is the occasional low accuracy of the prediction of the loads acting on the horizontal plane. The sway force, as well as the roll and yaw moment are governed also by other non-linear effects (spray generation, flow separation at chine and transom), that are not computed in potential flow models. In Chapter 5 this issue will be tackled in detail; the experimental data collected in Chapter 3 and 4 will be used to implement and validate the potential flow BEM in the prediction of the ship loads in following waves. The final aim is to guarantee both a qualitative and quantitative description of the broaching behaviour of the high-speed craft.

2.4.1. STEERING AND CONTROL OF THE SHIP

Particular attention must be devoted to the steering of the vessel when it is sailing in following and stern-quartering waves. Differences in the steering capabilities of the vessel could lead to very different broaching behaviour, and the steering parameters have to be set carefully.

The NH-1816 rescue vessel taken as object of the investigation is equipped with waterjets. The steering and propulsive forces and moments of the waterjets are modelled

with a semi-empirical model into the BEM simulation tool, as shown in Equations 2.15 to 2.18:

$$X_A = \rho Q(u_{NOZ} - c_M u \cos\beta_R)\cos\delta \tag{2.15}$$

$$Y_A = \rho Q(u_{NOZ} - c_M u \cos\beta_R)\sin\delta = Y_\delta \delta \tag{2.16}$$

$$K_A = Y_R z_{NOZ} \tag{2.17}$$

$$N_A = -Y_R x_{NOZ} = N_\delta \delta \tag{2.18}$$

The steering sway force and roll, yaw moments are described with the terms $Y_\delta\delta$, $K_\delta\delta$ and $N_\delta\delta$, that express the loads with polynomials linearised with respect to the steering angle δ. The term Q denotes the flow rate through the waterjet duct, that depends on the impeller rate; β_R is the flow incidence angle at the waterjet inlet; u_{NOZ} is the flow speed at the waterjet nozzle, located at the longitudinal and vertical coordinate x_{NOZ} and x_{NOZ}; c_M is an empirical coefficient representing the flow momentum due to the impeller suction.

The steering angle δ of the waterjets is set by an autopilot when the ship is freely sailing in waves. The autopilot is meant to keep the vessel at the same incidence angle with respect to the quartering waves; the desired steering angle δ is evaluated by means the autopilot in Equation 2.19:

$$\delta = b_{\delta\psi} r + c_{\delta\psi}\psi \tag{2.19}$$

This equation corrects the ship heading error net of the initial steady yawing moment from the waves; in other terms, the autopilot is meant to keep the vessel at relative angle with the wave while sailing in straight ahead direction. The autopilot is composed by a proportional and a derivative part that keep into account the instantaneous change of heading and turning speed from the initial straightforward sailing direction of the vessel in equilibrium. The autopilot parameter will be treated in detail in Chapter 6.

2.5. CONCLUDING REMARKS

SAR NH-1816 rescue boat controllability in following seas will be studied by means of experimental and numerical techniques.

Captive model tests were preferred to free-sailing model tests, because it will be possible to characterise and understand the dynamics of the vessel in waves and during the onset of dangerous dynamic instability events. The captive model tests will be carried out both in calm water and in following and stern-quartering waves.

A time domain, potential flow 3D boundary panel element method will be used to predict the hydrodynamic forces and moments acting on the hull in waves, and the overall behaviour of high-speed craft freely sailing in following seas. BEM are mature tools to predict the behaviour of the vessel in waves. Still some improvements are needed in the computation of the manoeuvrability loads, and this will be an object of the study.

3

HIGH-SPEED CRAFT MANOEUVRABILITY IN CALM WATER

The manoeuvrability of high-speed craft was investigated in calm water by means of experimental and numerical techniques. The results of experimental and numerical captive model tests on the SAR NH-1816 craft are presented in this chapter. The results are expressed in terms of manoeuvrability coefficients. These terms were implemented in the motion equations in order to understand the effect of the characteristics of the vessel manoeuvring. The manoeuvrability coefficients in calm water are highly dependent on the forward speed and on the trim variation of the vessel; in the pre-planing regime, the manoeuvrability coefficients of the high-speed craft are more important because they are higher in absolute value. The loads induced by static heel, by sway and yaw velocities have different effects on the vessel behaviour, and their estimation is crucial for a reliable prediction of the manoeuvre. Their effect on the initial turning of the vessel was estimated: the dynamics of the vessel changing its heading from an initial stable course is mainly dominated by the yaw moment due to the vessel sway and yaw velocities and the static heel. The hydrodynamic coupling between heel and the loads in sway and yaw is not commonly considered in controllability research. However, this coupling can be significant for small and fast craft. This effect was investigated: the results show that the loads induced by the heel cause the vessel to be less manoeuvrable, thus making turning more difficult.

3.1. INTRODUCTION

THE first step into the investigation of high-speed craft manoeuvrability-in-waves is to analyse their controllability in calm water. This allows the understanding of the difference between the more commonly studied calm water case and the less investigated following waves dynamics, examined in the successive chapters of this thesis. From the

Parts of this chapter have been published at the 14th International Conference of Fast Sea Transportation (FAST 2017) [53], at the 11th Symposium of High-Speed Marine Vehicles [54] and in The Transaction of the Royal Institution of Naval Architects [55].

point of view of the numerical simulations, insights into the controllability in calm water is helpful to separate the forward speed effects, such as wave making and the hydrodynamic pressure distribution, from the wave contribution.

The aspects that are studied in this chapter are the hull loads in sway, roll and yaw due to the sway and yaw velocities of the manoeuvring vessel, and its static heel. The motions in sway and yaw are commonly taken into consideration in manoeuvrability studies. For small, fast craft also the heel can play an important role. Often neglected in ship manoeuvrability [49], the heel induced sway force and yaw moment can significantly influence the manoeuvring of a vessel. When statically heeled on one side, the non-symmetric submerged geometry produces a force and a moment in the earth-fixed horizontal plane; this effect is particularly big on small vessels, since they are more sensitive than bigger ships to the change of wetted surface.

The hull manoeuvrability characteristics of the SAR NH-1816 craft were estimated by means of experimental captive model tests at the towing tank of the Ship Hydromechanics Department at Delft University of Technology (TU Delft). The sway induced and the heel induced loads were measured obtaining the respective hydrodynamic coefficients. The effect of the trim, considered particularly important for the distribution of hydrodynamic pressure and thus for the yaw dynamics of the small craft, was investigated. This effect was studied in order to estimate the variation of the manoeuvrability coefficients when the craft is trimmed "bow down". This is a very typical and dangerous condition for the vessel in the following sea: the incoming following wave pushes the stern up trimming the vessel with the bow deep in the water. Such dangerous position might play a role in the inception of a broach.

Oblique tests [48], also known as static drift tests were carried out to obtain the coefficients in sway Y'_v, K'_v and N'_v. The model was towed longitudinally with a turning angle in the horizontal plane (drift) with respect to the towing direction. The asymmetric motion causes forces and moments on the horizontal plane (sway and yaw) and on the transverse plane (roll). The static heel tests were performed towing the model longitudinally without drift angle but with a static heel angle: this asymmetric submerged geometry caused loads in sway, roll and yaw and the coefficients Y'_ϕ, K'_ϕ and N'_ϕ were obtained.

Rotating Arm tests [48] were simulated numerically using the BEM described in Section 2.4, with the aim to estimate the yaw rate induced linear coefficients Y'_r, K'_r and Y'_r. Due to the experimental set-up and time limitations, it was not feasible at this stage to perform experimental oscillating pure yaw PMM tests. These coefficients were already estimated experimentally by De Jong et al. in [26].

The results of the numerical and experimental investigations are given as the manoeuvrability coefficients introduced in Chapter 2. The linear hydrodynamic coefficients were obtained by fitting the hull loads with a polynomial using the least-squares method, as shown in Figure 3.1 for a pure-drift test. The polynomial fit is function of the orientation and velocities of the model during the captive tests (sway velocity, heel angle and yaw velocity). The first order coefficients of the polynomial fit are the manoeuvrability linear hydrodynamic coefficients. The forces, the moments and the velocities values used to estimate the coefficients are non-dimensional, and the angles in radians.

The ranges of heel angle, sway (drift angle) and yaw velocities were chosen in or-

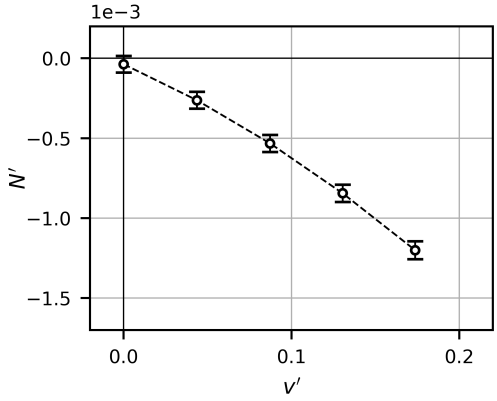

Figure 3.1: Example of the measured values of the yaw moment due to the sway velocity of the model in calm water depicted as function of the non-dimensional sway velocity at $Fr = 0.48$. The dashed line indicates the polynomial fitting of the measured values.

der to investigate the linear behaviour of the vessel, that is important in the stability problem: all the coefficients derived in this section are linear. The values of the velocity components of the vessel in the captive tests are shown in Table 3.1. The use of non-dimensional values allows a better comparison between the different coefficients, then the heeling, the sway and the yaw velocities are comparable, at least in the linear domain. The hydrodynamic manoeuvrability coefficients obtained with the experiments and the numerical simulations are presented in Section 3.4.

Manoeuvring Test	Motions range
Heeled model	ϕ [deg] = 0 to 12, ϕ' [rad] = 0 to 0.21
Oblique tests (drift)	β [deg] = 0 to 10, $v' = sin(\beta)$ = 0 to 0.17
Rotating arm	$r' = rL/U$ = 0 to 0.20

Table 3.1: Heel angle, sway and yaw velocity ranges investigated during the model tests. With good approximation for the NH-1816 hull, the loads due to these motions in these ranges are linear.

The parameters obtained were implemented in the motion equations (see Chapter 2, Section 2.1), in order to investigate the effects on each coefficient during the initial turning dynamics. This analysis, presented in Section 3.5, will highlight the most important parameters of the vessel during the initial turning from a stable condition of straight ahead motion. The dynamics of an initial turning is indicative of the stability of a vessel, and can also give useful information about a broach inception, i.e. a loss of stability in following seas. The characteristics of a ship during the initial change of heading represents rather well the behaviour of instability events that would make the vessel lose its initial stable straight course. The analysis is meant to outline the important factors that govern the dynamics of the vessel in these situations. In Section 3.5, also the not well-known and not widely considered heel-sway and heel-yaw hydrodynamic coupling effects on the manoeuvrability of the vessel was examined by performing standard ma-

noeuvres.

This chapter can be seen as a preliminary investigation of the manoeuvrability of high-speed craft, aimed to highlight the most important terms for the future investigation in the sea waves. Although the steering in calm water can be substantially different from the dynamical phenomena in following waves, this study gives a good initial understanding of the characteristics of the high-speed craft.

3.2. CAPTIVE MODEL TESTS SET-UP IN CALM WATER

CAPTIVE model experiments were conducted in the rectilinear towing tank of TU Delft. The model was tested fully captive at different speeds: the heave, trim and heel angles were fixed during each run. The model scale was 10. The rotations were set around the centre of gravity of the model. The orientation of the model was set by a 6 DOF oscillator that is based on the principle of the Stewart platform [76], also known as the Hexapod. The Hexapod can move in every direction in space using six electrical actuators. The forces in surge, sway and heave, and the moments in roll, pitch and yaw are measured through a frame composed by three horizontal and three vertical strain gauges, positioned between the Hexapod and the model. Figure 3.2 shows the set-up of the captive model experiments.

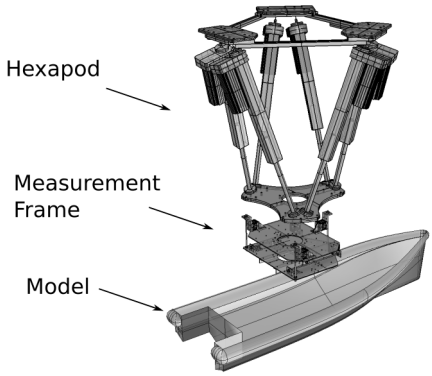

Figure 3.2: Exploded view of the model tests set-up. On top the Hexapod; below, the ship model is connected to the Hexapod through a measurement frame that measures the loads acting on the vessel in 6 DOF.

The experiments were divided into four phases. In the first phase (A), the heel induced loads were measured by statically heeling the model on one side at different heel angles. In the second phase (B), the drift induced loads were measured by statically rotating the model around the z-axis in order to run the model at a range of drift angles and thus different sway velocities. In these first two phases of the experiments, the heave and pitch of the model were constrained to the equilibrium running condition at speed. In the third and fourth phases, the effect of trim on the heel (C) and drift (D) induced loads was investigated. Two additional "bow down" trimmed conditions were tested; the heave of the model at these two additional trim conditions was kept at a constant deeper im-

mersion under the water surface. Table 3.2 summarises the runs performed. Figure 3.3 shows two pictures of the runs performed, for the heeled and drifting model cases.

Phase	Fr	σ $[m]$	θ $[deg]$	β $[deg]$	ϕ $[deg]$
A	0.38	0.09	0.80	0	0, 4, 8, 12 and 16
	0.48	0.13	2.64		
	0.57	0.08	3.38		
	0.67	-0.01	3.67		
	0.77	-0.11	3.84		
	0.86	-0.20	4.07		
	0.96	-0.29	4.30		
	1.05	-0.35	4.24		
	1.15	-0.40	4.07		
	1.25	-0.43	3.90		
	1.34	-0.46	3.67		
B	0.38	0.09	0.80	0, 5 and 10	0
	0.48	0.13	2.64		
	0.57	0.08	3.38		
	0.67	-0.01	3.67		
C	0.38	0.05	-0.8,-3	0	0, 4, 8, 12 and 16
	0.48				
	0.57				
	0.67				
D	0.38	0.05	-0.8,-3	0, 5 and 10	0
	0.48				
	0.57				
	0.67				

Table 3.2: Forward speed Froude numbers and orientations of the SAR NH-1816 during the four phases of the experimental static captive model tests in calm water. The values of the sink/rise are expressed in full scale.

The objective of the experiments was to derive the hydrodynamic coefficients in sway, roll and yaw when the ship is statically heeled at one side or has a sway velocity component.

- Y'_ϕ, K'_ϕ, N'_ϕ for statically heeled model;
- Y'_v, K'_v, N'_v for drifting model.

As the focus was directed towards the linear forces and moments, only a limited range of angles was considered. The heel induced coefficients were determined with the heel angle in radians; the sway induced ones were determined with the non-dimensional sway velocity v'. The coefficients are expressed according to the ship moving frame shown in Figure 2.1.

The forward speed range investigated in Phase A was between Froude numbers 0.4 – 1.3, corresponding to 10 – 35 knots full scale. The investigation covered the entire oper-

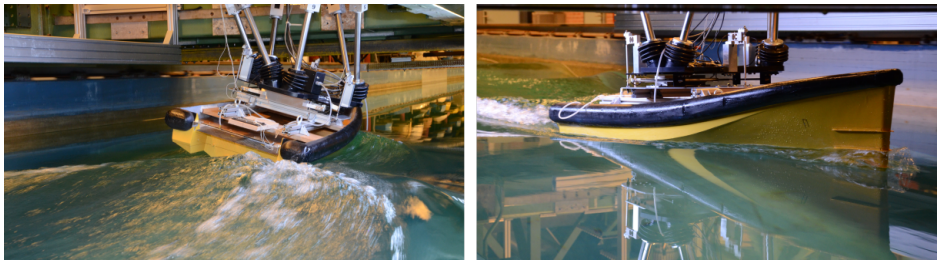

Figure 3.3: Pictures taken during the model tests. On the left, stern view of the heeled model: $Fr = 0.57$, $\phi = 8$ deg. On the right, bow view of an oblique drift run: $Fr = 0.48$, $\beta = 5$ deg.

ational speed range of the SAR NH-1816. At Phase B only the first lower Froude numbers between 0.35 and 0.7 were considered, since similar experimental data were available from [26] at the highest speeds.

The experimental uncertainty was calculated accordingly to [77]. The uncertainty analysis is explained in detail in Appendix A. The calculation takes into account the repeatability of the runs, the systematic errors of the set-up and the data fitting error.

3.3. NUMERICAL ROTATING ARM

THE forces and moments induced by the yaw velocity of the vessel were evaluated numerically, by means of the 3D BEM described in Section 2.4. Rotating Arm tests [48] were simulated, within the same forward speed range tested during the captive model tests. The yaw rate depends on the speed U; r' is only function of the model length and the distance from the centre of the circular tank R along the rotating arm, as formulated in Equation 3.1:

$$r' = r\frac{L}{U} = \frac{U}{R}\frac{L}{U} = \frac{L}{R} \tag{3.1}$$

The non-dimensional yaw velocity r' reaches a maximum of 0.20; with good approximation for the vessel in object, the forces and moments caused by a r' below this value can be considered linear (see Table 3.1). The coefficients Y'_r, K'_r and N'_r are then determined with the non-dimensional yaw velocity, similarly to what done for the other terms. The calculated loads were fitted with a polynomial, using the least squares method.

3.4. RESULTS

RESULTS are shown in terms of the hydrodynamic coefficients obtained from the experimental and numerical data. All the terms are non-dimensional and refer to the ship-fixed reference frame depicted in Figure 2.1.

3.4.1. SWAY VELOCITY INDUCED MANOEUVRABILITY COEFFICIENTS

Figure 3.4 shows the obtained manoeuvrability hydrodynamic coefficients in sway, roll and yaw induced by the sway velocity of the vessel.

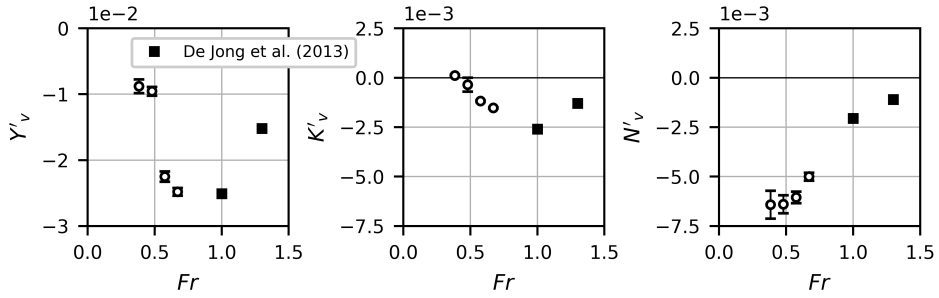

Figure 3.4: Non-dimensional experimental manoeuvrability coefficients induced by sway velocity, for sway force, roll and yaw moments plotted as a function of the Froude number.

The hydrodynamic coefficients in sway Y'_v, K'_v and N'_v are made up of the contributions of hydrodynamic pressure and wave making effects. Viscous effects can be neglected since the drift angles are small.

Y'_v and K'_v increase in absolute value up to Froude number 1.0. The effect of sway speed is in fact greater at higher forward velocities: the hydrodynamic pressure and the wave making effects become significant and increase the lateral resistance and the roll moment. At very high speed ($Fr = 1.34$) in the planing regime both Y'_v and K'_v are smaller in absolute value, since the vessel rises because of the hydrodynamic lift, then decreasing the sensitivity to the sway speed.

A different behaviour is observed in the yaw moment coefficient due to sway: N'_v is maximum in absolute value at the lowest speeds and decreases towards positive values. As the hydrodynamic lift increases with speed, the bow is progressively lifted out of the water reducing the total yaw moment.

3.4.2. HEEL INDUCED MANOEUVRABILITY COEFFICIENTS

Figure 3.5 shows the heel induced sway force and yaw moment coefficients and the roll restoring moment coefficient.

Although the model was heeled during the experiments, the coefficients Y'_ϕ and N'_ϕ are expressed according to the ship-fixed reference frame shown in Figure 2.1, that is a yawed-only coordinate system. Therefore, they do not account of the weight and the hydrostatic pressure, but only of the hydrodynamic effects.

Y'_ϕ, K'_ϕ are maximum in absolute value at the lower forward speeds, i.e. when the vessel is more immersed in the water. N'_ϕ is minimum at the lowest speed, whereas it increases after $Fr = 0.5$ and after that the behaviour is like the other two coefficients. It is not clear at this point the reason of this fluctuating behaviour; one of the explanations could be connected to the submergence of the transom, the flow separation at the chine or the bow wave development. From Figure 3.6 it is possible to appreciate the progressive development of the wave pattern around the model with increasing speed.

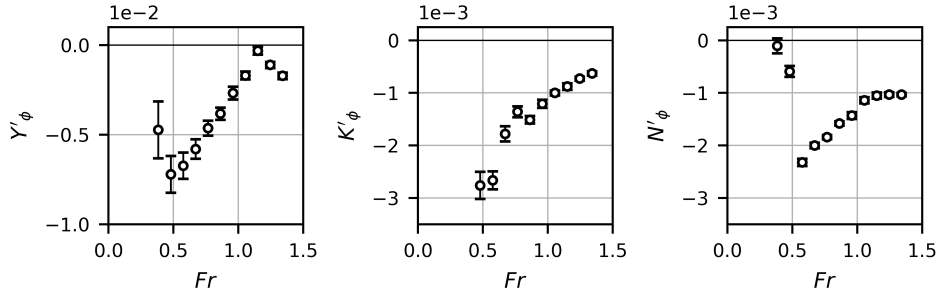

Figure 3.5: Non-dimensional experimental manoeuvrability coefficients induced by the static heel angle, for sway force, roll and yaw moments plotted as a function of the Froude number.

Some more detailed numerical investigations should be carried out to understand this behaviour; experimental tests alone cannot provide such insight into the hydrodynamics of the phenomenon.

The heel induced sway force and yaw moment show slight non-linearities at heel angles greater than 10 degrees. This is shown in Figure 3.7. For the purposes of this thesis, only the first order coefficients of the fitting polynomial are going to be considered. The offset of the sway force induced by heel in Figure 3.7 is caused due to a not correct alignment of the model along the direction of the basin. However, this does not have a significant effect on the estimation of the hydrodynamic coefficients, that represent the sensitivity of the hull loads with respect to the change in heel.

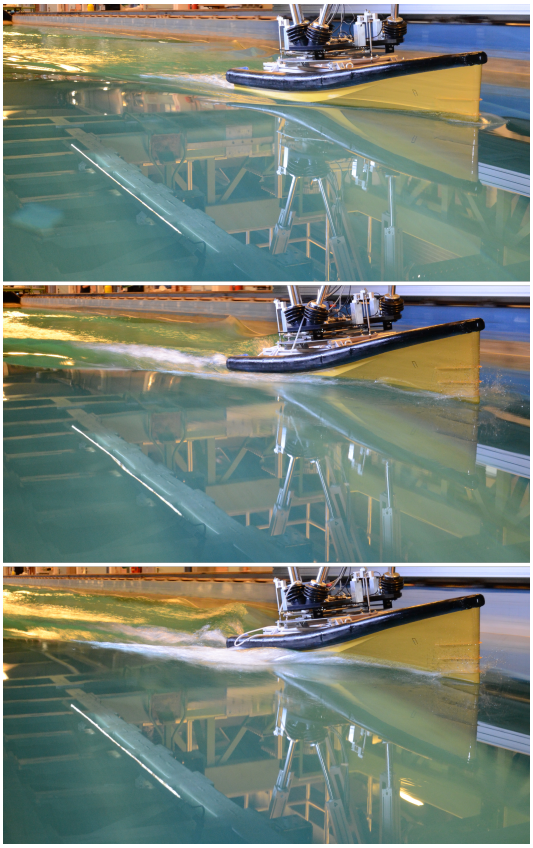

Figure 3.6: Three photos of the experimental tests of the heeled model. For all the photos $\phi = 8$ deg; on the top $Fr = 0.38$, in the centre $Fr = 0.57$ and at the bottom $Fr = 0.76$.

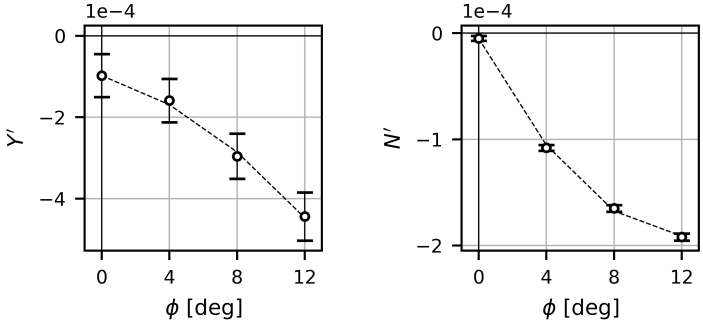

Figure 3.7: Measured values of the heel induced sway force (left) and yaw moment (right) in calm water depicted as function of the heel angle, for $Fr = 1.05$. The dashed line indicates the non-linear fitting of the data; a second order polynomial was used to highlight the slight non-linearity of these coupling loads.

K'_ϕ originates from the sum of the hydrodynamic lift and sway forces, but also from the hydrostatic restoring moments, as shown in Equations 3.2 and 3.3:

$$\Delta = \rho g \nabla \tag{3.2}$$

$$K'_\phi = K'^*_\phi - \Delta' GM'_T \tag{3.3}$$

The roll hydrodynamic coefficients K'^*_ϕ at the forward speeds investigated are shown in Figure 3.8 as function of Froude number. The hydrodynamic coefficients are compared with the linearised restoring moment coefficients $-\Delta' GM'_T$. The static restoring moment was calculated numerically using the vessel geometry, i.e. the immersed volume for each speed at the calm waterline taking into account the heave and trim of the vessel. The change in hydrodynamic pressure acting on the hull due to the change of the wave pattern around the vessel was considered as part of the hydrodynamic component.

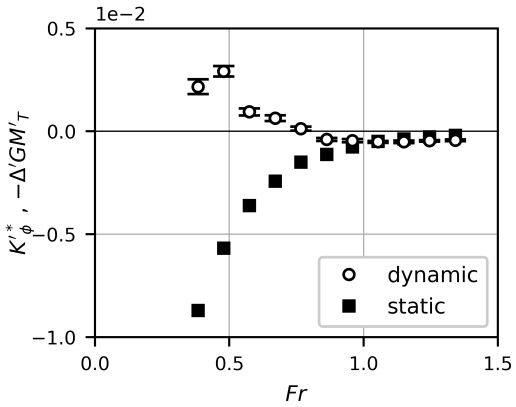

Figure 3.8: Hydrodynamic (K'^*_ϕ) and hydrostatic ($-\Delta' GM'_T$) components of the total roll restoring coefficient plotted as a function of the Froude number.

At lower speeds, the hydrodynamic component of the total roll moment is positive. This means that the hydrodynamic pressure distribution developed on the heeled hull creates a roll moment in the same direction as the vessel is heeled. This decreases the effect of the restoring static moment, that however is dominant at low forward speed. At higher speeds, the bow wave builds up significantly, as well as the separation from the chine on the heeled side: this generates a negative roll hydrodynamic moment that counter-acts the heeling of the vessel. At very high speed the dynamic and static components are of the same order of magnitude. The static restoring roll moment decrease with speed because of the effect of the lift, that raises the vessel out of the water.

3.4.3. YAW RATE INDUCED MANOEUVRABILITY COEFFICIENTS

Figure 3.9 shows the sway force and the roll, yaw moments induced by the yaw velocity of the vessel. The values are obtained from numerical Rotating Arm tests, simulated by the potential flow mathematical model described in Section 2.4.

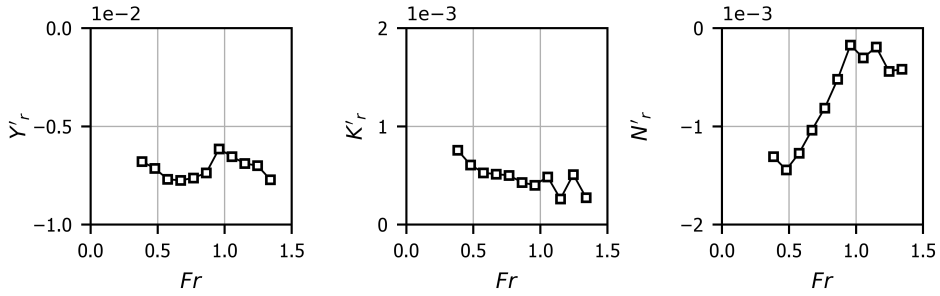

Figure 3.9: Non-dimensional numerical manoeuvrability coefficients induced by the yaw velocity, for sway force, roll and yaw moments plotted as a function of the Froude number.

The values of Y'_r are comparable with the term Y'_ϕ and Y'_v; instead, K'_r and N'_r are significantly smaller than the respective coefficients K'_ϕ, K'_v and N'_ϕ, N'_v. Y'_r and K'_r are not greatly dependent on the forward speed; instead N'_r decreases in absolute value at higher Froude number: this is similar to what observed for N'_v. At very high speed ($Fr > 1.0$) the coefficients K'_r and N'_r appear to be quite scattered. This is due to some numerical instabilities induced by the high pressures acting on the hull and by the low damping caused by the small submerged wetted surface.

3.4.4. THE EFFECT OF THE TRIM

In the experiments, also the effect of trim on the values of the manoeuvrability coefficients induced by heel and sway was investigated by trimming *bow-down* the model. The trim angles are summarised in Table 3.2, at Phase C and D. Figures 3.10 show the different orientations of the trimmed model. Hereby, the terminology *bow-up* refers to the normal running equilibrium of the vessel at the speed: the bow is lifted out of the water due to the action of the hull hydrodynamic lift.

In following waves the vessel might dive the bow into the water under the action of the wave front that raises the ship stern. This can be a very dangerous situation: with the bow deep below the water surface the risk of losing the control of the vessel can be a real risk. The position of the vessel trimmed in calm water is not an exact representation of the dynamics in a seaway, since the wave orbital components of the flow speed are not considered. However, this analysis can provide a good preliminary estimation of the sensitivity of the manoeuvrability loads with respect to the different running attitudes that a vessel may assume in the seaway.

The results of the trim effect investigation are summarised in Figure 3.11 and 3.12, that show the comparison between experimental sway and heel induced coefficients of the *bow-up* equilibrium configuration, already shown in the previous sections, and the trimmed vessel conditions.

As Figure 3.11 suggests, N'_v is the most sensitive coefficient to the change in trim of the vessel. This is because the trim changes the longitudinal distribution of the hydrodynamic pressure, affecting mainly the yaw moment. The sway and roll moment are instead less sensitive to the change of trim.

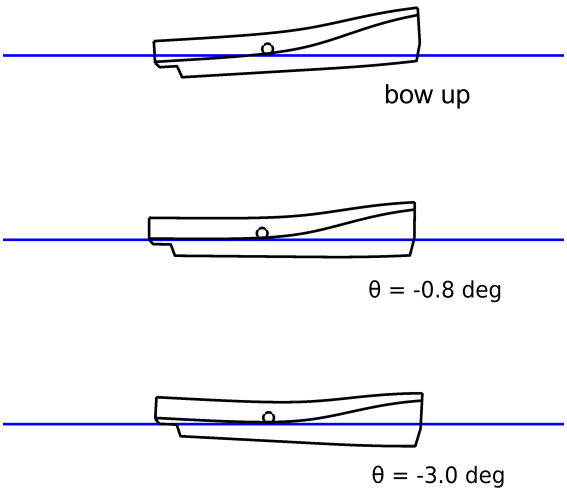

Figure 3.10: Different trimmed conditions of the SAR NH-1816. On the top the equilibrium running attitude; in the middle a "zero trim" situation, and at the bottom a *bow-down* situation. The lateral submerged areas change significantly with respect to the trim variation.

Figure 3.12 shows that the heel-sway coupling coefficient Y'_ϕ is the most affected by the change of the vessel trim; K'^*_ϕ and N'_ϕ are instead not particularly affected by it.

These different effects of the trim variation are not simply caused by a different submerged geometry. A *bow-down* trim changes the vertical lift produced on the hull bottom, the wave making characteristics, the submergence of the chine and the transom flow conditions. Those are aspects that change the dynamic loads on the vessel, acting differently on each of the directions interesting for the manoeuvrability.

The change in trim was also reproduced numerically, imposing the vessel orientations in heave and trim in the simulations computed with the 3D BEM. This analysis aimed to understand the effect of the trim on the yaw rate induced coefficients. The largest differences are expected to be in the yawing moment coefficient due to the vessel turning rate N'_r. The coefficient N'_r is compared to N'_v in Figure 3.13, in the *bow-up* and trimmed *bow-down* conditions.

The relative variation of the two coefficients is similar: both moments $N'_v v'$ and $N'_r r'$ increases of the same percentage when the hull is trimmed *bow-down*. However, the variation in the sway velocity induced moment is more relevant, since the values of $N'_v v'$ are larger than the ones induced by the yaw rate.

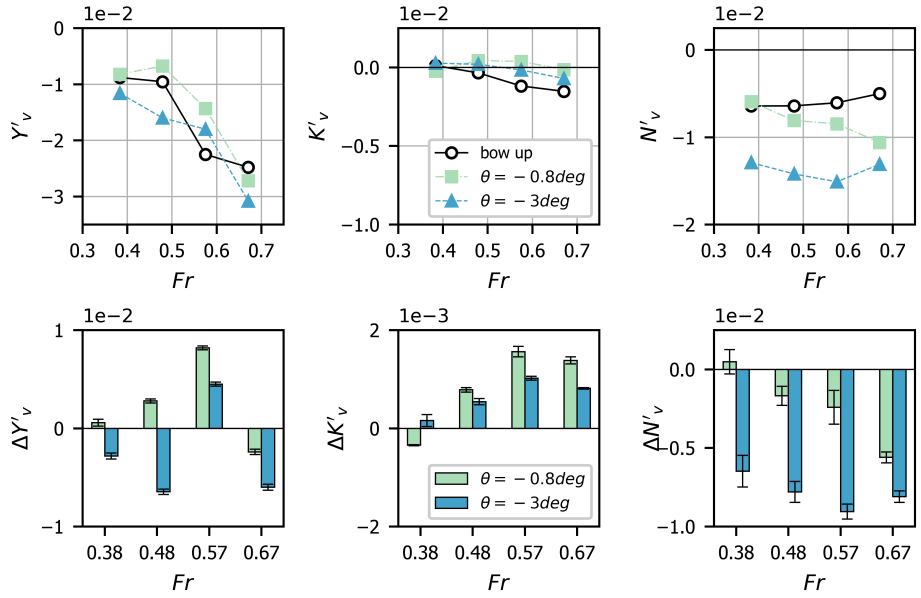

Figure 3.11: Top row: comparison between the sway velocity induced hydrodynamic coefficients for the different trim conditions. Bottom row: histogram of the absolute difference between the two trimmed *bow-down* and the equilibrium position coefficients.

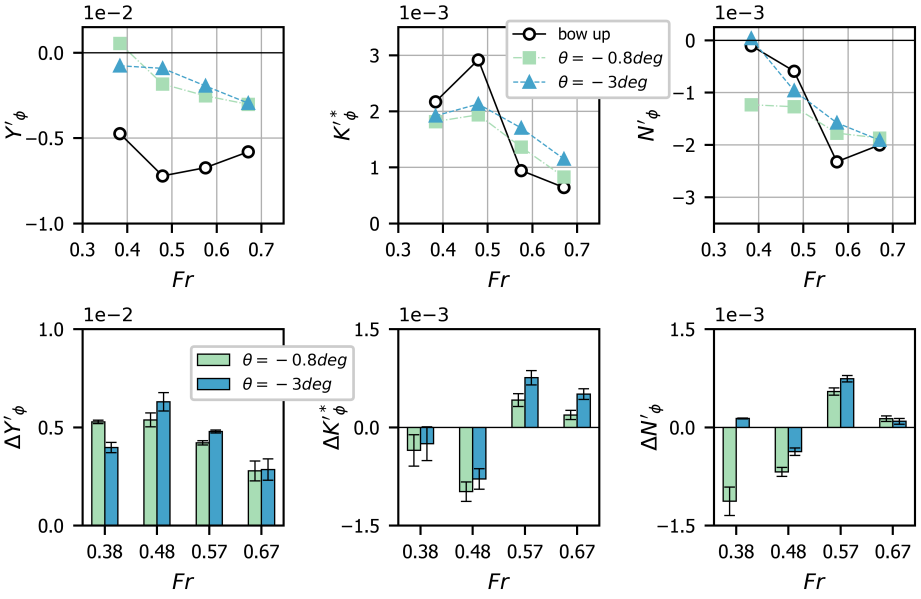

Figure 3.12: Top row: comparison between the static heel velocity induced hydrodynamic coefficients for the different trim conditions. Bottom row: histogram of the absolute difference between the two trimmed *bow-down* and the equilibrium position coefficients.

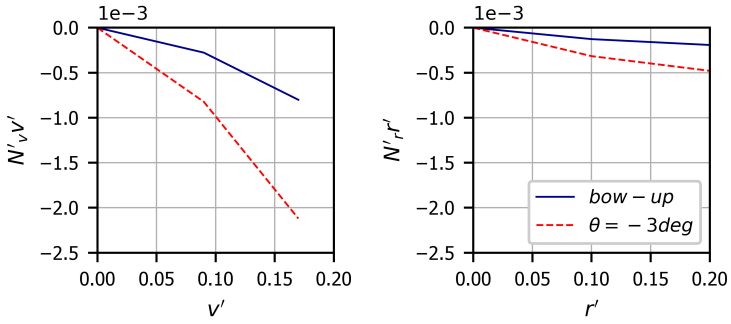

Figure 3.13: Comparison of the yaw moments induced by sway (left) an yaw (right) velocities in the two trim conditions, obtained by numerical simulations of oblique and Rotating Arm captive tests at $Fr = 0.6$.

3.5. DISCUSSION ON THE CALM WATER MANOEUVRABILITY

THE hull manoeuvrability coefficients were evaluated for the SAR NH-1816 craft, by means of captive model tests and numerical simulations. The data obtained are hereby utilised to estimate the characteristics of the manoeuvring high-speed craft.

The first aspect to consider is the ability of the high-speed craft to maintain its straight course after an external disturbance, without the steering action. This ability is quantified by the hull course directional stability index C' [48], reported in Equation 3.4.

$$C' = Y'_v N'_r - (Y'_r - m')N'_v \tag{3.4}$$

This term is obtained as the Jacobian of the system of differential equations in sway and yaw. A positive coefficient C' means that the vessel is directionally course stable. A hull is stable when the ship is able to keep a straight course without any steering actions after a little disturbance. On the contrary, a negative index means that the ship hull is course unstable: without utilizing the control devices, after a small disturbance the hull keeps a turning rate and a drift speed.

Although neglected for the study of displacement ships, the heel induced loads must be included in the directional stability assessment of fast vessels. Yasukawa et al. [42, 52] proposed a formulation of the directional stability coefficient considering also the heel coupling terms Y'_ϕ, N'_ϕ and the hydrodynamic restoring roll moment K'^*_ϕ. The latter coefficient C'_ϕ, reported in Equation 3.5, is obtained similarly to C', keeping into account also the third differential motion equation in roll. Basically, Equation 3.5 corrects Equation 3.4 for the dynamical behaviour in roll during a manoeuvre.

$$C'_\phi = C' - \frac{(N'_v K'_r - N'_r K'_v)(Y'_v N'_\phi - Y'_\phi N'_v)}{N'_v K'^*_\phi - N'_\phi K'_v} \tag{3.5}$$

As shown in Figure 3.14, the SAR NH-1816 craft shows a negative C'_ϕ, meaning that the vessel is course unstable in calm water. Contrarily to the case of big displacement

ships, this is not a result of a bad design: course instability on high-speed craft can be desired to achieve a greater ability to manoeuvre and turn. Moreover, the limited ability to keep a straight course is compensated by a great steering power and a high and quick turning responsiveness.

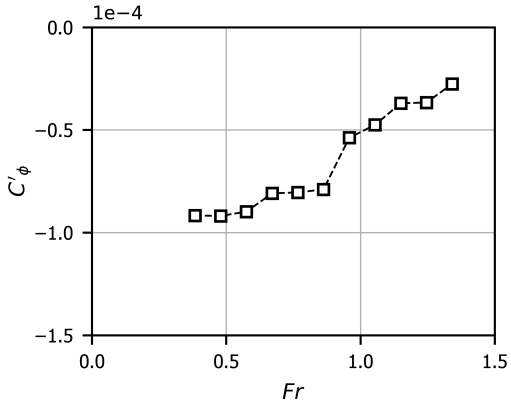

Figure 3.14: Directional stability index C'_ϕ plotted as a function of the Froude number.

3.5.1. THE TURNING DYNAMICS OF THE HIGH-SPEED CRAFT

The coefficients were implemented in the motion equations and the initial turning of the vessel under a constant steering action was investigated. The aim of this analysis was directed to the understanding of the most important hull coefficients that govern a change of heading. This represents well the dynamics following a loss of straight course due to external disturbances.

A sensitivity analysis of the hull terms was carried out. Each hull hydrodynamic coefficient was modified by 20%: the effect of this variation was assessed by applying a steering angle and calculating the response of the hull. This response was considered in terms of a time interval taken by the vessel to change its heading after the steering action. A longer time interval means that the vessel is more course stable and therefore the steering action is less effective.

In order to preserve linearity, the angles considered were small: under a steering deflection of 5 degrees, the interval between the start of the steering action and the moment in which the vessel heading changes of 5 degrees was taken as the reference quantity for the judgement of the course keeping ability of the vessel. This interval of time is hereby called execution time t_{EXE}.

In most common manoeuvrability studies, standard manoeuvres as Turning Circle and Zig-Zag are taken into account to estimate the manoeuvrability of the ship. However, this investigation is focused on the inception of the loss of dynamic equilibrium that causes the vessels not to be able to maintain its straight course. A Turning Circle, or Zig-Zag, highlights other important characteristics in manoeuvring that are not of interest at this stage. Moreover, in standard manoeuvres in calm water the non-linear loads of

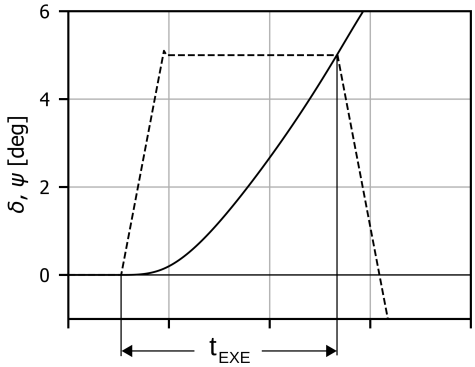

Figure 3.15: Definition of the execution time: interval of time between the first execution of the rudder and the instant where the vessel heading reaches the steering angle deflection. This is similar to the beginning of a Zig-Zag manoeuvre.

the vessel play a role. However, non-linear terms are secondary in the problem of the dynamic course instability.

The results of this analysis are shown in Figure 3.16, that shows a histogram of the relative percentage variation of t_{EXE}.

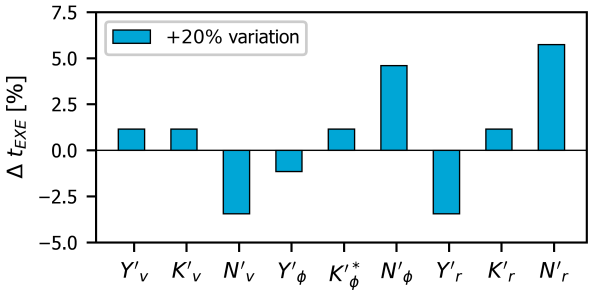

Figure 3.16: Sensitivity analysis of t_{EXE} with respect to a relative variation of the 20% of each linear coefficient.

The most important coefficients responsible of the dynamics of the high-speed craft turning are N'_r, N'_ϕ, N'_v and Y'_r. N'_r and N'_ϕ have a stabilizing effect: their 20% increase extends the execution time. On the contrary, Y'_r and N'_v have a destabilizing effect.

3.5.2. THE EFFECT OF THE HEEL INDUCED HYDRODYNAMIC LOADS

In the past, researchers evaluated the heel induced loads on fast vessels [42, 50, 52]. The sway force and yaw moment induced by the static heel of the high-speed craft can influence their manoeuvrability, but this effect is still rather unclear.

The heel induced loads were measured and the results in terms of the hydrodynamic coupling coefficient Y'_ϕ, K'_ϕ and N'_ϕ, presented in Section 3.4.2. Their effect on the manoeuvrability of the SAR NH-1816 was estimated looking into the common standard ma-

noeuvres Turning Circle and Zig-Zag. A detailed explanation of the two manoeuvres can be found in [48]. These two manoeuvres highlight the main characteristics of the ship manoeuvrability: the course stability, the turning ability, the responsiveness to a rapid change of heading due to external steering action, among the others.

The manoeuvrability of high-speed vessels has a strong non-linear characteristic, especially when considering tight manoeuvres with full steering as in the Turning Circle. Viscous effects are dominant in the appendages dynamics; flow separation at chine, transom and the keel can play an important role in the manoeuvrability behaviour of hard chine hulls. These effects were neglected in this analysis: only the linear characteristics of the vessel were taken into account. The lack of non-linear forces and moments does not allow a good representation of the ship manoeuvres. However, the vessel linear dynamics is accurate enough to discuss the role that the heel coupling has when manoeuvring.

The standard manoeuvres Turning Circle and Zig-Zag were simulated numerically. As done in the previous section, the coefficients obtained with the captive model tests (induced by static heel and sway velocity) and the numerical simulations (induced by yaw velocity) were implemented in the motion equations 2.2, 2.4 and 2.6, and the system of differential equations was solved in the time domain. In order to analyse the effect of the loads induced by static heel on the standard manoeuvres, two cases were investigated: the first without the heel coupled terms N'_ϕ and Y'_ϕ, the second with these coupled terms. K'_ϕ was included in both cases to realise a correct roll dynamics.

The ship manoeuvres were determined by the waterjets steering force. The ship speed was kept constant during the entire manoeuvre; this is an approximation because the speed-drop, typical in tight manoeuvres, is not modelled. Such approximation was considered acceptable seen the aim of this analysis, that is the comparison of the two standard manoeuvres with and without heel coupling terms. In the case of Turning Circle, the steering angle is set at the maximum of 23 degrees, whereas in the Zig-Zag it changes alternatively between +10 and −10 degrees, as soon as the vessel heading reaches the same value. The two manoeuvres are shown in Figure 3.17 and 3.18.

The results presented in Figure 3.17 and 3.18 show that the heel-sway and heel-yaw hydrodynamic coupling have the effect of making the vessel less manoeuvrable, increasing its directional stability. In the Turning Circle, due to the action of the heel-yaw and heel-sway coupling, the yaw velocity is reduced and the diameter of the manoeuvre becomes larger. The heel induced yaw moment $N'_\phi \phi'$ compensates the steering yawing moment. When steered towards portside, the vessel heels on portside inward in the turning because of the action of the steering devices that are located lower than the centre of gravity. According to the reference frame in Figure 2.1, ϕ' is negative, N'_ϕ is also negative: this results in a positive yaw moment that is opposite to the negative one produced by the steering action.

The same happens in the Zig-Zag manoeuvre. The heel induced loads cause the vessel to be less manoeuvrable the time interval to change heading becomes larger, the drift is higher and yaw rate decreases. Although in the case of a low rudder and low heading Zig-Zag 10-10 the heeling of the vessel is moderate, the difference in the manoeuvring behaviour is significant.

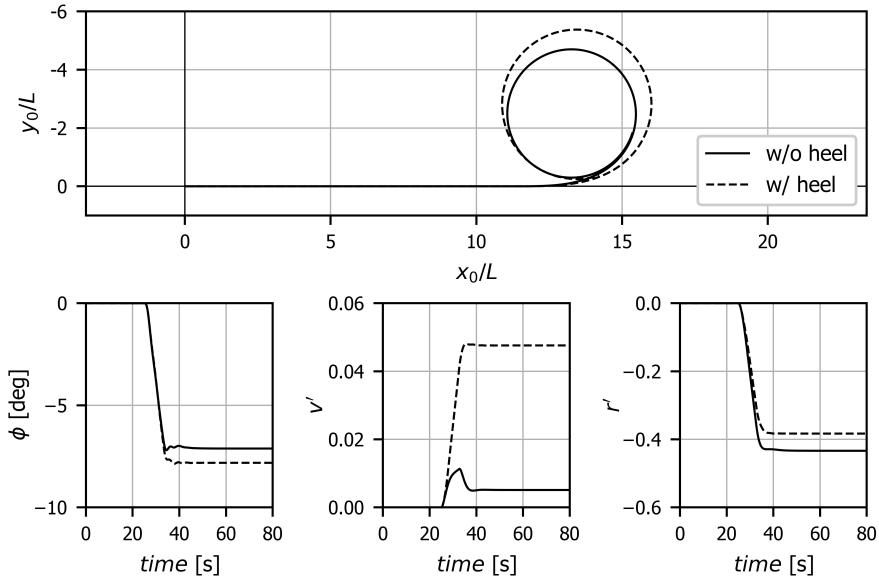

Figure 3.17: Turning Circle at full steering angle of the SAR NH-1816 craft at $Fr = 0.6$, without and with heel induced hydrodynamic sway force and yaw moment.

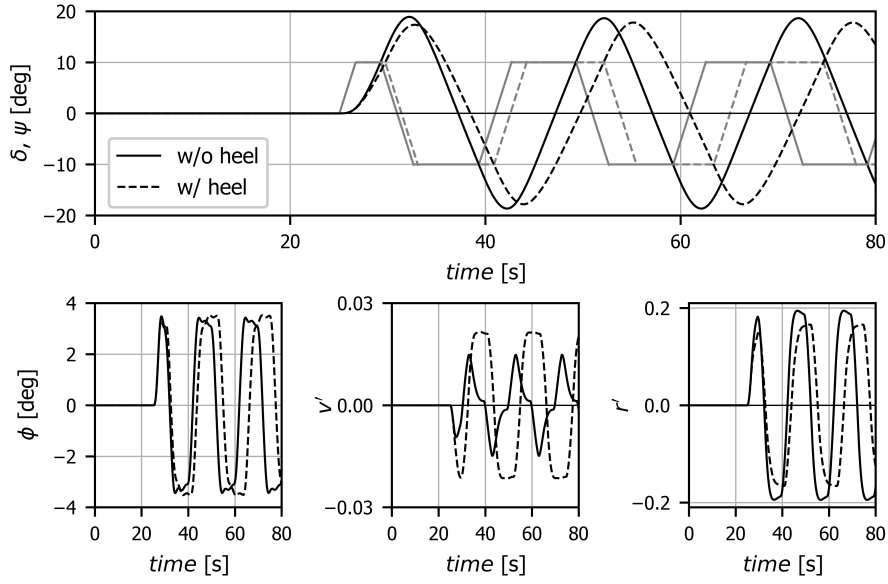

Figure 3.18: Zig-Zag 10-10 of the SAR NH-1816 craft at $Fr = 0.6$, without and with heel induced hydrodynamic sway force and yaw moment.

3.6. CONCLUDING REMARKS

EXPERIMENTAL and numerical captive model tests in calm water were carried out in order to obtain the manoeuvrability characteristics of the SAR NH-1816 craft; from the data acquired the hull hydrodynamic manoeuvrability coefficients in sway, heel and yaw were obtained. These coefficients were implemented into the motion equations in order to investigate and understand their effects on the turning and the course keeping abilities of the vessel.

The static heel and sway velocity induced coefficients were obtained by means of experimental measurements. The yaw velocity coefficients were obtained by simulating numerically the Rotating Arm captive tests. Pure yaw PMM tests were not feasible at this stage; in view of the future investigation in a seaway, it is extremely complex to obtain such terms in following waves [57].

The hydrodynamic coefficients are highly dependent on the forward speed. For all the conditions examined, their values are higher in absolute value at low-medium speed (Froude number between 0.4 and 0.7), whereas they decrease at higher velocities. This is mainly caused by the fact that at high speed, the hydrodynamic lift becomes great raising the model out of the water: then the sensitivity of the hull loads to the vessel orientations becomes lower. The speed range where the coefficients are significant correspond to the range of speeds where a dynamic instability in the following sea can occur. This is a hint of the important role that the hull characteristics can play in such scenarios.

The trim has a great influence on the manoeuvring characteristics of the vessel. In following waves, the small craft are subjected to large vertical motions. The incoming waves change the trim of the vessel, modifying the lateral hydrodynamic pressure and thus the hull yaw moment. The yaw moment due to the sway velocity of the vessel is greatly influenced by the vessel pitching: a change in trim of about 4 degrees can cause a modification of 100% of the N'_v coefficient, and this can lead to dangerous situations with the vessel unable to keep its course.

Each of the coefficients estimated in this section has an influence on the characteristics of the craft when the heading is changed from the initial straight course at speed. The most important coefficients that dominate the high-speed craft turning dynamics are N'_v, N'_ϕ, Y'_r and N'_r. As already discussed, the estimation of N'_r is complicated in following waves. The other terms will be estimated experimentally in the successive chapters, along with the forces and moments that are relevant for a reliable prediction of the craft manoeuvring-in-waves.

The heel induced sway force and yaw moment have the effect of stabilizing the ship during a turning. This results in larger Turning Circle diameter and larger period of the Zig-Zag manoeuvre. Those differences are significant even when the heel angle of the vessel is moderate, as it is in the case of a low angles Zig-Zag 10-10.

The numerical estimation of the yaw rate coefficients by means of a BEM model was considered as the only feasible option in the assessment of the manoeuvrability characteristics of the high-speed craft. Although during the initial turning in calm water the yaw rate is significant, the yaw dynamics in the following waves is rather different; as a matter of fact, in an inception of a dynamic instability in stern-quartering waves the yaw turning of the vessel is the final effect; the causes must be sought in other factors that act on the vessel dynamics.

4

CAPTIVE MODEL TESTS IN FOLLOWING AND STERN-QUARTERING WAVES

The manoeuvrability of the rescue boat SAR NH-1816 was analysed by means of captive model tests and numerical simulations for the calm water case. In this chapter, the results of captive model tests in following and stern-quartering regular waves are presented. The manoeuvrability loads due to the static heel and to the drift velocity of the vessel were measured. Also the force and moments induced by the wave in stern-quartering directions and induced by the control devices were estimated. The results showed that the loads in waves depend highly on where the vessel is located in the wave, and less on the wave and speed conditions tested. The hull manoeuvrability loads are significantly different from the calm water values: this suggests that applying a calm water characterisation into manoeuvring-in-waves problems is not accurate enough to judge the behaviour of high-speed craft in these conditions.

4.1. INTRODUCTION

NOT many researchers estimated the loads acting on the ships in waves. In more common seakeeping studies, the focus is usually directed to the measurement of motions and accelerations. Moreover, captive experiments in waves are complex and therefore time consuming, then they must be often limited only to very few wave conditions and forward speeds. Although it is impossible to estimate the safety level of the vessel through captive tests directly, the measurement of the forces and moments acting on the model gives helpful information into the dynamics of the problem, as well as useful data to be used in conjunction with mathematical tools.

Parts of this chapter have been published in the Journal of Marine Science and Technology [51] and are under review at Ocean Engineering [78].

The experimental measurements in following and stern-quartering waves presented in this chapter have three main objectives. First, it is necessary to quantify and describe the loads acting on the hull, particularly the forces and moments acting in the horizontal plane, and provided by the steering devices. In the case of the vessel under investigation, the SAR NH-1816, the steering is provided by two waterjets. Second, the forces and moments measured will be used to validate the 3D BEM simulation tool (see Chapter 2): although very suitable to predict the vessel behaviour in the seaway, potential flow mathematical models need improvements in the calculation of the manoeuvrability loads. Third, the experiments were carried out in several wave and model speed conditions in order to characterise the loads over a large range of wave characteristics and vessel speed scenarios.

The model tests presented in this chapter are the results of two experimental campaigns on the SAR NH-1816 model. The loads measured refer to the bare hull of the craft without skegs. The heel induced loads were measured at the rectilinear towing tank of TU Delft in following waves. The loads due to the incoming wave, to the vessel sway velocity and to the steering devices were measured in the Seakeeping and Manoeuvring Basin (SMB) of MARIN. This is because in this basin it was possible to produce the waves in stern-quartering directions and to run the model also with a sway speed component keeping the waves incidence angle at zero: this is not possible in a rectilinear towing tank. The model tested at the SMB was slightly larger than the one tested at TU Delft, in order to measure larger loads and thus to limit the effects of the vibrations induced by a wider and less stiff carriage. Figure 4.1 and Table 4.1 illustrates the towing tanks and their main characteristics.

Figure 4.1: Pictures of the Ship Hydromechanics Laboratory towing tank at TU Delft (left) and of the SMB MARIN (right).

Characteristics	TU DELFT	SMB
Main dimension	140 x 4.5 m	120 x 40 m
Depth	2.4 m	3 m
Maximum carriage speed	7 m/s	6 m/s
Model scale	10	6

Table 4.1: Main characteristics of the facilities at TU Delft and at SMB MARIN, and model scale of the experiments.

When sailing in waves, the model must assume its natural vertical orientation in heave and pitch at every location in the wave. This is an important requirement: Chap-

ter 3 showed the great influence of the running attitude on the manoeuvrability loads, especially the trim of the vessel. It is then crucial that the vertical running attitude of the model in waves is realistic. During the tests at the SMB the model was constrained in surge, sway, roll and yaw, but it was free to move in heave and pitch in order to be in vertical equilibrium in each location in the wave. In the tests at TU Delft instead the model was fully constrained in every direction by the Hexapod, with the same set-up used for the experiments in calm water. The motions in heave and pitch were prescribed to the Hexapod by means of numerical simulations: in order to ensure the model vertical equilibrium and thus the correct realization of the experiments, the full synchronization of carriage, wave maker and Hexapod was necessary. The detailed procedure of the tests is presented in Section 4.2.1.

The two experimental campaigns covered different following and stern-quartering regular wave conditions. The ship forward speed and the wave length were chosen in order to cover a large region of conditions where a course dynamic instability event could occur, within a reasonable number of tests to be performed. Since the loss of directional control usually happens when the ship speed is accelerated approximately to the wave celerity, the following wave crests were chosen to overtake the model at a low encounter frequency. The conditions investigated are depicted in Figure 4.2 in the Fr - λ/L space and summarised in Table 4.2. The wave slope, H/λ, was 0.06 (about 1/16) in all the conditions tested. The choice of the steepness was dictated by the limitation of the wave making process in the towing tank. Although the dynamic course stability events could happen at higher steepness, 0.06 was the upper limit to guarantee good quality waves, avoiding breaking.

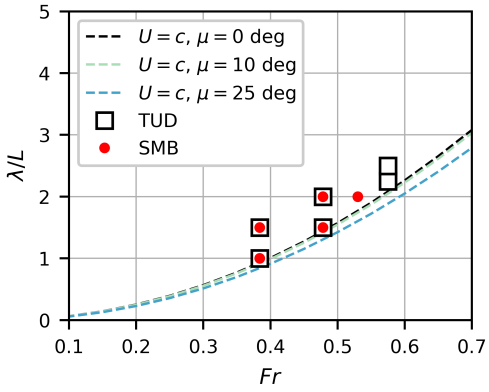

Figure 4.2: Model tests conditions at TU Delft and at SMB. The dashed line indicates the zero encounter-frequency at different wave incidence angle μ: above the line the waves are faster than the ship, under the line the ship is faster than the wave. The cases investigated at TU Delft and at SMB are slightly different because of the different limitations of the two facilities in the wave generation process.

As already explained in Chapter 3, the yaw velocity induced coefficients are not measured in the two experimental campaigns. Renilson [6] and Mastuda and Umeda [57] proposed methods to obtain these coefficients. The idea would be to perform pure yaw

Basin	TU DELFT						SMB MARIN				
Fr	0.38	0.38	0.48	0.48	0.57	0.57	0.38	0.38	0.48	0.48	0.53
λ/L	1.0	1.5	1.5	2.0	2.25	2.5	1.0	1.5	1.5	2.0	2.0
H/λ	0.06						0.06				

Table 4.2: Summary of the captive model tests runs in terms of forward speed Froude number, non-dimensional wave length and wave steepness.

PMM tests in every positions in the wave, i.e. moving the model exactly at the same wave crest celerity of the following wave; when rotating however, the model is at an incidence angle with the wave, then the loads induced by the waves must be subtracted, as shown in Equation 4.1:

$$N = N_\mu \mu(t) + N_r r(t) = N_\mu(\mu - \psi(t)) + N_r r(t) \tag{4.1}$$

Such complexity would make the tests very time consuming and of difficult realisation. Also ensuring a sufficient level of accuracy would be challenging, due to the subtraction of the measured force components to obtain the final result, the yaw velocity induced loads. At this stage the evaluation of the other characteristics of the vessel were preferred. The experimental estimation of Y'_r, K'_r and N'_r must be object of future research.

The results of the experiments are presented as the hull manoeuvrability coefficients due to heel and drift velocity, the steering loads coefficients, and the wave related parameters: the wave surging force and the manoeuvrability wave loads incidence angle coefficients. A summary of the terms obtained in the captive model tests with the relative angles tested is shown in Table 4.3. Regarding the tests carried out at TU Delft, un uncertainty analysis was carried out accordingly to [77]; the procedure is shown in Appendix A. For the tests at SMB, only the precision limits obtained by the 10 repetitions of a run were available.

	TU DELFT	SMB	Angles tested
Heel induced coefficients	Y'_ϕ, K'_ϕ, N'_ϕ		ϕ=0,8,12,16 deg
Wave surging force	X'_W	X'_W	μ=0 deg
Wave induced loads		Y'_μ, K'_μ, N'_μ	μ=0,5,10,15,25 deg
Sway induced coefficients		Y'_v, K'_v, N'_v	β=0,5,10 deg
Steering induced coefficients		Y'_δ, K'_δ, N'_δ	δ=0,5,10,15,20

Table 4.3: List of terms obtained from the captive model tests in following and stern quartering regular waves.

4.2. CAPTIVE MODEL TESTS AT TU DELFT: HEEL COUPLING

THE experiments were conducted in the rectilinear towing tank of TU Delft, the wave incidence angle, μ, and the drift angle, β, being zero during the entire experimental campaign. Thus, the manoeuvrability loads were caused exclusively by the heel angle.

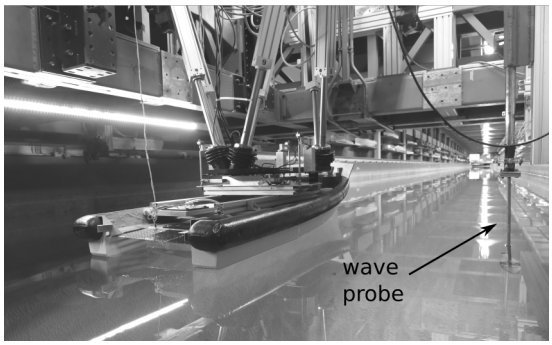

Figure 4.3: Model of the SAR NH-1816 craft during the captive tests at TU Delft. The wave probe located at the same longitudinal position of the model centre of gravity *G* measures instantaneously the wave elevation during each run.

The model was statically heeled on one side at different angles, up to 16 degrees. The wave elevation was measured by a wave probe installed next to the model at the longitudinal location of the centre of gravity. Figure 4.3 shows the set-up of the experiments.

4.2.1. EXPERIMENTAL SET-UP

As already anticipated in the Introduction, during every run the oscillations of the Hexapod were synchronized with the carriage start and the wave generation process, in order to guarantee the model vertical equilibrium attitude in the wave. The model was towed in the same direction of the waves propagation, as depicted in Figure 4.4.

The time traces of the motions and rotations in heave and pitch were calculated by the 3D time domain potential flow BEM that is described in Chapter 2. Each planned run for the captive model tests was reproduced numerically in advance, constraining the model in surge, yaw, sway, and heel, while being free to move in heave and pitch. These motions were used as input of the Hexapod that controls the model movements.

Fully constraining the model to an oscillator ensures a better stiffness of the experimental set-up: a not-completely stiff set-up might interfere with the measurement of the loads in an unpredictable manner. Moreover, the use of an oscillator allows the model to be oriented in every desired direction allowing to measure the sensitivity of the loads with respect to well defined positions of the model. This is very meaningful for manoeuvring and seakeeping applications: it is possible to measure all the forces and moments acting on the model in waves in static conditions or with forced oscillations. In these particular tests, the model was forced to assume its equilibrium position in the wave; more in general, the model can be forced to assume every prescribed position or to perform every oscillation in waves.

Figure 4.5 shows an example of the comparison between the computed prediction and the measured data resulting from the synchronization. The synchronization phases can be described as follows. At the run start the wave-maker is activated: the model is out of the water until a stable wave train is generated. After this waiting time, the carriage starts automatically according to the speed time trace specified by the user input. At this point the Hexapod is triggered and the model moves towards the desired wave position

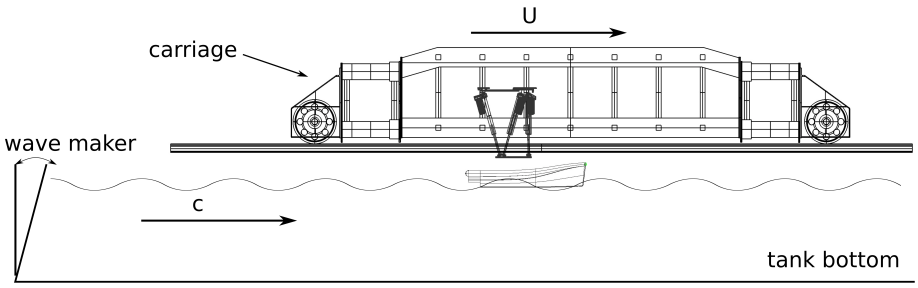

Figure 4.4: Picture of the global set-up of the experiments in following waves. The model is towed from the wave maker towards the beach, in the same direction of the waves propagation. The carriage moves with speed U, whereas the wave crests move with celerity c.

ξ_G/λ at its prescribed vertical position. Once the model reaches the desired position the measurement starts. After a complete or partial wave cycle the carriage decelerates, the model is lifted out of the water and the measurement ends. Figure 4.6 shows three photographs taken during a measurement run.

The synchronization process consists of two steps. First it is necessary to know how the waves develop along the tank. There is a phase shift, φ_P, between the wave elevation measured at the probe and the sinusoidal input signal from the wave maker controller. The phase φ_P was obtained by means of a least-squares fitting of the signal of the wave probe positioned at the model's starting location. The second step consists of the estimation of the longitudinal position in the tank corresponding to the first position of the model on the wave. For that Equation 4.2 is solved iteratively for time t as the independent variable, until the match between the carriage longitudinal position x_T^* and the desired wave elevation ζ^* is reached:

$$\zeta^* = a \cdot cos(\omega t – k x_T^*(t,U) + \varphi_P) \tag{4.2}$$

The time t is summed to obtain the waiting time needed for the wave to be fully developed. In order to characterise the wave propagation along the tank, an extensive series of wave measurements was carried out during the preparatory phase of the experiments. These measurements had two aims. The first aim is to set the correct amplitude for the input to the wave maker, and to determine the time that is required to achieve a stable regular wave train. The second aim is to determine the celerity of the wave crests, making use of the definition of encounter frequency. The method consists of moving the carriage along with the wave at a higher encounter frequency in order to be able to record several wave periods. The wave elevation was measured using the wave probe installed on the carriage. The model was not present at this stage. The wave encounter period was then measured, and the wave celerity was calculated according to Equation 4.3:

$$\lambda / T = c = \frac{U}{(1 - \frac{T}{T_E})} \tag{4.3}$$

The wave amplitude and celerity are considered to be constant along the length of the tank.

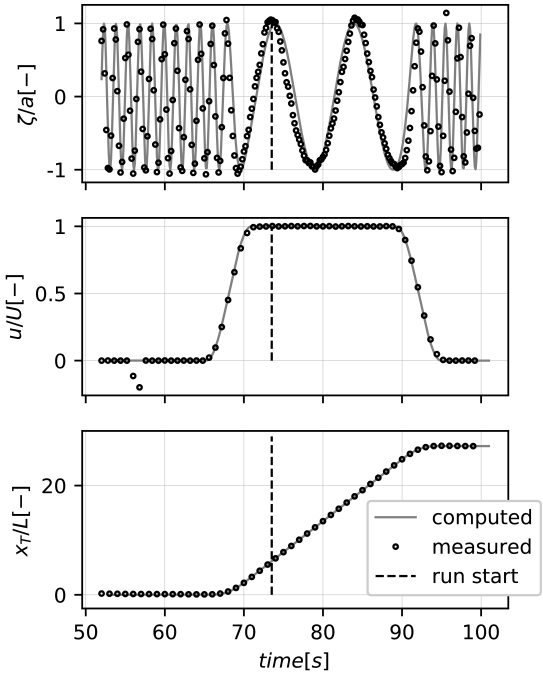

Figure 4.5: Comparison between the computed and measured time histories of the main outputs of the synchronization: wave elevation at model G (top), carriage speed (middle) and carriage position (bottom). The dotted line highlights the instant at which the measurement starts. In this figure $\lambda / L = 2$, $Fr = 0.48$.

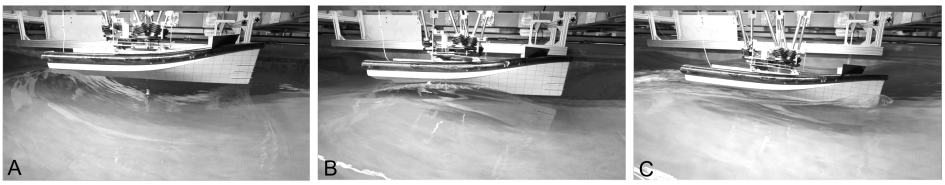

Figure 4.6: Examples of three different phases during a run. A): the waves are generated, and the ship model is out of the water. The carriage speed is zero. B): the carriage has accelerated to its nominal speed and the model is in its initial position on the wave. The measurement starts. C): measurement interval, the ship model oscillates in heave and pitch according to the wave positions; the carriage speed is stationary. The forces and moments, the wave elevation and the vertical position of the model are measured.

4.2.2. NUMERICAL CORRECTION OF THE MODEL VERTICAL EQUILIBRIUM

The use of the calculated vertical positions in the time domain (heave and pitch) as input to the Hexapod motions in the wave can have advantages, however it introduced a potential error. The calculated vertical positions did not ensure exactly the vertical equilibrium in the model tests, resulting in a non-zero heave force and pitch moment measured during the runs. It meant that a new vertical position must be found such to satisfy the vertical equilibrium. The approach followed was the same as that presented in the work of Hashimoto [50]. As a first step it is necessary to evaluate the sensitivity derivatives of the force and moments in heave σ and pitch θ. In this study those derivatives were calculated numerically using the 3D time domain potential flow BEM described in Chapter 2, Section 2.4. The derivatives are evaluated by varying the model's vertical attitude systematically at each longitudinal location in the wave. Figure 4.7 shows the outcome of this analysis on the heave force and pitch moments for one condition investigated in one location in the wave. Each point in the plot represents a different heave or pitch value at the location in the wave ξ_G/λ. The range of the values of heave σ and pitch θ is chosen accordingly to their maximum variation in the measurements.

The new heave and pitch values can be calculated solving the system of equations:

$$\begin{cases} Z'(t) + Z'_\sigma \Delta\sigma'(t) + Z'_\theta \Delta\theta(t) = 0 \\ M'(t) + M'_\sigma \Delta\sigma'(t) + M'_\theta \Delta\theta(t) = 0 \end{cases} \tag{4.4}$$

The terms Z' and M' are respectively the non-zero heave force and pitch moment measured in the tests. The variations in heave for the six conditions tested are in average about the 10% of the maximum heave excursion of the model on the wave. For the pitch the same average relative variation is around the 2.5%. Figure 4.8 shows the values of heave and pitch before and after the correction for one condition.

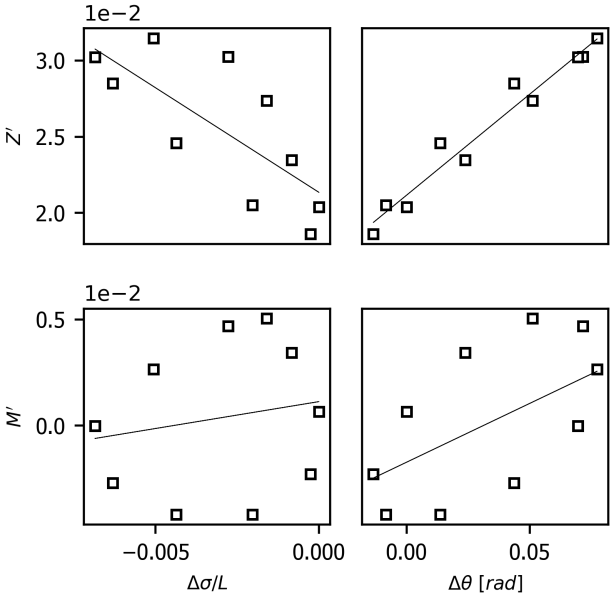

Figure 4.7: Sensitivity coefficients of heave force Z' (top row) and pitch moment M' (bottom row) with respect to the variation of heave $\Delta\sigma$ (left column) and pitch $\Delta\theta$ (right column) with respect to the equilibrium value. This Figure refers to the condition of $\lambda/L = 1$ and $Fr = 0.38$, at the location in the wave correspondent to $\xi_G/\lambda = 0.5$; $H/\lambda = 0.06$.

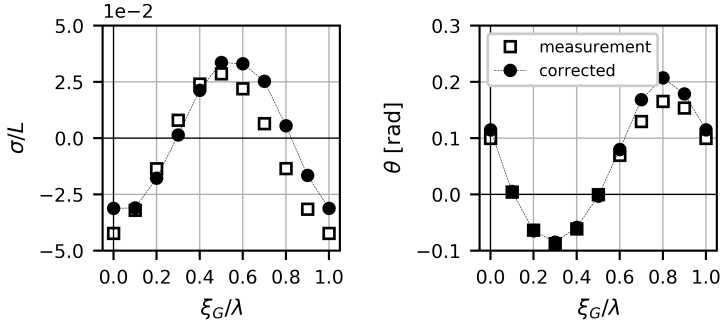

Figure 4.8: Plots of the original measured vertical motions and the values after correction (left: heave; right: pitch). Condition examined: $\lambda/L = 1.5$, $Fr = 0.48$; $H/\lambda = 0.06$.

4.3. CAPTIVE MODEL TESTS AT SMB: WAVE, SWAY VELOCITY AND STEERING INDUCED LOADS

Figure 4.9: Picture of the SAR NH-1816 craft model at MARIN facilities.

DIFFERENTLY from the tests at TU Delft, the SMB set-up let the model free to move in heave and pitch, thus assuming its natural vertical position in the wave. Moreover, the wave making of SMB allowed to perform tests not only in following waves, but also in stern-quartering directions; the carriage could also move in the direction of the sway of the model. In this way, a clear separation between the loads induced by the waves and by the sway velocity was possible. The model of the SAR NH-1816 used at SMB is shown in Figure 4.9. During this tests campaign, the model was also equipped with two waterjets: the steering force provided by the waterjets in waves were measured. Therefore, three different types of experiments were performed:

(a) *Tests at incidence angle with zero sway velocity.* The wave induced loads are measured at different wave incidence angles up to 25 degrees. At this stage the model is running at zero sway velocity, see Figure 4.10, and hence there is no contribution to the sway force or yaw moment from the sway velocity. Thus, the only loads being measured are due to the wave.

(b) *Tests at pure sway motion in following waves.* The sway induced loads are measured while the model is running with constant drift in waves. The incidence angle between the direction of the waves and the ship longitudinal axis is zero, see Figure 4.10, and hence there is no contribution from the wave to the sway force or yaw moment. Thus, the only loads being measured are due to the sway velocity.

(c) *Tests with waterjets steering angles.* The steering loads of the waterjets are measured in waves at different steering angles. In this condition the sway motion and the wave incidence angle are zero, and hence there is no contribution to the loads from either the sway motion or the wave, see Figure 4.10. Thus, the only loads being measured are due to the waterjets steering angle.

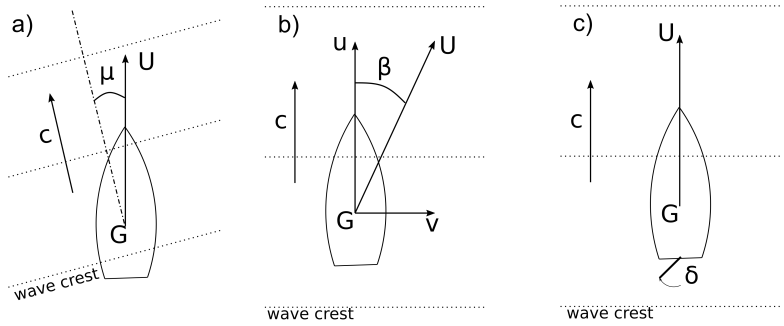

Figure 4.10: Schematic representation of the captive model tests performed at the SMB of MARIN as described in the text items.

4.4. RESULTS

ALL the terms were evaluated for each conditions tested as function of the longitudinal position of the centre of gravity of the vessel in wave ξ_G/λ, defined by Figure 2.2 of Chapter 2. Figure 4.11 shows two pictures of the model tests taken during one run.

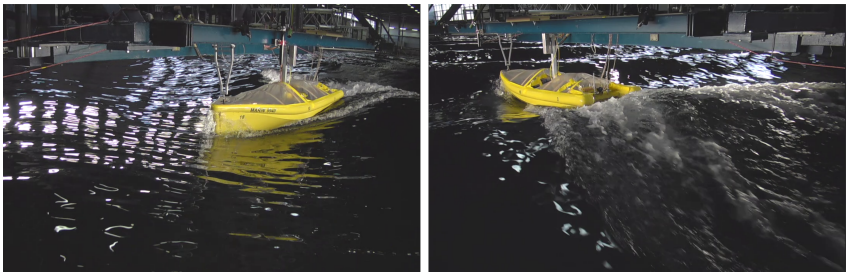

Figure 4.11: Bow and stern views taken from a captive test run at the SMB of MARIN, in stern-portside-quartering waves. $\lambda/L = 2$; $Fr = 0.48$; $\mu = 25$ deg; $H/\lambda = 0.06$.

The loads measured were fitted along the wave locations with a sinusoidal signal of the same frequency as the excitation wave encounter frequency: this is reasonable for the manoeuvrability loads at low angles under the hypothesis of linearity between the wave excitation and the output load. Figure 4.12 shows an example of the sinusoidal fitting of the sway force induced by sway velocity.

In each location in the wave ξ_G/λ, the coefficients were obtained similarly to the case of calm water, as depicted in Figure 4.13. Forces, moments, translations and rotations are referred to the centre of the ship-fixed reference system shown in Figure 2.1 of Chapter 2, located at G.

This section will be subdivided in the results for:

- wave surging forces;
- the sway force, roll and yaw moments hydrodynamic coefficients induced by the wave incidence angle;

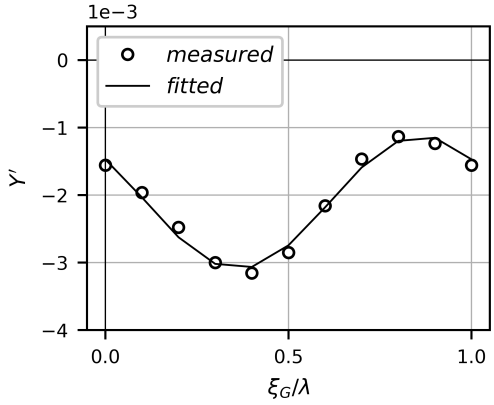

Figure 4.12: Sinusoidal fitting of the non-dimensional sway force induced by sway velocity measured at SMB for one run in regular waves. $\lambda/L = 1.5$; $Fr = 0.38$; $\beta = 5$ deg; $H/\lambda = 0.06$.

- the sway force, roll and yaw moments hydrodynamic coefficients induced by the sway velocity of the model;
- the sway force, roll and yaw moments hydrodynamic coefficients induced by the static heel of the model;
- the sway force, roll and yaw moments hydrodynamic coefficients induced by the waterjets steering on the model.

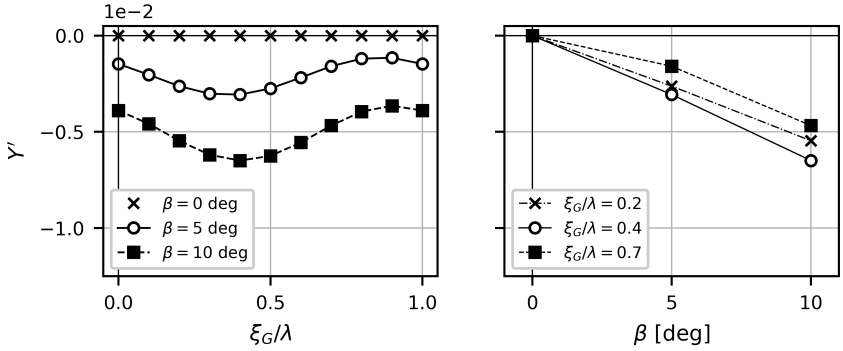

Figure 4.13: Non-dimensional sway velocity induced sway force measured at SMB. On the left, Y' is depicted as function of ξ_G/λ at different drift angle β; on the right the same force is shown as function of β at three different location in the wave. $\lambda/L = 1.5$; $Fr = 0.38$; $H/\lambda = 0.06$.

4.4.1. WAVE SURGING FORCE

The surge force in following waves was measured during both tests, at TU Delft and at SMB at MARIN. For all the cases investigated, the wave surging force measured during

the two experimental campaigns were very similar to each other. Figure 4.14 shows the term X'_W plotted against ξ_G/λ for the conditions investigated at TU Delft. For $Fr = 0.38$ the wave surging force is influenced by the wave length to a larger extent than the other two higher speed cases. At $Fr = 0.48$ and $Fr = 0.58$, X'_W does not depend on the wave length. For all the different cases, the maximum surging force is located around $\xi_G/\lambda = 0.3$, on the wave front; while the minimum is located around $\xi_G/\lambda = 0.8$, on the wave back.

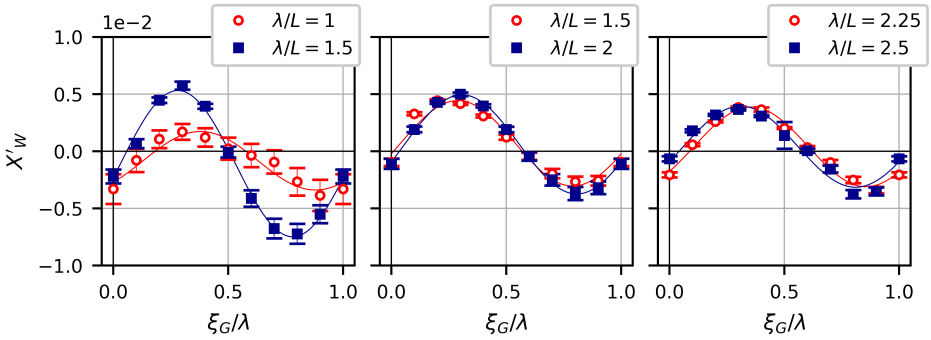

Figure 4.14: Wave surging force X'_W measured during the model tests at TU Delft for $\phi = 0$ degrees. Left: $Fr = 0.38$, centre $Fr = 0.48$, right $Fr = 0.57$; $H/\lambda = 0.06$.

The knowledge of the wave surging force is very important to predict in which location in a wave the vessel can surf, i.e. where a dynamic instability might occur. This prediction can be achieved by considering the equilibrium of forces during a surf-riding, as explained in details by Renilson in [32]. The total hydrodynamic surge force acting on the hull can be split in two terms: the calm water resistance $R_T(U)$ at the measurement speed U and the wave surging force X'_W. Assuming that during a surf the surge acceleration is zero, the surf-riding equilibrium equation is:

$$X'_W + R_T(c) + X_P = 0 \tag{4.5}$$

The total surge force is equal to X'_W plus the calm water resistance of the ship at the wave celerity c: during a surf the ship is captured by the incoming wave thus having the same speed. The engine revolution rate and the thrust are kept constant: X_P is equal to the calm water resistance $R_T(U)$ to ensure the forward motion equilibrium at the initial reference speed U. Substituting in Equation 4.6:

$$X'_W = -(R_T(c) - R_T(U)) = -\Delta X \tag{4.6}$$

The term $-\Delta X$ is the difference between the calm water resistance during a surf, i.e. at speed c and the starting resistance at the reference speed U. In Figure 4.15 the term $-\Delta X$ is denoted with a horizontal constant dashed lines. This line crosses the X'_W curve in two points. The first, at about $\xi_G/\lambda = 0.1$ near the wave crest, is a point of

unstable equilibrium: moving slightly forward or backward the ship will go further than that equilibrium, pushed away by the wave surging. The second one, at about $\xi_G/\lambda = 0.5$ near the wave through, is a point of stable equilibrium: moving forward or backward, X'_W pushes the ship back to the equilibrium location. This means that during a surf-riding event, the ship will spend most of its time near a wave trough.

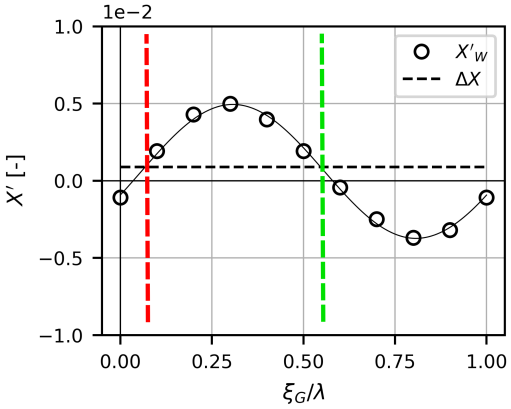

Figure 4.15: Wave surging force X'_W for the condition of $\lambda/L = 2$, $Fr = 0.48$, $H/\lambda = 0.06$. The red vertical dashed line indicates the location in the wave of unstable surf equilibrium, near the crest. The green vertical one indicates the surf equilibrium location in the wave where the vessel is most likely to be during the inception of a dynamic instability.

4.4.2. WAVE INCIDENCE ANGLE INDUCED COEFFICIENTS

The model tests in stern-quartering regular waves were carried out at positive μ, i.e. with the waves hitting the model at portside. Figure 4.16 shows an example of the measured wave yawing moment as function of the steady wave incidence angle μ, for one case investigated and two locations in the wave.

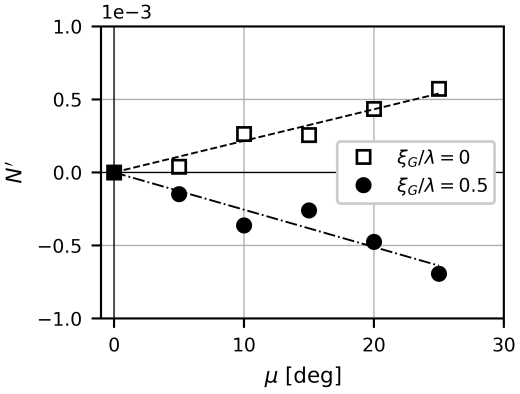

Figure 4.16: Measured wave yawing moment and linear fitting plotted as function of the wave incidence angle μ, for two locations in the wave. $\lambda/L = 2$, $Fr = 0.53$, $H/\lambda = 0.06$.

The coefficients of the wave loads with respect to the wave incidence angle obtained are shown in Figure 4.17.

The wave induced coefficient in sway Y'_μ and in roll K'_μ have a similar shape. Y'_μ is positive when the vessel is on the front of the wave ($\xi_G/\lambda < 0.5$), meaning that the vessel is pushed towards starboard. On the contrary on the back of the wave ($\xi_G/\lambda > 0.5$) the vessel tends to go back towards portside under the effect of the counter-acting orbital velocities of the wave. Similarly, the ship tends to roll outwards to starboard, being K'_μ positive, and the opposite happens on the back of the wave.

The wave yawing moment coefficient N'_μ instead has a different shape. N'_μ has a maximum around the through of the wave ($\xi_G/\lambda = 0.4 - 0.5$); close to that location it is negative, meaning that at portside-quartering waves the ship is turned towards portside. This agrees with the dynamic of a broaching-to: the ship is turned as to lie broadside to the incoming waves, beam-to-sea. Moreover, the wave yawing moment is bigger close to the equilibrium surfing location, where the dynamic instability inception usually begins.

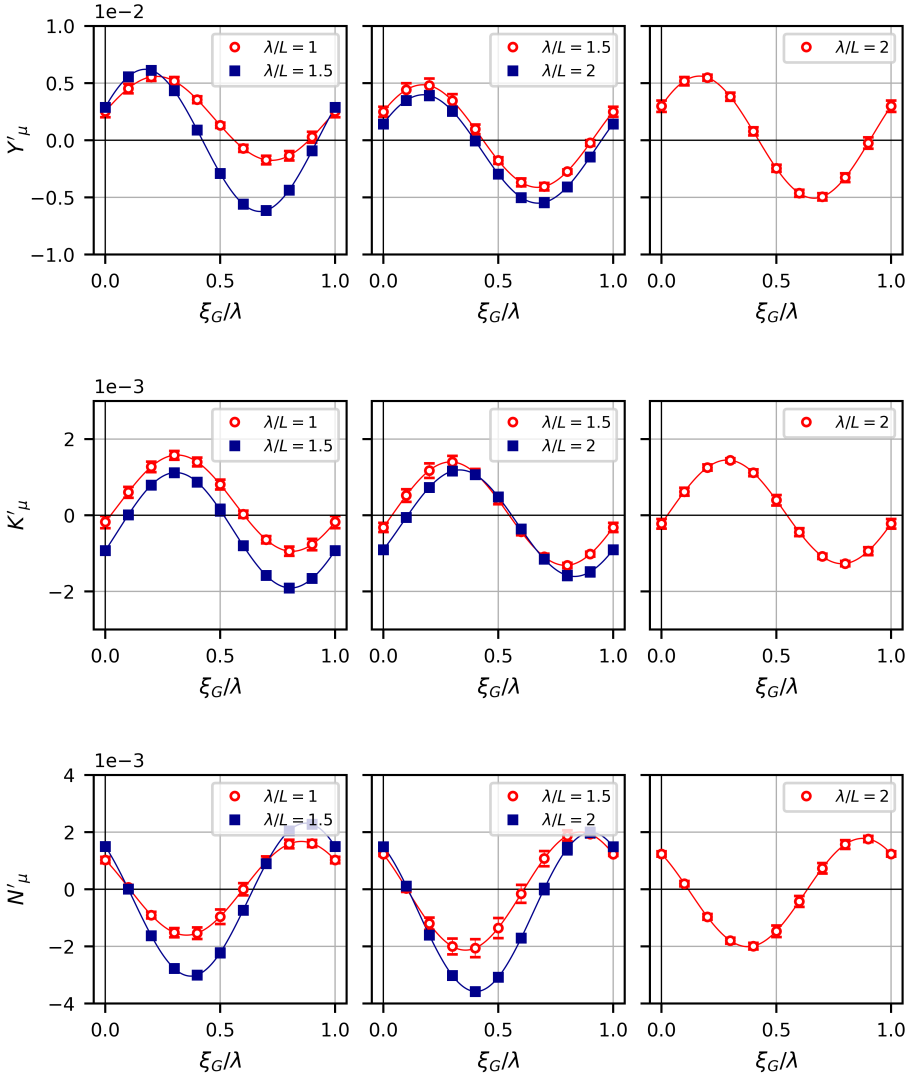

Figure 4.17: Non-dimensional wave induced coefficient Y'_μ (top), roll coefficient K'_μ (centre), yaw coefficient N'_μ (bottom) as a function of the ship location in the wave. Left column: $Fr = 0.38$; central column: $Fr = 0.48$; right column: $Fr = 0.58$; $H/\lambda = 0.06$.

4.4.3. SWAY INDUCED HYDRODYNAMIC COEFFICIENTS

Figure 4.18 shows the measured yaw moment due to sway as function of the non dimensional sway velocity v' for one case investigated and two locations in the wave.

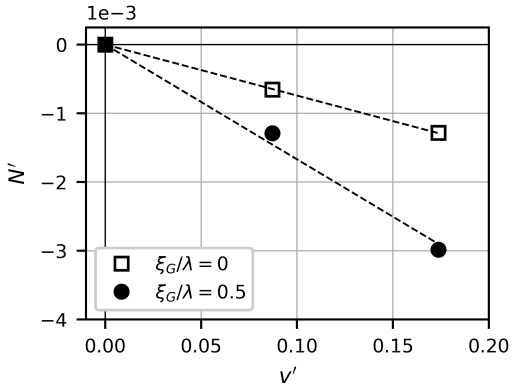

Figure 4.18: Measured yawing moment induced by the sway velocity and linear fitting plotted as function of the non -dimensional sway velocity v', for two locations in the wave. $\lambda/L = 1.5$, $Fr = 0.38$, $H/\lambda = 0.06$.

The sway induced coefficients obtained in regular following waves are shown in Figure 4.19. The results measured in waves are plotted together with the value measured in calm water at the correspondent speed (see Chapter 3, Section 3.4.1.

Similarly to the wave induced roll moment coefficient, K'_v is positive on the wave front, whereas it is negative on the back. This means that a drift motion on the wave front would increase the roll towards the direction of the sway motion; on the back the effect is contrary and the roll reduced by the sway velocity. The values of K'_v in calm water are within the range of the variation caused by the wave effect. However, differently to what found for the heel induced roll restoring coefficient K'_ϕ, the variations of K'_v due to the position in the wave are significant.

The values of the sway Y'_v and yaw N'_v hydrodynamic coefficients in waves are very different from the calm water ones. In both cases, the coefficients in waves are between 2 or 3 times the calm water ones. Both Y'_v and N'_v are maximum in absolute value near the surfing equilibrium location in the wave. This is important especially for the yaw moment coefficient N'_v. Near the wave front-through at portside-quartering direction, the waves cause the vessel to sway towards starboardside (see Section 4.4.2): this positive sway motion causes a negative yaw moment $N'_v v'$ that makes the vessel turn towards portside beam-to-sea. This is a destabilizing moment that is added to the wave yawing one.

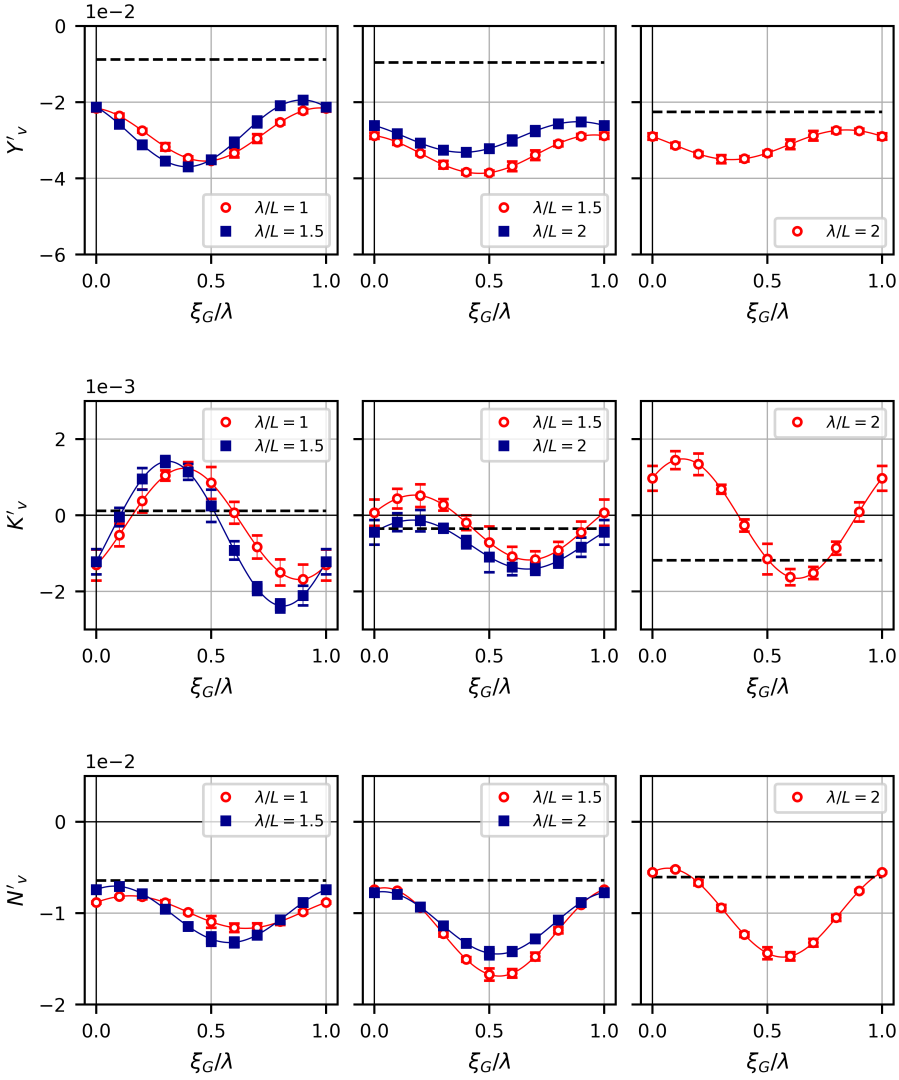

Figure 4.19: Non-dimensional sway velocity induced hydrodynamic coefficient Y'_v (top), roll coefficient K'_v (centre), yaw coefficient N'_v (bottom) as a function of the ship location in the wave. Left column: $Fr = 0.38$; central column: $Fr = 0.48$; right column: $Fr = 0.58$; $H/\lambda = 0.06$. The dashed black line denotes the value of the coefficients in calm water at the respective Froude number, taken from Chapter 3, Section 3.4.1.

4.4.4. HEEL INDUCED HYDRODYNAMIC COEFFICIENTS

The experiments of the heeled model were carried out for positive heel angles (model heeled to starboard). At each position on the wave the hydrodynamic derivatives were calculated by linearly fitting the loads measured as a function of the heel angle. Figure 4.20 depicts the fitting of the heel induced sway force and yaw moment on the front and on the back of the wave as function of the heel angle for one condition tested. The yaw moment is linear with the heel angle, whereas the sway force shows a slight non-linear behaviour over 10 degrees when the vessel is on the front of the wave. For simplicity, a linear fit of the loads was chosen in every position in the wave. A more accurate insight into the nature of the non-linear behaviour of the heel induced loads is still needed and must be object of future research.

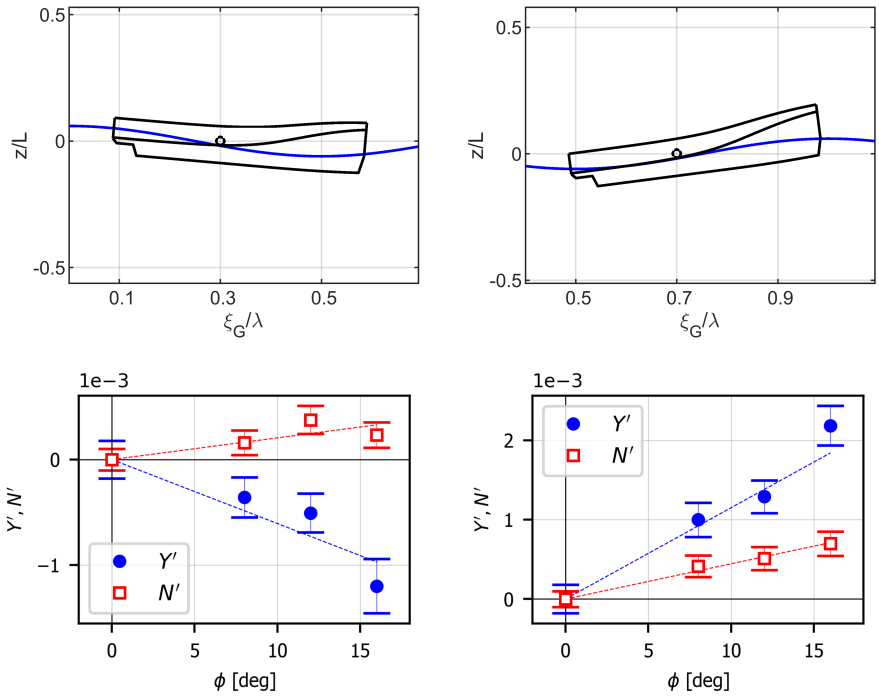

Figure 4.20: Non-dimensional sway force and yaw moment as function of the heel angle ϕ for two positions in the wave. Left column: the vessel is in the front of the wave ($\xi_G/\lambda = 0.3$); right column: the vessel is in the back of the wave ($\xi_G/\lambda = 0.7$). Plots refer to the case of $\lambda/L = 2$, $Fr = 0.47$; $H/\lambda = 0.06$.

The heel-induced coefficients are shown in Figure 4.21. The amplitude and the mean value of the sinusoidal signals of Y'_ϕ are larger for increasing values of Froude number. Between the lowest speed $Fr = 0.38$ and the other two higher speed cases $Fr = 0.48$ and $Fr = 0.58$, a phase shift of about half wave length was observed. The variations with respect to the calm water values are quite significant, see Chapter 3, Section 3.4.2. The

value of Y'_ϕ is mostly negative at $Fr = 0.38$ for all the locations ξ_G/λ, meaning that when heeled at starboard, the sway force is directed to port. For the higher speeds, the sign of Y'_ϕ changes from negative on the wave front to positive when the ship is located on the wave back.

At the forward speeds investigated, interesting for the vessel dynamics in the following sea, the hydrostatic component of the total roll moment K'_ϕ is dominant, as shown in Figure 3.8. The values of the total restoring roll moment K'_ϕ in waves are very close to the calm water ones in all the cases investigated, meaning that the wave has a limited effect on it.

Unlike the values of N'_ϕ in calm water that are negative for the speed range investigated, in following waves the heel-yaw coefficient changes sign. Whereas at $\mathrm{F}r = 0.38$ N'_ϕ is always positive for all the longitudinal locations in the wave, for the other two cases the coefficient is negative on the front of the wave, and positive on the back of the wave. Thus on the front of the wave a heel angle to starboard means that the coupling effect makes the vessel to turn to port. The opposite occurs on the through and the back of the wave.

The heel induced loads originate from the non-symmetrical hull submerged geometry and by the vertical position of the vessel in the wave. They are caused by the lift developed on the hull bottom, the Froude-Krylov, radiation and diffraction effects, and by more complex viscous phenomena such as the flow separation at the chine. Since only the total forces and moments are measured during a captive model experimental tests, it is very hard to examine the characteristics of these loads in detail. Advanced numerical simulations (CFD) might provide a better insight in the study of these loads.

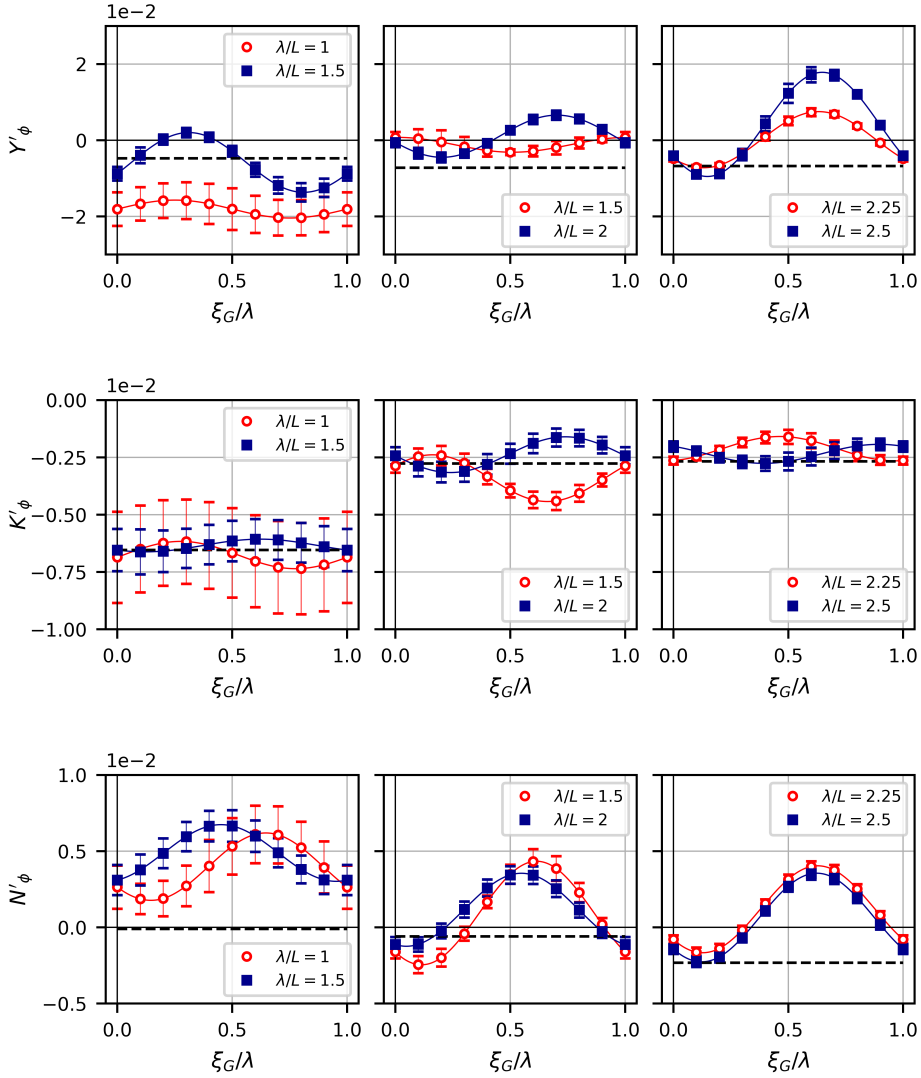

Figure 4.21: Non-dimensional heel-sway coupling hydrodynamic coefficient Y'_ϕ (top), total roll restoring coefficient K'_ϕ (centre), heel-yaw coupling hydrodynamic coefficient N'_ϕ (bottom) as a function of the ship location in the wave. Left column: $Fr = 0.38$; central column: $Fr = 0.48$; right column: $Fr = 0.58$; $H/\lambda = 0.06$. The dashed black line denotes the value of the coefficients in calm water at the respective Froude number, taken from Chapter 3, Section 3.4.2.

4.4.5. STEERING INDUCED COEFFICIENTS

The model of the SAR NH-1816 rescue boat was equipped with waterjets; Figure 4.22 shows a view of the stern of the model with the waterjets arrangement.

Figure 4.22: View of the waterjets arrangement of the NH-1816 model.

The objective of the tests with active waterjets was the estimation of the steering loads in following waves, and to ascertain the differences with the calm water case. The steering loads were in fact also measured in calm water. The RPM were set to match the calm water resistance and kept constant during the runs in waves.

Figure 4.23 shows the measured total steering lateral force provided by the waterjets for one case investigated in two locations in the wave.

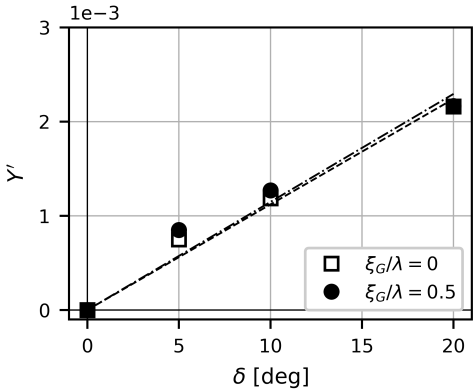

Figure 4.23: Measured sway force induced by waterjets steering and linear fitting plotted as function of the steering angle δ, for two locations in the wave. $\lambda/L = 2$, $Fr = 0.53$, $H/\lambda = 0.06$.

Figure 4.24 shows the hydrodynamic coefficient in sway Y'_δ, roll K'_δ and yaw N'_δ due to the action of the steering devices, in this case the waterjets. The coefficients were obtained by rotating the waterjets nozzles at different δ, up to 20 degrees. Only two cases were investigated for this stage.

Differently from the hull loads coefficients, the waterjets coefficients are barely affected by the presence of the wave, because they are very close to the calm water values

along all the locations in the wave. This means that the waterjets are very effective also in the seaway: the orbital velocities induced by the presence of the wave have a minimum effect on the force provided by the waterjets. This would not be the case for usual appendage control devices such as rudders: in waves the rudder lift can fluctuate because of the wave induced effects, and in some unfortunate cases they can also ventilate [6].

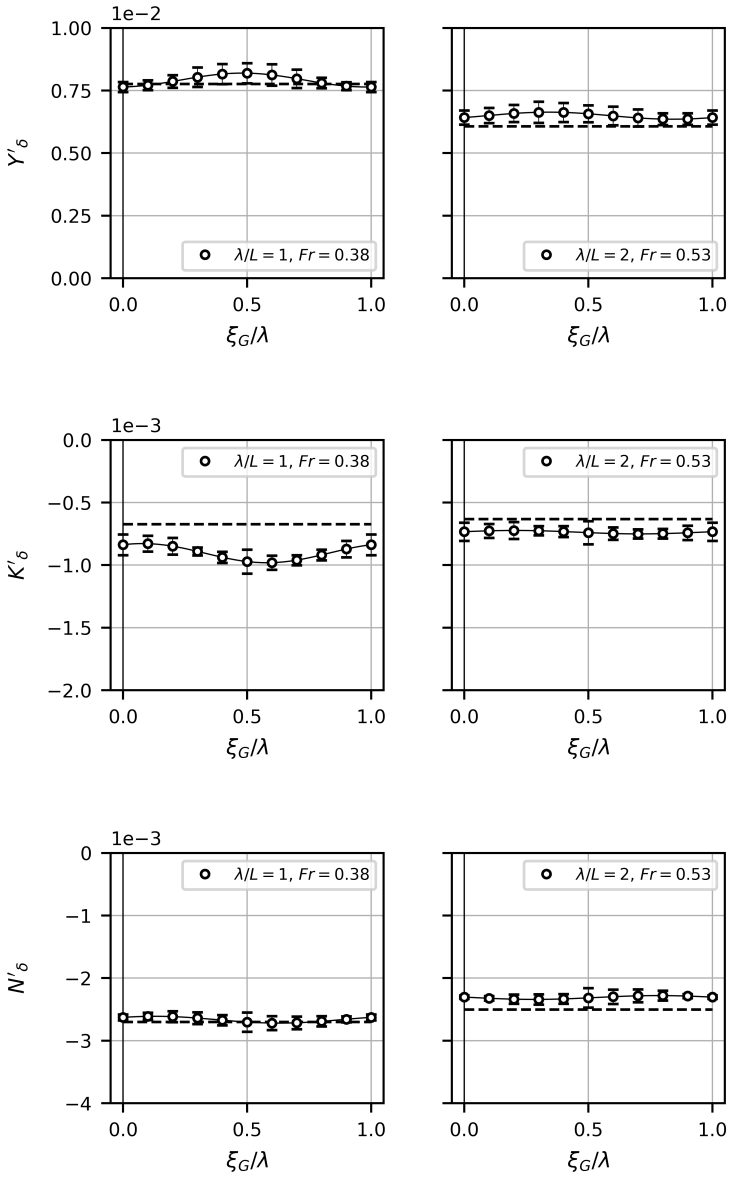

Figure 4.24: Steering induced coefficients Y'_δ (top), K'_δ (centre) and N'_δ (bottom) for all the test cases investigated. The left column refer to $Fr = 0.38$ and the right column to $Fr = 0.53$; $H/\lambda = 0.06$.

4.5. CONCLUDING REMARKS

THE main manoeuvrability characteristics of the SAR NH-1816 craft were measured by means of captive model tests in regular following and stern-quartering waves. The experimental campaign consisted of two parts, one at the towing tank of TU Delft Ship Hydromechanics Laboratory towing tank and one at the Seakeeping and Manoeuvring Basin of MARIN. The experiments covered several combinations of ship forward velocities and wave lengths, in order to describe the manoeuvrability loads over the widest possible range of conditions that may occur in the following sea and cause a dynamic instability. The wave steepness H/λ was kept constant at 0.06, because that was the upper limit for the regularity of the wave generation. From the experimental data the hydrodynamic coefficients were obtained as a function of the location of the vessel in the wave ξ_G/λ for all the cases investigated.

As a general observation, the hull and wave terms are highly dependent on where the vessel is located along the wave, and they are less affected the wave lengths and Froude number. Moreover, the hull coefficients in sway and in heel are significantly different from the calm water values at the correspondent forward speed: this means that a calm water characterization of the high-speed craft manoeuvrability does not apply in waves. This is not valid for the waterjets steering coefficients: Y'_δ, K'_δ and N'_δ are barely affected by the presence of the wave and they are very close to the respective value in calm water.

The coefficients N'_μ and N'_v are both negative and maximum in absolute value in the location where the vessel is more likely to surf on the wave. They both have a destabilizing effect, increasing the rate of turning towards the beam-to-sea position in the following waves. On the contrary, N'_ϕ is positive in that position, meaning that if the vessel rolls in the same direction of the wave propagation. This has a stabilizing effect against the undesired yawing motion. These considerations are preliminary: they must still find a confirmation through free sailing numerical simulations, together with the effects of the other coefficients.

As already mentioned in Chapter 3 and in the Introduction, the coefficients induced by the yaw velocity are hard to obtain in following waves. Experimental investigations on this effect must be object of future research.

The variability of the coefficients is governed by very complex hydrodynamic phenomena, connected to the wave dynamics and the non-linear viscous effects on the hull, such as flow separation at the chine or transom, wave making and spray generation. To the purpose of a better investigation of the phenomena, detailed analysis of numerical simulations should be carried out. This would give a deeper understanding of the shape of the hydrodynamic coefficients in waves.

From an experimental point of view, the latter objective is hard to achieve. Global forces and moments are measured during a captive model tests, and the hydrodynamic insights can not be estimated directly. However, the experimental technique shown in Section 4.2 developed to evaluate the heel induced loads, can be utilised to obtain more detailed information about the loads acting on the ship in waves. In fact, being able to perform model oscillations in waves, would make possible to describe certain trends of variation of the coefficients with respect to different velocities and orientations.

These detailed investigation of the hydrodynamics acting on the hull is not the object of this thesis. The terms evaluated in this chapter will be used to implement and validate

the 3D BEM tool (see Chapter 2) meant to predict the manoeuvrability-in-waves of high speed craft and their vulnerability to dynamic instability in the following sea. The next chapter will deal with this task.

5

THE NUMERICAL SIMULATION OF THE CAPTIVE MODEL TESTS

The manoeuvrability loads acting on the high-speed craft due to the effects of the wave, the sway velocity, the heel of the vessel and the steering devices were estimated by means of captive model tests in regular following and stern-quartering waves. One of the objective of those experiments was to implement and validate the capabilities of the numerical methods to predict such loads in a reliable manner. In this chapter, a three-dimensional Boundary Element Method (also known as panel method or BEM) was utilised to reproduce the experimental captive tests numerically in order to compare the numerical and measured outcomes. Whereas the forces and moments from the incoming wave are predicted by the potential flow BEM well, some corrections to this tool are needed to compute correctly the manoeuvrability loads acting on the hull due to the sway velocity and the static heel. The comparison between numerical and experimental results and the procedure to correct the manoeuvrability loads is shown.

5.1. INTRODUCTION

THE objective of the experimental campaigns shown in the previous chapters was to understand the characterisation of the manoeuvrability loads acting on the high-speed craft NH-1816 sailing in calm water and in following waves. The experiments were carried out over a range of wave lengths and vessel forward speeds: the results of the tests in waves shown in Chapter 4 were carried out over 5-6 combinations of Fr and λ/L. This allowed a rather extended description of the ship manoeuvring loads, with respect to waves external conditions and speeds.

In this chapter, the data collected during the experiments are used to formulate an empirical description of the ship manoeuvring loads. Every hydrodynamic coefficient is expressed as function of Fr and λ/L. Thanks to these formulations, the manoeuvrabil-

Parts of this chapter have been published in the Journal of Marine Science and Technology [51] and are under review at Ocean Engineering [78].

ity loads were extrapolated also in other conditions not investigated during the experiments. Although this can seem unnecessary in a deterministic "regular waves" view of the problem, in realistic scenarios (irregular sea states) the combination of "local" wave length and height and the forward speed change constantly. The numerical tools must be able to cope with this variability. Therefore, it is very important to describe the loads acting on the ship over the widest range of conditions that are expected in sea operations.

The empirical description of the manoeuvrability coefficients is function of Fr and λ/L. Another important factor that influences the ship loads in waves is the wave steepness. Unfortunately, due to experimental towing tank limitations, the model tests were carried out at a single value of steepness: $H/\lambda = 0.06$ was the upper limit for the realisation of good quality regular waves. In the next chapter, the effect of varying the wave steepness on the manoeuvrability coefficients will be treated numerically.

The empirical description of the manoeuvrability loads is implemented into the BEM simulation tool. The wave induced loads are expected to be predicted satisfactorily by boundary element methods, since the Froude-Krylov pressures are well described by the potential flow theory, and are computed over the actual wavy submerged geometry. The same cannot be said for the manoeuvrability loads, that are governed by other complex non-linear and viscous effects: flow separation at the chine and transom, wave making, among the others. The manoeuvrability of ship is particularly sensitive to the distribution of hydrodynamic pressure on the hull: because of the lack of mass restoring term on the horizontal plane, even the smaller inaccuracy in the computation of the hydrodynamic loads can lead in some cases to large prediction errors.

Therefore, the computation of the manoeuvrability loads in sway and heel by means of the BEM are corrected keeping into account the experimental results. The captive model tests were reproduced numerically, and the BEM prediction was corrected taking into account the differences with the measured results.

The Froude-Krylov force and moment were not corrected, since the BEM can predict them well. The yaw velocity induced loads were estimated only numerically and in calm water, and thus they are not considered in this chapter. The steering loads of the waterjets are not influenced by the presence of the waves. Thus, the numerical and experimental values of the steering coefficients are compared only in calm water.

The procedure of the ship manoeuvring loads in waves is shown in Section 5.2. The comparison between experimental and numerical results is shown in Section 5.3 for some of the conditions investigated; Appendix B includes the complete comparison between experimental and numerical data also in other conditions not tested during the experiments. The manoeuvrability coefficients obtained by the numerical prediction are calculated over a larger number of combinations of Fr and λ/L.

5.2. EMPIRICAL DESCRIPTION OF THE SHIP LOADS IN WAVES

AN empirical description of the manoeuvrability coefficients in following regular waves is proposed in this section. The coefficients were obtained up to 6 combinations of vessel Froude number and wave lengths; these results can be interpolated and extrapolated to other conditions different from the cases considered in the captive model tests.

For this purpose, it is useful to express concisely the coefficients in waves using only

few parameters, i.e. the amplitude, the mean value and the phase, as shown in Figure 5.1. Those terms can be obtained by the least square fitting of their sinusoidal signal as functions of the location of the ship in the wave ξ_G/λ. Each coefficient can be then expressed as in Equation 5.1, with the term N'_v taken as example.

$$N'_v = a'_{N_v} cos(2\pi\xi_G/\lambda + \varphi'_{N_v}) + \bar{\eta}'_{N_v} \tag{5.1}$$

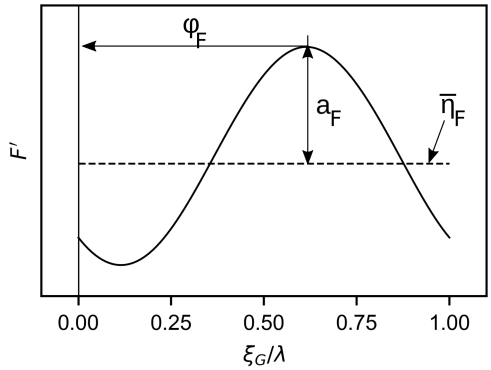

Figure 5.1: The amplitude a, phase φ and mean value η are depicted for a generic sinusoidal term F'.

Each of these terms can be plotted as a function of the Froude number and wave length, i.e. for every condition tested. The values of amplitude, phase and mean of the experimental cases can be fitted using a plane as shown in Figure 5.2. Thanks to this plane, each parameter of the coefficients, amplitude, phase and mean value, can be expressed using the plane polynomial coefficients p_0, p_1 and p_2. As example, the amplitude a'_{N_ϕ} is formulated in Equation 5.2:

$$a'_{N_\phi} = p_0 Fr + p_1 \lambda/L + p_2 \tag{5.2}$$

Using this formulation, the coefficients can be expressed over a larger number of combinations of Fr and λ/L, other than the 6 experimental conditions. A planar fit was chosen as first approximation of the coefficients in waves: as shown in Chapter 4, the variation of the manoeuvrability coefficients due to different wave length or forward speed are small enough to consider the planar fit satisfying.

This empirical description was used to correct the mathematical BEM described in Chapter 2. The captive model tests are reproduced numerically at the same conditions tested in the experiments. Similarly to what done for the model tests results, the coefficients obtained numerically with the BEM can be used to define a numerical description by fitting the data with a plane as done in Figure 5.2. The differences between the *experimental* and *numerical* plane fits are calculated and used to correct the 3D BEM in every Fr - λ/L combination other than the experimental cases.

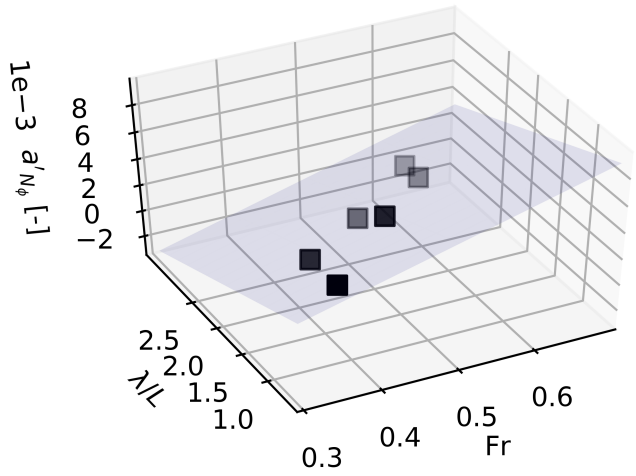

5

Figure 5.2: Planar fit of the amplitudes of the manoeuvrability coefficient N'_ϕ. The black squares are the experimental values; the grey plane fits these data within the domain of Fr and λ/L.

This correction allows a (although imperfect) reasonable agreement with the experimental results over a wide range of forward speeds and wave lengths. The correction in fact depends on how well the terms are distributed over the plane, and on how the initial numerical coefficients are different from the experimental description. The complete numerical-experimental comparison of amplitude a, phase φ and mean value η is shown in Appendix B, for the coefficients induced by the waves, the heel and the sway velocity of the vessel. In Appendix B the polynomial terms of the plane fit are also given, for coefficients induced by sway velocity and static heel.

5.3. VALIDATION OF THE VESSEL LOADS NUMERICAL COMPUTATION

THE 3D BEM was used to reproduce the captive model tests described in Chapter 4 numerically. In the simulations, the vessel was able to move in heave and pitch, assuming its natural vertical attitude on the wave, while the other motions in surge, sway, roll and yaw were set to zero. This was done in a similar fashion as in the captive model experiments carried at the TU Delft and in the SMB of MARIN.

The results are presented in terms of wave loads in surge, sway, roll and yaw, and in the hydrodynamic coefficients induced by sway velocity, static heel and the steering action. For each term only one condition tested is shown; a more complete overview of the outcomes in all the numerical conditions is shown in Appendix B. The following results are presented in this section:

- the wave loads;
- the steering induced loads;

- the sway velocity induced loads;
- and the heel induced loads.

5.3.1. THE WAVE LOADS

The wave loads are computed using the 3D BEM considering the Froude-Krylov pressures on the actual wavy submerged geometry. Since the wave exciting forces originate from potential flow hydrodynamic effects, boundary element mathematical methods are expected to predict these loads with good accuracy. Figure 5.3 shows the numerical and experimental wave loads, confirming the initial expectations. Some discrepancies can still be observed, especially in the roll moment; however, the 3D BEM provides a reasonable prediction of the excitation by the waves. The computation of the wave forces and moments will not be corrected, considering the reasonable results of the 3D BEM. This is valid also for the values of the wave induced coefficients over the conditions not tested during the experiments, as shown in Appendix B.

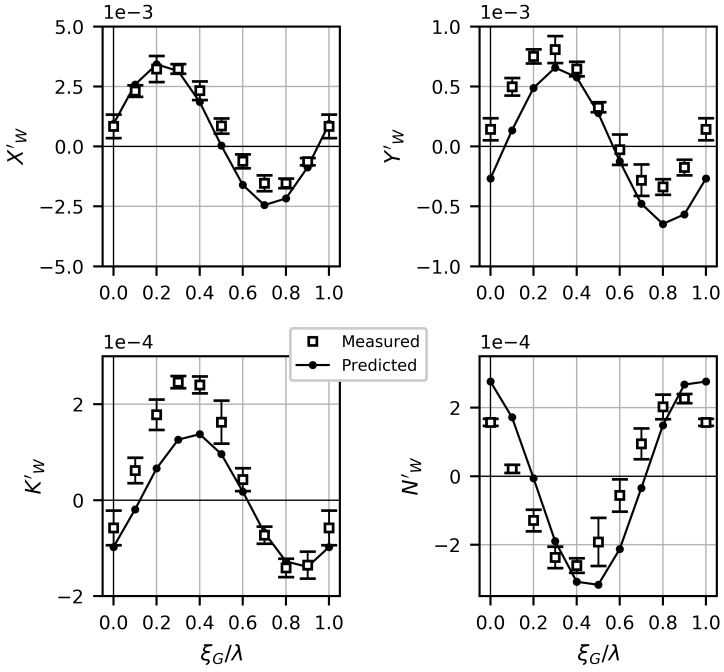

Figure 5.3: Comparison between experimental and numerical wave surge, sway forces and roll, yaw moments. Condition: $\lambda/L = 1$; $Fr = 0.38$; $\mu = 10$ deg; $H/\lambda = 0.06$.

5.3.2. THE STEERING-INDUCED LOADS

The steering loads in sway, roll and yaw provided by the waterjets installed on the NH-1816 craft are computed according to a semi-empirical mathematical model summarised in Equations 2.15 to 2.18, in Chapter 2, Section 2.4.1. The experiments in following waves

(see Chapter 4) showed that the waterjets loads are not influenced by the presence of the wave. The sinusoidal oscillations due to the incoming wave are negligible; the hydrodynamic coefficients due to the steering action in wave are very similar to the ones in calm water at the respective forward velocities. Therefore, the experimental results are compared with the numerical simulations only in calm water, because this represents well the steering characteristics in waves. Figure 5.4 shows the hydrodynamic coefficients Y'_δ, K'_δ and N'_δ, that represent the loads derivative with respect to the steering angle δ.

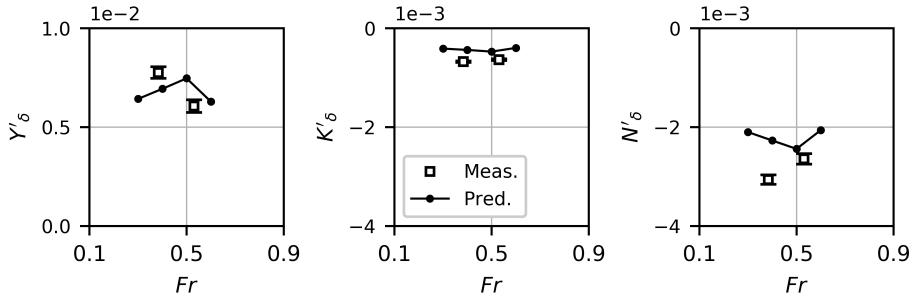

Figure 5.4: Comparison of the experimental and numerical values of the coefficients Y'_δ, K'_δ and N'_δ obtained in calm water as a function of Froude number.

5.3.3. THE SWAY VELOCITY INDUCED LOADS

Much more difficult than the previous contributions it is to accurately predict the forces and moments caused by a sway velocity, using potential methods. The forces and moments acting on hard-chine craft due to sway velocity are governed by complex phenomena such as wave making effects, separations at the chine and at the transom. The presence of the wave increases the complexity of the phenomena acting on the hull. The results of the predictions obtained using the 3D BEM were corrected to account for the differences between the numerical and experimental captive tests, as explained in Section 5.2. A comparison between the corrected BEM and the experimental sway hydrodynamic coefficients is shown in Figure 5.5. The complete comparison of the numerical and experimental results in the conditions not tested during the experiments is shown in Appendix B.

When a free running ship is sailing in following waves it is subjected to large fluctuations in its velocity - known as surging. In extreme cases the ship is forced to travel at wave speed, known as surf-riding. As discussed above, surf-riding is a prerequisite of broaching-to. It is very important that the 3D BEM is also capable of predicting the change in the hydrodynamic loads due to forward speed. The captive tests were performed at constant forward speed; then a good match between experimental and simulated model tests in principle is not enough to predict the behaviour of the vessel when it is freely running in the following sea, because the effect of the variation of speed must be taken into account. Figure 5.6 depicts the comparison between the numerical and experimental coefficients Y'_v, K'_v and N'_v in calm water as a function of Froude number over the speed range investigated. The comparison shows that the 3D BEM can quali-

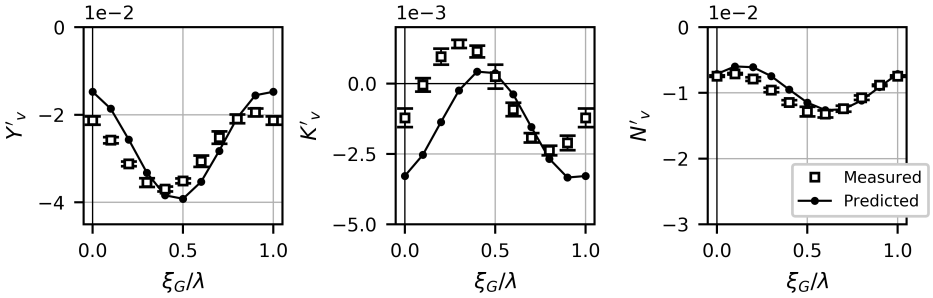

Figure 5.5: Sway velocity induced coefficients in sway, roll and yaw. Comparison between the measured experimental coefficients and the predicted numerical results. $\lambda/L = 1.5$; $Fr = 0.38$; $H/\lambda = 0.06$.

tatively predict the trend of the hydrodynamic coefficients with respect to the forward velocity.

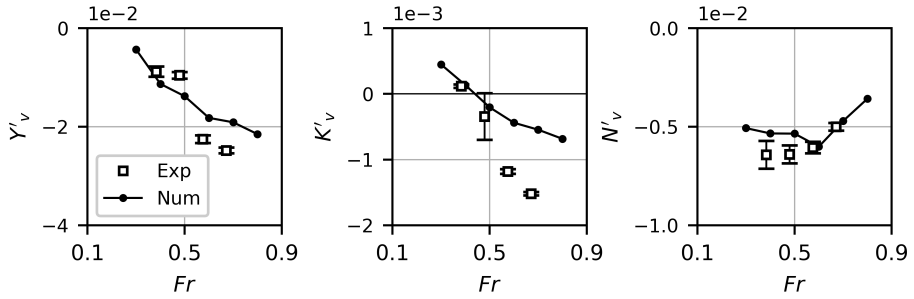

Figure 5.6: Comparison of the experimental and numerical values of the coefficients Y'_v, K'_v and N'_v obtained in calm water as a function of Froude number.

5.3.4. THE HEEL INDUCED LOADS

Also the heel induced manoeuvrability coefficients were corrected to account for the experimental results, as described in Section 5.2. The comparison between experimental and corrected numerical coefficients is shown for one test condition in Figure 5.7; the complete comparison of the conditions not tested during the experiments is shown in Appendix B.

Contrary to what can be expected for the sway velocity induced loads, the effect of the forward speed on the heel induced terms is not significant. As shown in Chapter 4, Section 4.4.4, the heel induced coefficients obtained in calm water are smaller in absolute value than the values measured in waves. This means that the influence of the forward speed is negligible with respect to the effect of the waves. Moreover, the heel restoring moment is mainly caused by the hydrostatic pressures, that are well predicted by numerical tools.

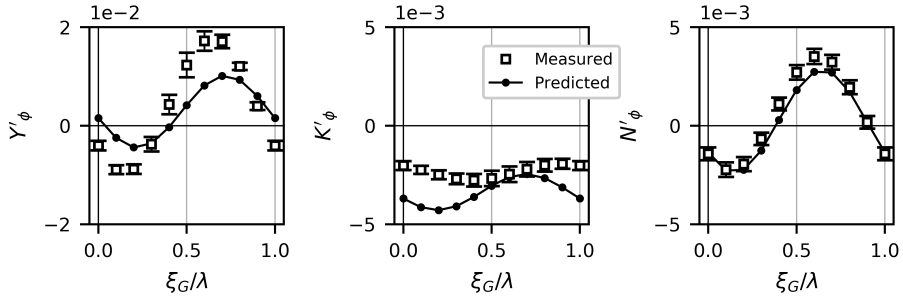

Figure 5.7: Static heel induced coefficients in sway, roll and yaw. Comparison between the measured experimental coefficients and the predicted numerical results. $\lambda/L = 2.5$; $Fr = 0.57$; $H/\lambda = 0.06$.

5.4. CONCLUDING REMARKS

THE manoeuvrability loads in waves on the hard-chine craft SAR NH-1816 were measured by means of captive model tests in following and stern-quartering waves at the towing tank of TU Delft and at the Seakeeping and Manoeuvring Basin of MARIN, in Wageningen. The results of the experiments, presented in Chapter 4, were used to tune a 3D time domain potential flow BEM. The capability of this mathematical tool in the prediction of the loads in waves was verified for the experimental conditions and also over a wider range of forward speeds and wave lengths, different from the conditions investigated experimentally. This was aimed to allow a reliable numerical prediction of the ship loads over the widest possible conditions that are interesting for the vulnerability assessment of dynamic instability in following seas. The complete overview of the results is reported in Appendix B.

It was assumed that the loads acting on the ship sailing in waves had a sinusoidal shape as the regular wave excitation. Such hypothesis is valid under the assumption of linearity between the wave excitation and the resulting loads. This is a reasonable assumption for the manoeuvrability loads at low incidences angles. The ship coefficients were therefore expressed using three fundamental parameters: amplitude, phase and mean value. This was a handy and easier formulation of the manoeuvrability terms over a wide range of ship speed and wave combinations. A more extended use of this approach is foreseen in the continuation of the research on this topic and on the study of the broaching phenomenon in irregular, realistic sea states.

The 3D BEM can predict the wave induced Froude-Krylov force and moment well. Also the steering loads are predicted well by the semi-empirical model implemented into the simulation tool. On the other hand, the manoeuvrability loads caused by the sway velocity and the static heel of the vessel need to be corrected in order to match the measured results.

This analysis and the correction applied to the computation of the manoeuvrability loads increases the confidence that the 3D BEM is able to simulate the behaviour of high speed craft in waves not only *qualitatively* but also *quantitatively*. However, it has to be noted that for a proper validation of the mathematical tool, numerical simulations of the free running vessel manoeuvring-in-waves should be compared with full scale or

free-running model data.

Further investigations are required to improve the numerical prediction of the forces caused by the sway velocity and the heel of the vessel. As already mentioned in Chapter 3 and 4, the yaw velocity induced terms must be still investigated with experimental techniques. The forces and moments due to the yaw velocity are taken into account in the 3D BEM, but these numerical outcomes must still be validated.

6

THE ONSET OF DYNAMIC INSTABILITY IN FOLLOWING SEAS

The last chapter of this thesis investigates the effects of the steering qualities of the SAR NH-1816 on the inception of broaching when the craft is sailing in following and stern-quartering waves. The behaviour of the vessel is simulated by means of a 3D time domain potential flow BEM in the time domain. In the previous chapter, the 3D BEM was validated by the captive model tests in regular waves carried out at TU Delft and at MARIN. The effect of the vessel static heel, the course keeping and turning ability of the high-speed craft were investigated. It was shown that the static heel in stern-quartering waves tends to decrease the vulnerability to broaching for the rescue boat SAR NH-1816 under investigation. Afterwards, four different designs of the NH-1816 with modified steering and course keeping characteristics were analysed: an increase in the directional stability or in the steering effectiveness of the craft is beneficial to avoid dynamic instabilities, although they have different consequences on the dynamics of the vessel in the following sea.

6.1. INTRODUCTION

As its first aim, this thesis aims to describe the loads acting on the high-speed craft when manoeuvring in calm water and in waves. This task was accomplished in Chapters 3 and 4. These loads were used to check and correct the capabilities of the 3D BEM simulation tool in predicting the manoeuvrability loads, as described in Chapter 5. The numerical prediction of the sway velocity induced components of the total loads was corrected keeping into account the empirical results. The second aim is to understand the effect of the loads acting on the hull have on the inception of dynamic instability events in following seas, namely broaching-to. This latter objective will be the subject of this chapter.

Parts of this chapter have been published in the Journal of Marine Science and Technology [51] and are under review at Ocean Engineering [78].

As already explained in the Introduction, the latter objective formulated above is the result of a long-standing debate in the naval architecture community. Broaching-to and surf-riding are known phenomena that threaten the survival of certain types of ships in particular sea state scenarios. The characteristics of these phenomena have been studied and analysed throughout the last 50 years. However, it is still not clear why some vessels are more unstable than others. The answer to this question must be sought thinking about the inherent characteristics of the controllability of a vessel.

Designers and researchers have been debating about the most important factors causing a broach. As first approximated approach, reported by Renilson [6, 16] and in more recent years by De Jong et al. [26], the steering devices effectiveness was considered predominantly important in a dynamic instability inception in the following sea. The effect of the other manoeuvrability characteristics, namely the sway and yaw loads induced by the motions and velocity components of the vessel, was neglected. Due to the complexity of these aspects, the hull manoeuvrability of fast vessel is in fact hardly considered during the design.

In common manoeuvrability research, the hull directional stability, quantified by the index C' [48], is one of the most important parameters meant to judge the controllability of a ship. It is not clear to which extent the level of directional stability of a vessel could affect the broaching behaviour. This question is particularly interesting when considering high-speed craft: as shown in Figure 3.14, Chapter 3, the SAR NH-1816 presents a negative C'_ϕ (directional stability index which accounts also for the heel induced loads), meaning intrinsic hull directional instability. This can be a common feature for small, fast craft, because the ability to turn and perform tight manoeuvres can be an undeniable property. The question is whether this characteristic can cause a poor dynamic behaviour in the following sea. The objective of this chapter is to solve the ambiguity of the contribution to the inception of broaching-to between the turning ability of a fast craft and its inherent hull directional stability.

The first aspect investigated in this chapter is the heel-sway-yaw hull hydrodynamic coupling, an aspect rarely considered in manoeuvrability research [49]. The heel induced loads in sway and yaw are considered and their effect on the broaching behaviour of the vessel is assessed. In Chapter 3, the effect of the heel-coupling hydrodynamic coefficients Y'_ϕ and N'_ϕ was estimated in calm water standard manoeuvres (Turning Circle and Zig-Zag). These terms have significant consequences on the calm water dynamics; in a seaway these consequences could be even amplified, since the vessel in waves experience larger roll angles. The effect on this hydrodynamic coupling was already investigated by previous researchers, showing contradictory results. In [79], Renilson and Manwarring used the heel-yaw and heel-sway coupling loads obtained experimentally in calm water for a fishing trawler to assess their effect on the inception of broaching-to. The outcomes showed that the heel induced loads increase the likelihood of broaching-to. Hashimoto et al. [50] measured the heel induced loads in steep following waves for a fishing trawler, proving that the heel induced loads have the consequence of stabilizing the ship contrarily to what found in [79]. In this Chapter the experimental results of the captive-heeled model tests in following waves were considered, extending the research in [50] to a higher number of wave and vessel speed conditions.

The course keeping and turning ability of a vessel are representative of its manoeu-

vrability performance. These characteristics are well described by the terms in sway and yaw. The second part of this chapter presents a sensitivity analysis is performed by changing these two craft features by modifying the hull and steering coefficients, and therefore their role during the inception of broaching-to events is determined. The sensitivity analysis is carried out considering four different designs. The course keeping and turning ability of a vessel are usually predicted in an early design phase for the calm water case; from a designer point of view, the information provided by a connection between this simple characterisation and a more complex description in the seaway would be extremely valuable to improve the vessel dynamic stability in an initial design phase.

In order to assess the dynamic instability of a vessel, such events must be defined precisely. Many definitions of broaching-to were given in the past; in the naval architecture community, an univocal quantitative definition of broaching-to has not been formulated yet. Section 6.2 contains an attempt to clarify this aspect and the definition of broaching-to used in the continuation of this chapter is given.

As already explained previously, some manoeuvrability parameters of the high-speed craft are considered and their effect on the broaching dynamics is studied. Many free-sailing vessel simulations are carried out, for different wave and initial forward speed conditions. The combinations in which a broaching occurs highlight the so-called *broaching zone*. The plots of the broaching zones were firstly conceived by Nicholson [15], with the aim to show in which experimental conditions of a free-sailing model test a broaching had occurred. The broaching zone plot was used later on in other several works as a very powerful tool to visualise the vulnerability of a ship to the following sea dynamic instability events. [18, 19, 21, 26, 34, 50]. A broaching zone allows to assess the broaching behaviour of a vessel with respect to the main parameters involved, typically the vessel speed, the wave length and the wave steepness. In this chapter, the broaching zone approach is used to compare the broaching behaviour of the vessel for each of the four different manoeuvrability designs.

6.2. DEFINITION OF BROACHING-TO

BROACHING-TO was described qualitatively in the Introduction of this thesis. The action of the waves, the yaw turning, the drift and the steering devices have different consequences on the resulting motions of the vessel, and they act together during the realisation of a broach. The understanding of each single contribution to the total vessel dynamics is important to describe in detail an instability event.

In order to assess the behaviour of the high-speed craft in the following sea, it is necessary to define the instability phenomena that are important for this study, namely surf-riding and broaching-to. Earlier in this thesis the qualitative definitions of such phenomena were given; however, it is necessary to formulate criteria to detect instabilities event during a numerical simulation.

In the past, several authors gave a definition of broaching-to. Renilson et al. [16, 80] and more recently De Jong et al. [26, 34] quantified a broach as the situation in which the yaw velocity, r, and the yaw acceleration $\dot{r}$, are of the same sign, while the steering angle, δ, is at the maximum value in the direction opposite to the yaw motion, and the change of ship's heading angle ψ is higher than 20 degrees. This definition is summarised in Equation 6.1.

$$\delta = \delta_M, \quad r > 0, \quad \dot{r} > 0, \quad \psi > 20 deg \tag{6.1}$$

Umeda et al. in [17, 27], gave a slightly different definition of broaching-to, without including the threshold on the ship heading. This is shown in Equation 6.2.

$$\delta = \delta_M, \quad r > 0, \quad \dot{r} > 0 \tag{6.2}$$

The reason for this definition is that a broach is recognised by the mariners by their inability to counteract the involuntary increasing yawing motion of the vessel, without considering the amount of such turning motion quantified by the change in heading. The choice of a threshold on the minimum heading variation appears to be quite arbitrary in such events.

In the present study the definition of Equation 6.2 was used. In the majority of the cases, a broach that occurs according to the criteria in Equation 6.2 also leads to a significant change in the heading angle. In some cases, during the numerical simulations those criteria are met but for a very short interval of time, after which the vessel regains his initial stable status. Therefore, also a minimum time duration threshold was considered to properly detect a broach. As a rule of thumb, an interval of 2 seconds was chosen.

Also surf-riding was detected and defined, in order to distinguish the case where surf-riding is occurring from the broaching events. The definition of surf-riding is simpler: the vessel, that is initially travelling slower than the waves, is captured by the following wave and thus accelerated to its celerity [26, 36]. A surf-riding event is detected when the vessel forward speed is greater or equal than the wave celerity.

In extreme situations a capsize due to broaching-to could occur, and this is coherently detected as the other phenomena. A capsize is detected when the roll amplitude

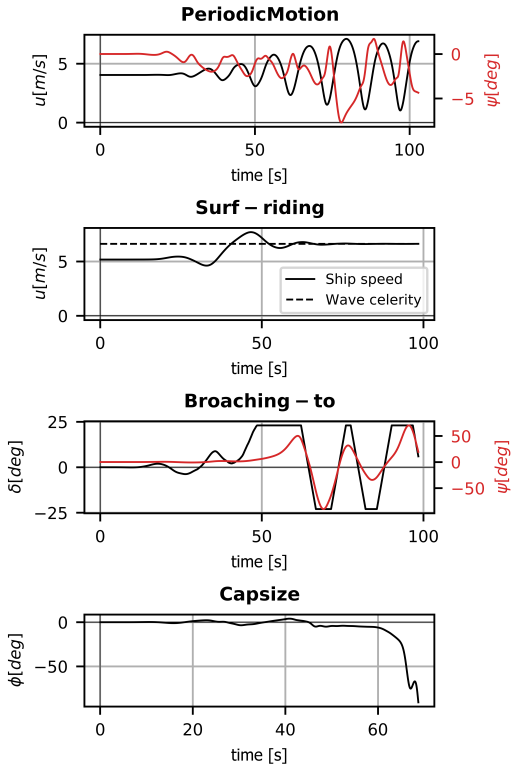

Figure 6.1: Four examples of possible phenomena occurring in following seas: periodic motion (non-occurrence of a dynamic instability event), surf-riding, broaching-to and capsize.

becomes larger than 90 degrees. It has to be noted that operators would consider lower roll angles unacceptable for safe operations. A value of 90 degrees represents the threshold of a total loss of the vessel.

When none of the aforementioned events occurs, a ship experiences only periodic motions in waves. The definitions used hereby to detect the surf-riding, broaching-to, capsize and periodic motions in the numerical simulations are summarised in Table 6.1. Figure 6.1 shows an example of typical time histories for each of these events.

Figure 6.2 shows a qualitative sketch of how a broach happens in quartering waves from starboard, in terms of the main motions, forces and moments involved. The vessel experiences a broach starboard to side-quartering regular waves. More details are given in Figure 6.3, showing the simulated time histories of the main variables of the vessel freely sailing in the following sea, for the rescue boat SAR NH-1816. The signs of the motions and of the loads involved in the dynamic phenomenon are important to estimate the single contributions of the quantity involved.

Dynamic Instability	Definition
Periodic motion	None of the previous conditions occurs
Surf riding	$Ucos(\mu) \geq c$
Broaching-to	$\delta = \delta_M$, $r > 0$, $\dot{r} > 0$, $t_{broach} > 2$ s
Capsize	broach and $\phi > 90$ deg

Table 6.1: Criteria for the detection of the main dynamic instabilities in the following sea. A periodic motion denotes the non-occurrence of a dynamic instability event in the following sea.

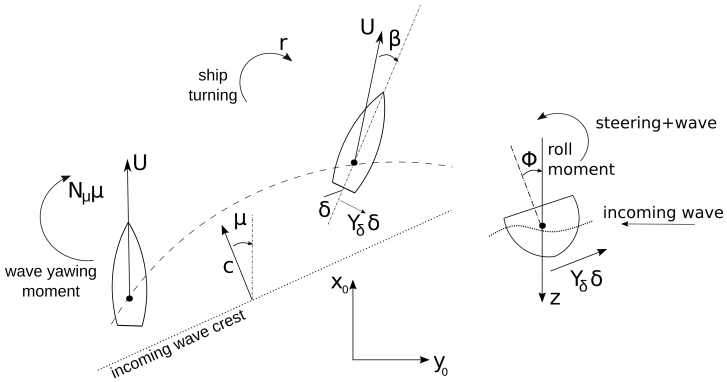

Figure 6.2: Schematic reproduction of the motions and loads acting on the a vessel during a common broaching-to event. The wave yawing moment $N_\mu\mu$ causes the vessel to turn with velocity r, to drift at an angle β in the same direction of the wave propagation direction. The steering devices counter-act this destabilising yaw turning, but at the same time increase the roll caused by the incoming wave, because rudders or waterjets are usually located below the centre of gravity of the ship.

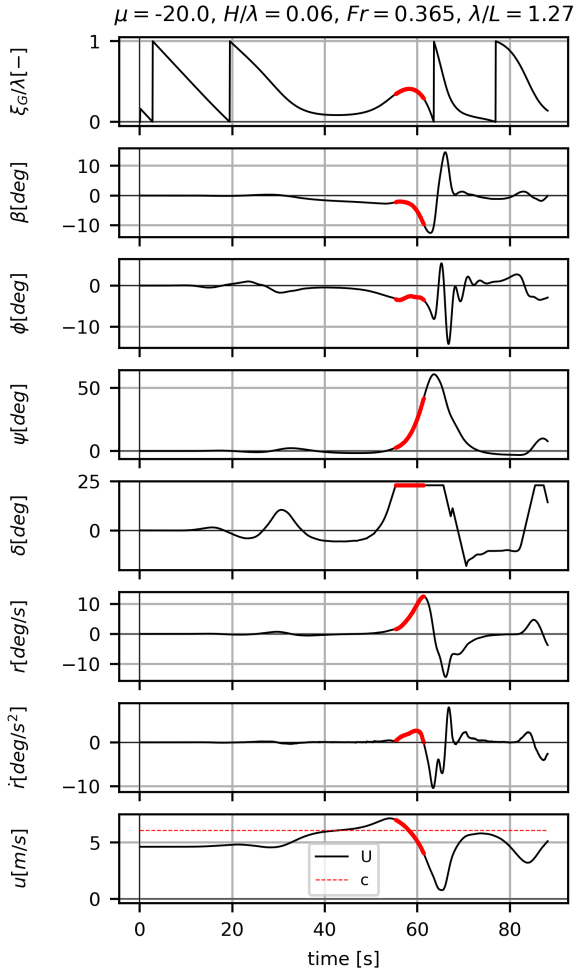

Figure 6.3: Time histories of the SAR NH-1816 freely sailing in starboard-quartering regular waves; the simulation constant parameters are summarised on the top of the picture. A broach occurs around 60 seconds after the start of the simulation and lasts for about 5 seconds: this time interval is highlighted in red in the plots. This picture shows (starting from the top): the longitudinal location in the wave ξ_G/λ, the drift angle β, the heel angle ϕ, the ship heading ψ, the steering angle δ, the yaw velocity r and acceleration $\dot{r}$, total speed U and wave celerity c. The location of the craft in the waves is near the wave front before the broaching event: a surf-riding is in fact occurring and preceding it, being U very close to the wave crest celerity c. The broach starts: ψ, r and $\dot{r}$ increases, while the waterjets are at the maximum opposite deflection. The drift and roll of the craft are both negative, meaning that the vessel is drifting in the same direction of the wave propagation and rolling outwards its turning trajectory.

6.3. NUMERICAL SIMULATIONS

FREE-SAILING vessel simulations are carried out in the time domain by means of the 3D BEM described in Chapter 2, Section 2.4. The motions and the forces are expressed according to the reference frame in Figure 2.1, Chapter 2. The SAR NH-1816 hull is discretised with quadrilateral flat panels; a semi-empirical transom flow condition [73, 81] is implemented at Froude numbers greater than 0.4. This condition corrects the hydrodynamic lift evaluated by the BEM at the transom, that must be equal to the atmospheric pressure when the transom is dry. Potential flow tools such BEMs are not fully capable to simulate flow separations, thus making empirical corrections necessary.

The vessel is initially running in its vertical equilibrium condition while the waves are ramped-up. The propulsion rate is kept constant during the entire simulation. The initial heave and pitch, the wave ramp-up factor, the propulsion rate and the other important simulation parameters are chosen in such a way to have the smoothest start and not to alter the final outcomes of the simulations. This was made sure by a preliminary sensitivity analysis of the main input parameters of the numerical simulations, namely time step, wave ramp-up period, speed, initial location in the wave. A small change of these parameter provoked only small changes in the simulation outputs.

The angle of the steering devices is automatically set by the autopilot equation given in Equation 6.3 and already introduced in Chapter 2.

$$\delta = b_{\delta\psi} r + c_{\delta\psi} \psi \tag{6.3}$$

The autopilot is meant to keep the initial course direction of the vessel correcting the deviation in heading ψ and its rate of change r, but not the relative incidence angle with the wave direction. The main characteristics of the vessel steering are shown in Table 6.2.

Steering parameters	Symbol	Value
Autopilot proportional coefficient	$c_{\delta\psi}$	3 deg/deg
Autopilot damping coefficient	$b_{\delta\psi}$	9.49 deg/(deg/s)
Steering rotation velocity	$\dot{\delta}$	10 deg/s
Maximum steering angle	δ_M	23 deg

Table 6.2: Summary of the main steering parameters of the waterjets of the SAR NH-1816 craft. These characteristics are taken by the previous work of De Jong et al. [26] for the same vessel.

The manoeuvrability forces and moments induced by the stationary heel and the sway velocity predicted by the 3D BEM are corrected keeping into account the experimental results, as explained in Chapter 5. After the correction over a wide domain of wave lengths and ship forward speeds (see Appendix B), the 3D BEM can be used to evaluate these loads reasonably well. However, the captive model tests in regular waves were carried out at a constant steepness $H/\lambda = 0.06$, judged as the highest limit to generate good quality waves. Dynamic instability events are more frequent at steeper waves: therefore, it is preferable to perform simulations at a steepness higher than 0.06. The 3D BEM takes into account the effect of steepness for the computation of the wave and

hydrodynamic loads. Also the correction of the manoeuvrability loads must keep into account of different steepness.

A generic force in wave can be seen as a sinusoidal curve function of the term ξ_G/λ, as shown Figure 5.1, Chapter 5. Then, every sinusoidal curve has its own amplitude, mean value and phase with respect to the exciting wave: a modification of wave steepness has the effect of changing these parameters. The effect of the wave steepness on the manoeuvring loads can be significant, especially on the loads caused by sway velocity, since the change in the submerged geometry is large, hence greatly affecting the distribution of the pressure over the hull. Figure 6.4 shows the predicted effect of the steepness on the amplitude and mean value of the hydrodynamic coefficient N'_v. A change of wave steepness affects only the amplitude and the mean value of the loads, not the phase. The effect of the wave steepness variation is computed by the 3D BEM for the wave and yaw velocity induced loads, and it is taken in account into the correction of the sway velocity and heel induced loads.

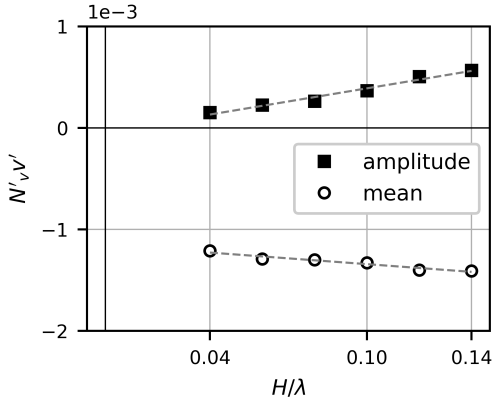

Figure 6.4: Amplitude and mean value of one wave length signal of the sway velocity induced yaw moment as function of the wave steepness. The values are obtained by means of numerical simulations, for the condition of $\lambda/L = 2$, $Fr = 0.48$.

6.4. THE EFFECT OF THE HEEL INDUCED LOADS

IN Chapter 3 the effect of the heel induced loads on the manoeuvrability of the rescue boat NH-1816 in calm water was investigated. The analysis was carried out simulating two standard manoeuvres, Turning Circle and Zig-Zag 10/10, that showed that the stationary heel of the craft had a stabilising effect that resulted in a larger Turning Circle diameter and a longer Zig-Zag period (see Figures 3.17 and 3.18, Chapter 3). The effect of heel on the inception of dynamic instability events in following waves was already discussed in past research [50, 79], showing contradictory results. It is therefore still necessary to assess clearly how important is the effect of the heel in the broaching dynamics.

In order to investigate the effect of the heel induced sway force and yaw moment on the likelihood of broaching of the high-speed craft, a series of free sailing vessel simula-

tions in regular stern-quartering waves were performed numerically in the time domain using the 3D BEM. The investigation covers 7 vessel initial forward speeds equally spaced between $Fr = 0.3$ and $Fr = 0.6$; for each speed 8 wave lengths are considered, between a minimum of $\lambda/L = 0.6$ and a maximum of $\lambda/L = 3.0$, resulting in 56 total conditions.The wave steepness coincides with the value used in the experiment, $H/\lambda = 0.06$, and the initial wave heading angle μ is equal to -20 degrees in all the conditions simulated. Those ranges were chosen to highlight a well defined broaching zone.

The effect of the heel induced loads is analysed by comparing the broaching zones within the range of the conditions examined with and without the utilization of the heel coupling terms Y'_ϕ and N'_ϕ. In the latter case, the coupling terms were set to zero by correcting the numerical captive tests outcomes. A similar approach of the numerical computations correction described in Chapter 5 was used. The results are presented in Figure 6.5.

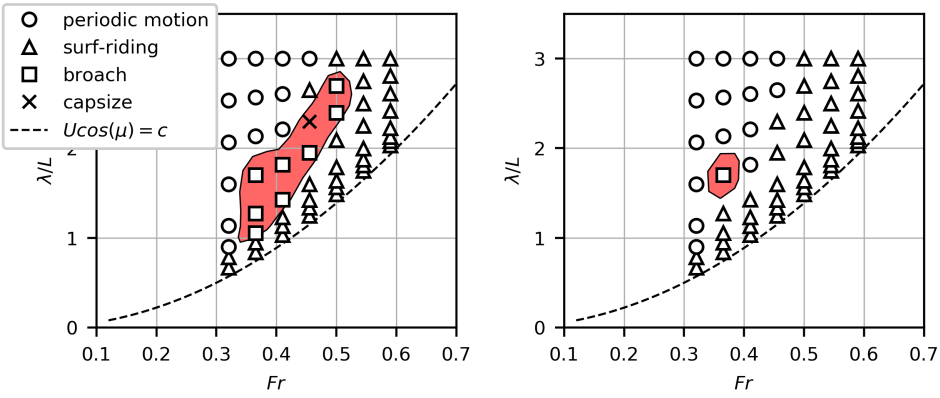

Figure 6.5: Broaching zone of the high-speed craft for $\mu = -20$ deg and $H/\lambda = 0.06$. Left: without heel-induced loads; right: with heel-induced loads. The red area identifies the broaching region.Simulations were carried out above the $Ucos(\mu) = c$ line, i.e. where the waves are faster than the initial speed of the vessel.

Figure 6.5 shows that the heel induced sway force and yaw moment stabilise the high-speed craft, reducing the likelihood of dynamic course instability events. In the conditions considered, that are not extreme, broaching-to inception builds-up during the surf-riding phenomenon: in this situation the vessel location is in the wave downslope near the through at $\xi_G/\lambda = 0.4 - 0.5$. This is confirmed by the results shown in Section 4.4.1, Chapter 4. Although the coefficient N'_ϕ changes sign along the wave, at the surf-riding position it is positive in all the conditions considered. According to the ship frame depicted in Figure 2.1, Chapter 2, when the waves act at quarter-starboard the vessel starts yawing towards starboard beam-to-sea, while heeling towards port. The heel being negative and the heel-yaw coupling coefficient positive, this results in a negative yaw moment caused by the vessel heel that counter-acts the positive destabilising moment.

As said, the conditions are not extreme but for the cases investigated the maximum roll of the vessel can reach values up to 50 deg. In one simulation without heel-sway-yaw coupling coefficients, the SAR NH-1816 experiences also a capsize. In the case without

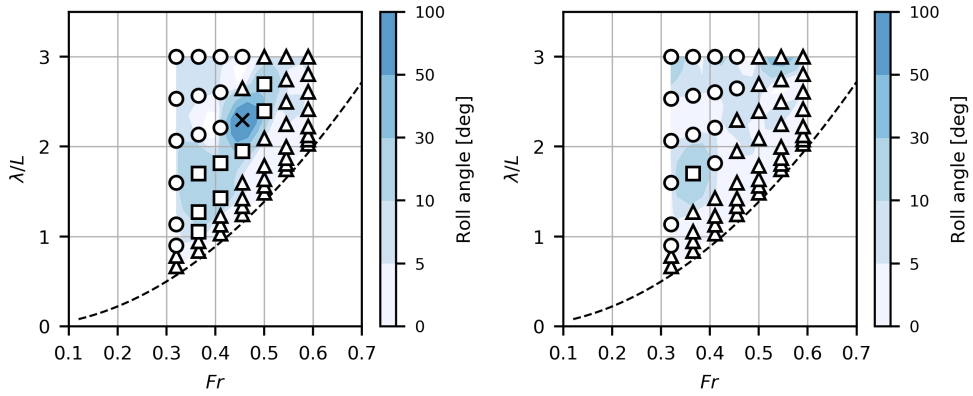

Figure 6.6: Contour plots of the maximum heel angle reached during the simulations by the SAR NH-1816, for the same simulations and conditions depicted in Figure 6.5. On the left, the simulations without heel induced terms; on the right, the simulations with heel induced terms.

heel induced coefficients, the roll angles are smaller; this can be explained by the fact that being the vessel more stable, the lateral motion and therefore also the roll are more moderate. Figure 6.6 shows the contour plots of the maximum roll angles computed during the simulations. The numerical time histories with and without the heel coupled coefficients are shown in Figure 6.7.

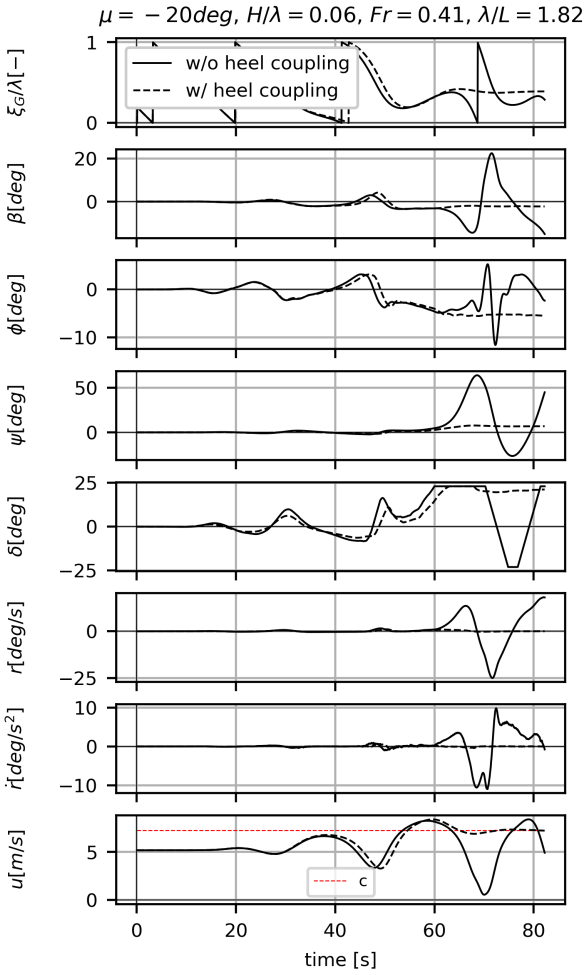

Figure 6.7: Plots of the main time histories of one simulation in stern-quartering waves of the SAR NH-1816. The continuous lines refer to the simulation without heel-induced loads where broaching-to occurs after 60 s; the dotted lines refer to the simulations with heel-induced loads, where the ship experiences only a surf-riding. The simulation conditions are summarised on the top of the plot. Without the terms Y'_ϕ and N'_ϕ, a broaching event occurs; with them the vessel manages to keep its equilibrium experiencing only a surf-riding.

6.5. THE EFFECT OF THE COURSE KEEPING AND TURNING ABILITY OF THE HIGH-SPEED CRAFT

FROM the previous analysis, it has been shown that the static heel induced loads contribute to making the vessel less vulnerable to the inception of broaching-to. This effect is similar to what can be observed in calm water: the heel has the effect of stabilizing the vessel thus reducing its ease to turn. This analysis suggests that the loads due to the terms Y'_ϕ and N'_ϕ cannot be neglected for a reliable prediction of the vessel motions.

However, it is hard to say how this information can be used by designers to improve the dynamic stability of the vessel in following waves. Allowing the vessel to reach higher heeling angles is obviously not an option.

From a design point of view, it is important to know which counter-action to utilise to avoid or at least mitigate the dynamic instability of the vessel. Usually, modifications to the manoeuvring of ships are applied to the appendage stern configuration, because it is the most effective way to enhance the steering quality of a vessel. The effect of such modifications on the roll characteristics of the vessel are usually considered to be secondary. Therefore, in this section the main characteristics of the manoeuvrability of a vessel in terms of sway and yaw dynamics are analysed, and their effect on the inception of broaching-to is assessed.

As done in Chapter 3 for the calm water case, the most important steering qualities of the high-speed craft are analysed. They can be summarised as in the following:

- the ability to maintain the desired course with the minimum steering effort after a disturbance (course keeping ability);
- the ability to change heading quickly and in a limited amount of longitudinal displacement (turning ability).

In this work, these two different, but related, aspects of the manoeuvrability of high-speed craft have been investigated in relation to their effect on the inceptions of broaching phenomena in stern-quartering waves. The elements investigated independently are:

- the directional stability; and
- the effectiveness of the steering devices.

Both these elements will affect the steering qualities identified above, and hence these were varied independently to study their effect on the inception of broaching in stern-quartering seas. The effectiveness of the steering can be modified by increasing the total steering force provided by the control devices. The directional stability of the high-speed craft was modified by considering the well-known index C [48], already defined in Chapter 3 and reported in the following Equation 6.4:

$$C' = N'_r Y'_v - (Y'_r - m')N'_v \tag{6.4}$$

The investigation is made up of four different designs, that originate from the bare hull of the NH-1816. Each of the designs have different directional stability and steering ability and are denoted as follows:

A. The bare hull of the NH-1816 is considered without modification;

B. The directional stability of the NH-1816 was improved by artificially modifying the linear hydrodynamic coefficients due to sway velocity Y'_v, N'_v and due to yaw velocity Y'_r, N'_r;

C. The steering ability of the vessel was improved by artificially increasing the steering side force, resulting in greater coefficients Y'_δ, K'_δ and N'_δ;

D. Both the directional stability and steering ability were improved at the same time.

For the designs B and D, the coefficients Y'_r and N'_v were decreased by 25%, and N'_r and Y'_v were increased by 25%. Also the roll coefficients K'_v and K'_r were increased by 25%, in order to realistically simulate the roll dynamics. The percentages of modification were chosen as to simulate the presence of the skegs, i.e. a condition of bare hull with appendages. The appendages were not added directly in the simulations in order to avoid the induced effects due to the fluctuations of the forward speed and the presence of the wave. In designs C and D the steering coefficients Y'_δ, K'_δ and N'_δ were increased by 25%. These percentages have been chosen to simulate a feasible increase of steering force available to the ship. A summary of the main aspects of the four designs is given in Table 6.3. Although present in the numerical simulations, the heel induced coefficients Y'_ϕ and N'_ϕ were not modified as the other coefficients. For the purpose of this section, only the modification of the more classic sway-yaw dynamics was taken into consideration to relate the dynamic stability of the high-speed craft to its steering qualities.

It must be noted that the modification of the coefficients was realistic but not physical. The hull coefficients were changed without considering a relative change in hull form, or an addition of appendages. The steering force was increased without considering the effect that a bigger sized rudder would have on the surge dynamics of the vessel, or that an increase in the waterjet steering forces would be achieved only by accelerating and increasing the waterjet impeller rate. The surge dynamic of the vessel was not modified so that it was possible to make a net comparison between different steering qualities of the vessel, disregarding the induced modifications on the vessel that would have an influence on the ship behaviour at sea.

Design A	**Design B**
No coefficients variation	Y'_v, N'_r increased by 25% Y'_r, N'_v decreased 25%
Design C	**Design D**
Y'_δ, N'_δ increased by 25%	Y'_v, N'_r increased by 25% Y'_r, N'_v decreased by 25% Y'_δ, N'_δ increased by 25%

Table 6.3: Scheme of the four manoeuvrability designs with relative coefficients variation.

Simulations in regular starboard-stern-quartering waves for the four designs were carried out at constant steepness $H/\lambda = 0.08$, for a range of Froude numbers from 0.32 and 0.59, and wave lengths from 1 to 3.5 ship lengths. The vessel autopilot was set to keep the initial heading of $\mu = -20$ degrees to the wave direction. The choice of these parameters was determined by the need of highlighting a clear and rather extended broaching zone. A too high or too low steepness would have not made the effect of the different manoeuvrability characteristcs visible.

The results of this analysis are presented in Figure 6.8. As done in Section 6.4, the results are visualized through graphs of the combinations of ship forward speed and wave

length. The broaching zone contains the conditions where a broach has occurred.

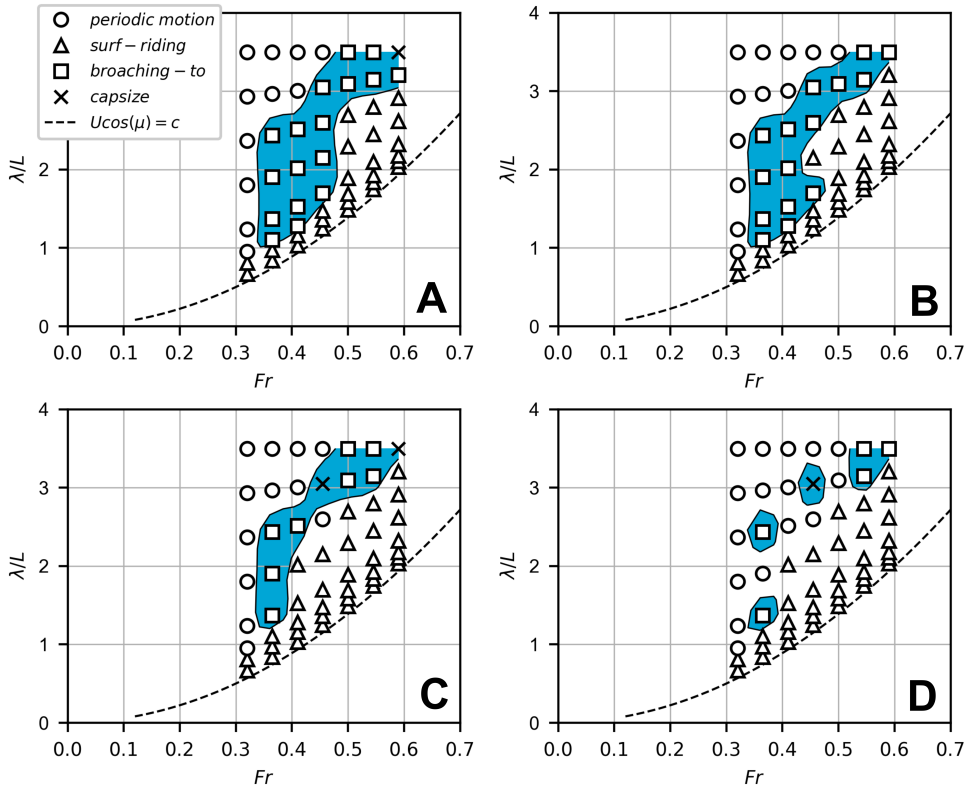

Figure 6.8: Broaching zone plots for the four designs A to D. The occurrence of broaching is highlighted within the coloured region; periodic motion, surf-riding, broaching-to and capsize are denoted with different symbols. Simulations were carried out above the $Ucos(\mu) = c$ line, i.e. where the waves are faster than the initial speed of the vessel.

Design A is the base condition of the bare hull vessel, showing a rather extended broaching zone covering almost the entire range of wave lengths and speeds simulated. Both the design with the increase in directional stability (B) and the design with the increased steering ability (C) show a reduced broaching zone. Design C has a smaller broaching zone than Design B, suggesting that, in this case, increasing the steering ability has a greater effect on reducing the broaching tendency than increasing the directional stability. However, a greater steering force would induce a roll moment in the same direction of the ship roll during the broaching-to inception, increasing the risk of capsize. This could happen in accordance with the autopilot specified in Equation 6.3, that is set-up to correct the ship heading but not the rate of heeling. The combination the two (Design D) results in a greater improvement. This suggests that a design with both increased steering effectiveness and increased directional stability would reduce the tendency of the vessel to broach in a following and stern-quartering sea even further.

6.5.1. DISCUSSION

From the results of Figure 6.8, it can be seen that an increase in the directional stability and the steering ability are both beneficial to reduce the broaching tendency of the high-speed craft in following and stern-quartering waves. However, the increase in directional stability produces a limited benefit when compared to the increase in steering ability, particularly at lower speeds and at the corresponding lower wave lengths.

Figure 6.9 shows the comparison of the simulation time histories in the same condition for the three Designs A, B and C. The starting speed of the vessel corresponds to $Fr = 0.41$ and the wavelength to ship length ratio is 1.53. Although the broach takes more time to build-up for the case with the increased directional stability (B), with respect to the other two cases, the increase in directional stability does not prevent a broach occurring. For higher initial forward speeds and the longer waves, the design with the increased steering ability (Design C) does not show the same benefits that are present at lower speeds and lower wavelengths. This is because the waves are longer and higher and thus are more powerful, and an increase in steering force alone is not capable of fully counteracting the wave induced yawing moment.

Figure 6.10 shows a comparison of the simulation time histories for the three Designs A, B and C, but this time at a higher initial forward speed corresponding to $Fr = 0.5$, and a longer wavelength corresponding to a wavelength to ship length ratio of 3.5. For this higher initial forward speed, it is possible to observe that the design with enhanced steering is less effective: the unstable region of Design C at higher Froude numbers is comparable with the region of Design B.

Figure 6.11 shows a comparison of the simulation time histories for Design B, C and D. The initial forward speed corresponds to $Fr = 0.41$ and the wavelength to ship length ratio is 2.51. As with the conditions shown in Figure 6.8, broaching occurs less for Design D: broaching occurs at both Design B and C but not for Design D.

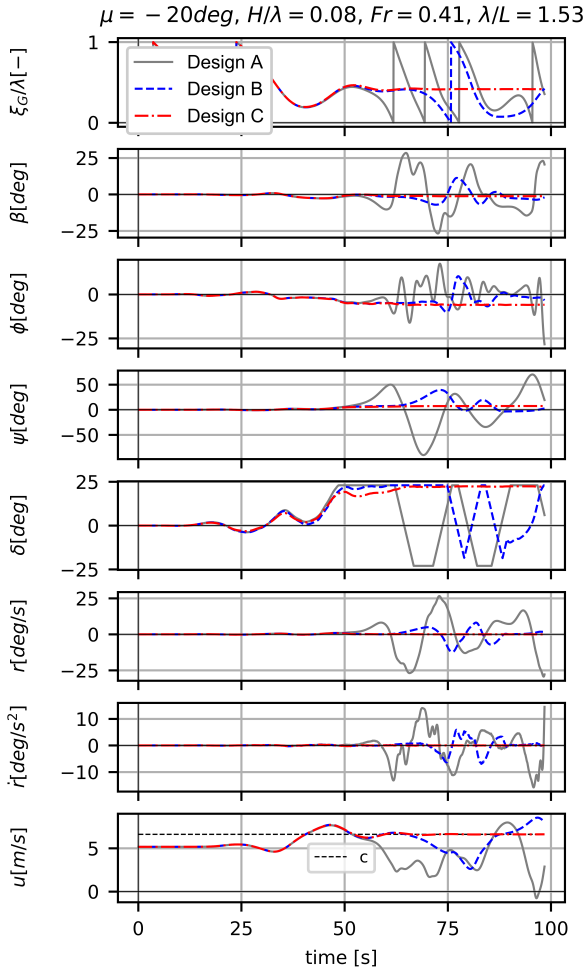

Figure 6.9: Comparison of the time histories of a numerical free-sailing run between Design A (original), Design B (increased directional stability) and Design C (enhanced steering ability). The initial vessel forward speed corresponds to $Fr = 0.41$ and the non-dimensional wave length to 1.53. The other constant simulation parameters are summarised on the top of the picture. Design A shows a rather quick inception of broaching-to, that occurs around 60 seconds after the start of the simulations. Design B also experiences a broach, but the increase of turning rate and heading deviation is retarded (it occurs 10 seconds later than the original Design A) and the turning acceleration is significantly lower. Design C instead managed to keep it course and surf-rides on the wave, only.

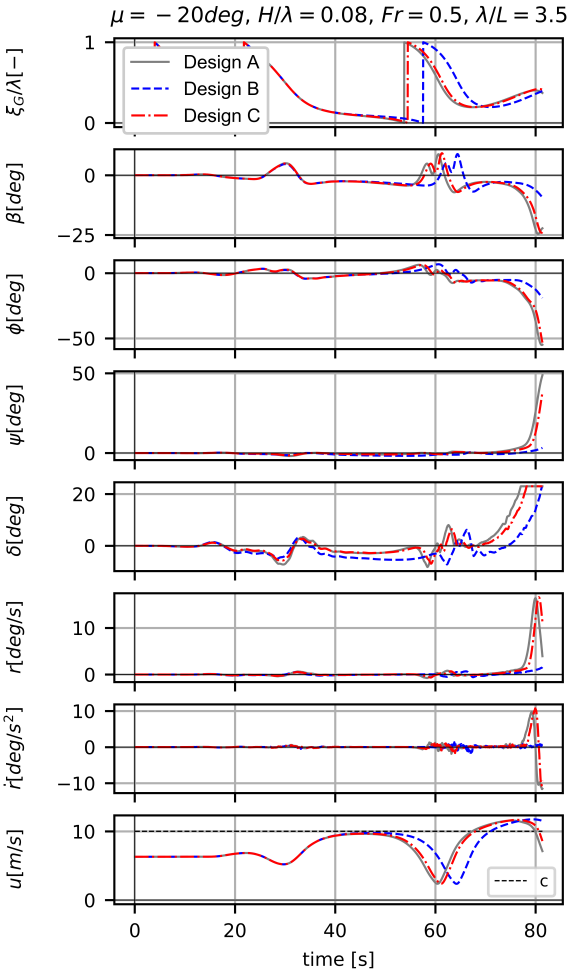

Figure 6.10: Comparison of the time histories of a numerical free-sailing run between the Design A (original), Design B (more course stable) and Design C (enhanced steering ability). The initial vessel forward speed corresponds to $Fr = 0.5$ and the non-dimensional wave length to 3.5. The other constant simulation parameters are summarised on the top of the picture. In this case the waves are longer, higher and more powerful. Broaching-to occurs for the design A and C: it is extremely quick, the drift angle β, the roll angle ϕ and the yaw turning velocity r reach frightening large values. The Design B instead does not experience the same instability; the vessel is sailing at high-speed thus being more directionally stable. At the very end of the simulation the heading starts to increase but it is retarded with respect to the other two cases and at significantly smaller turning acceleration.

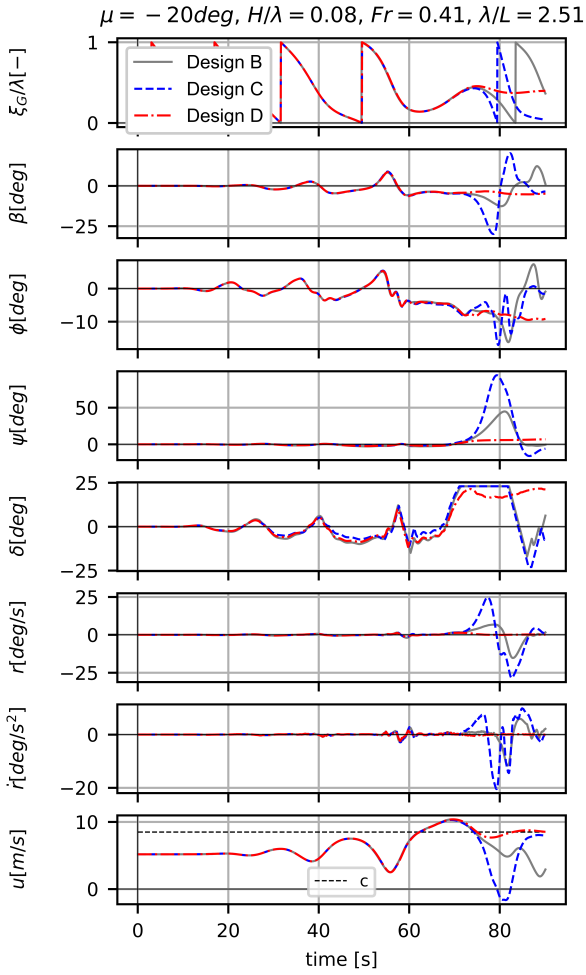

Figure 6.11: Comparison of the time histories of a numerical free-sailing run between the Design B (more course stable), Design C (enhanced steering ability) and Design D (both enhanced directional stability and turning effectiveness). The initial vessel forward speed corresponds to $Fr = 0.41$ and the non-dimensional wave length to 2.51. The other constant simulation parameters are summarised on the top of the picture. Broaching-to occurs for the designs B and C. The yaw turning rate and yaw turning acceleration of Design B is considerably lower than Design C. Design D is more effective: only a surf-ride occurs.

Design B does not show significant improvements with respect to the original design; however, a larger directional stability results in milder yaw turning velocity and accelerations. Design C is more effective, but the occurrence of broaching-to can be extremely quick. Design D appears to be the optimal design solution.

For the results presented above, the capabilities of the vessel have been modified assuming a realistic change in directional stability that would be expected due to the addition of skegs. To investigate this issue in more detail, the effect of directional stability was investigated by modifying the linear coefficients to improve the vessel directional stability further.

Figure 6.12 shows the three different C-indexes in calm water as function of Froude number. These indexes were obtained by modifying the sway and yaw velocity induced coefficients by 25% as done previously, obtaining the index C_1, and further by 50%, obtaining index C_2. The original design, C_0, has negative C-index, meaning that the vessel is course unstable in calm water.

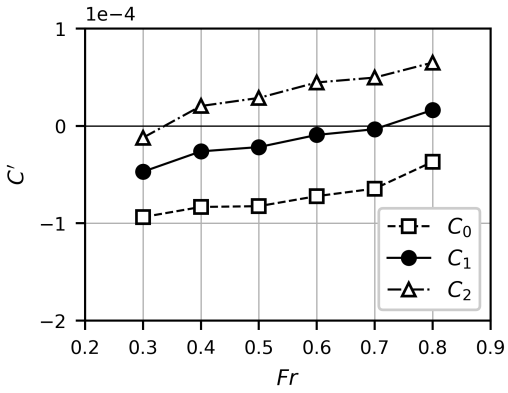

Figure 6.12: Comparison of the C-index in calm water as function of the Froude number. The values are obtained by modifying the linear coefficients in sway and yaw towards a more directionally stable hull.

Figure 6.13 shows a comparison of broaching-to vulnerability of the designs obtained with the progressive changes of the manoeuvrability coefficients, resulting in the three different directional stability indexes C_0', C_1' and C_2'.

The increase in directional stability significantly decreases the size of the broaching plot at the higher speeds. The same analysis was carried out for the steering ability. This was done by increasing the steering force from the waterjets by up to 50%. The results are shown in Figure 6.14. Increasing the steering force has a different effect compared to the effect of the more directionally stable design. A 50% increase in the steering force reduces the occurrence of broaching-to at lower speed, whereas broaching still occurs at higher wave length, height and forward speed.

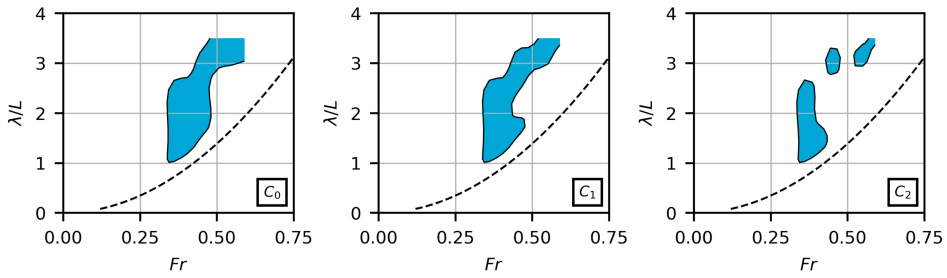

Figure 6.13: Three different broaching zone plots obtained by progressively increasing the directional stability of the vessel.

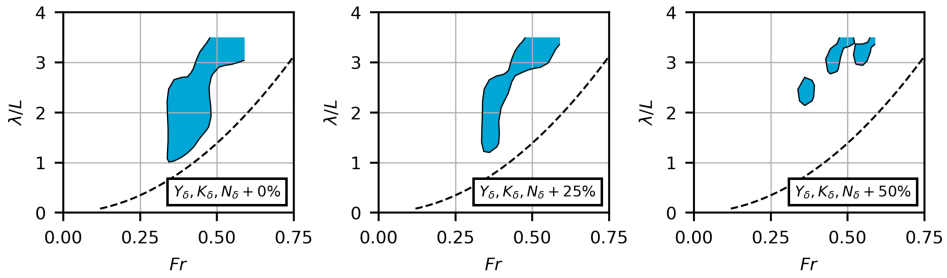

Figure 6.14: Three different broaching zone plots obtained by progressively increasing the waterjets steering effectiveness.

6.6. CONCLUDING REMARKS

THE 3D BEM simulation tool was used in this chapter to simulate the behaviour of the SAR NH-1816 freely sailing in stern quartering regular waves. The objective was to investigate the effect of the controllability characteristics of the vessel on the inception of dynamic instability phenomena in the following sea. Three aspects of the NH-1816 manoeuvrability were examined:

- the loads induced by the static heel of the vessel in sway and yaw;
- the directional stability of the vessel in sway and yaw, commonly assessed in the ship manoeuvrability design;
- the steering devices effectiveness.

The nature of heel-sway and heel-yaw coupling in the following sea is very different, even opposite, compared the case in calm water (see Chapter 3). The effects originating from the incoming waves are more significant than the dynamics of the lift and wave making in calm water, especially for the heel-yaw hydrodynamic coupling $N'_{\phi}\phi'$.

The heel induced sway force and yaw moment cause the craft to be more stable reducing the likelihood of broaching inception. The results agree with the investigation of Hashimoto et al. [50], confirming the validity of these considerations to several wave and ship speed conditions. The study of Renilson and Manwarring [79] shows instead an opposite result of the effect of the heel induced loads into the inception of broaching-to, although this latter work was based on a similar vessel, a fishing trawler. The influence that the heel induced loads have in the vessel broaching behaviour is still not unequivocally estimated; future research must address this issue to solve this ambiguity; since the complex fluid dynamic mechanisms involved, the use of more accurate modelling is foreseen.

From a design point of view, the prediction of the heel-coupling terms is difficult, and they are rarely taken into account in manoeuvrability studies. Moreover, the heel coupling loads cannot be used to improve the manoeuvrability design of a high-speed craft in a practical way. For this reason, the less sophisticated and more common sway-yaw dynamics was investigated afterwards: the effect on broaching-to inception of the hull directional stability, represented by the well-known index C' [48], and the steering effectiveness, represented by the hydrodynamic coefficients Y'_{δ}, K'_{δ} and N'_{δ}, were analysed.

The turning ability and the directional stability of the vessel were modified artificially into the 3D BEM. A sensitivity analysis over four different manoeuvrability variants of the same vessel was realised, focusing on the dynamic instability in the following sea. The results of this investigation show that:

- an increase in the steering ability, as a result of an increase in steering force available to the vessel, reduces the tendency to broach, particularly for low speeds and low wavelength to ship length ratios up to 2.5.
- An increase in directional stability has little effect on the tendency to broach below a wavelength to ship length ratio of around 2.5, however it does reduce the broaching tendency in case of longer waves.

- It was shown that the size of the broaching zone could be reduced compared to the original design by the enhancement of both the directional stability and the steering effectiveness. This is preferable because the modifications of the stern appendages configurations, aimed to improve the ship manoeuvrability, have often only a limited effect.

7

CONCLUSIONS AND RECOMMENDATIONS

7.1. CONCLUSIONS

THE doctoral investigation elaborated in this thesis deals with the problem of the small, fast vessels, commonly known in literature as high-speed craft, sailing in following seas. The demand for safer and better performing craft in rough sea is increasing: dynamic instability phenomena, such as broaching-to, can seriously threaten the safety on board. Although these events are well known and highly dreaded by mariners, there is no clear agreement within the Naval Architecture community about the main characteristics that lead a vessel to be more vulnerable than others in the following sea. The debate is still open: the objective of this thesis was to solve this ambiguity and to provide useful information for shipbuilders and ship designers. As suitable test case, the rescue craft NH-1816 in operation for the Royal Netherlands Sea Rescue Institution (KNRM) was chosen as subject of this research work.

The first part of the thesis consists of a broad acquisition of experimental and numerical data of the loads acting on the high-speed craft. An optimal level of dynamic stability in the following sea would not be achievable during the design process before a proper prediction of the loads acting on the vessel at sea. The knowledge of the vessel dynamics during the inception of dynamic instability events is necessary. Also a good understanding of the most suitable methods used to investigate them must be available.

The data collected in this phase are used in the second phase, that focuses on the behaviour of the vessel in the following sea in relation with its inherent manoeuvrability characteristics. The main purpose when studying these scenarios is to improve the design of the vessels, in order to make them less vulnerable to the inception of dynamic instability events. This concerns especially two features, namely the ability of maintaining the desired course despite an external disturbance (course keeping), and of changing it rapidly and safely (turning).

These two aspects, the characterisation of the physics and the design optimization

of the vessel sailing in the following sea, follow from the research questions of Chapter 1, Section 1.2. Hereby, the most significant findings of the thesis are listed as follow-up answers of the research questions.

- *How to predict the dynamics of the high-speed craft manoeuvrability and seakeeping in following and stern-quartering waves?*

The answer to this question has been addressed in three consequential steps. First of all, the manoeuvrability loads acting on the vessel were investigated in calm water at different forward speeds (Chapter 3). Second, the same loads were measured in regular following and stern-quartering waves (Chapter 4). These two investigations were carried out mainly by experimental captive model tests. Third, the prediction of such manoeuvrability loads by means of numerical tools was assessed (Chapter 5). The prediction of the loads in waves of a time domain 3D BEM was corrected and implemented taking into account the empirical results.

The manoeuvrability forces and moments acting on small fast vessels depend on the vessel forward speed, on the wave length and steepness, on the relative longitudinal location of the vessel in the wave and on the vertical running attitude that the vessel assumes in the wave determining the shape of the submerged geometry. Since the high complexity of this description, in literature there is a substantial vagueness about the characterisation of these loads in waves. The experimental and numerical investigations carried out in this work were meant to cover this lack of knowledge, highlighting the following results:

- the manoeuvrability loads are highly dependent on the position of the vessel in the wave. This variability is in most of the cases more significant than the differences due to the change in forward speed and wave conditions;

- the manoeuvrability loads in waves are significantly different than the calm water case. This implies that the common manoeuvrability-in-waves approach, that sums the Froude-Krylov and diffraction loads to a calm water characterization in the horizontal plane, is not applicable for small, fast craft above Fr = 0.3;

- the experimental and numerical investigations of the loads acting on the vessel hull cover a wide range of forward speeds and wave lengths. Important limitations on the number of conditions tested weigh on several past studies on the field. A larger picture of the dynamics of the vessel in following waves is advantageous for a comprehensive understanding of the problem.

The second question is connected to the behaviour of the vessel in the following sea, and to the study of the main factors leading to an unstabe ship design.

- *Which are the most important characteristics that lead a vessel to be dynamically unstable in following seas?*

The data collected in the experimental and subsequent numerical investigations allowed an accurate prediction of the behaviour of the high-speed craft NH-1816 in the

following sea. The manoeuvrability characteristics of the vessel were changed by modifying the directional stability and the steering effectiveness of the vessel. The results of this investigation show that the ability of keeping a desired course and of turning rapidly have both a significant influence on the inception of a broaching instability in following seas, regardless of the wave exciting loads. This was assessed by performing many free-sailing vessel simulations and highlighting a broaching zone. The results are summarised in the following:

- an increase in directional stability has little effect on the size of the broaching zone below a wavelength to ship length ratio of around 2.5, however it does reduce the size of the broaching zone for longer waves;
- an increase in the steering ability, as a result of an increase in steering force available, reduces the size of the broaching zone, particularly for low speeds and low wavelength to ship length ratios up to 2.5;
- the size of the broaching zone could be reduced compared to the original design by the enhancement of both the directional stability and the steering effectiveness. This is preferable because the modifications of the stern appendages configurations, aimed to improve the ship manoeuvrability, are often limited.

7.2. RECOMMENDATIONS FOR FUTURE DEVELOPMENTS

THE research developed in this thesis made use of both numerical and experimental techniques, that can be considered as state-of-the-art methods in the Naval Architecture field. As any other tool, they present limitations and therefore also some possibilities of improvement.

The assessment of the broaching-to behaviour of the vessel in following seas can also be expanded. In particular, this work is only an initial step towards a more systematic assessment of the quality of a vessel in following seas. Future research will point to methods meant to quantify the ship dynamic stability in order to be able to understand to what extent a vessel can be considered safe when sailing in realistic sea states. The International Maritime Organisation (IMO) have already been focusing on this issue with the Second Generation Intact Stability Criteria, and new developments on this issue are foreseen.

7.2.1. NUMERICAL TOOLS

A time domain potential flow 3D BEM was chosen to simulate the behaviour of the high-speed craft in following seas. This choice was motivated in the beginning of the project by the well-known suitability of these mathematical model in the prediction of the ship motions: panel methods are one of the most reliable and accurate tools to simulate the ship behaviour at sea at the cost of modest computational effort. However, especially for manoeuvrability problems, BEMs present some inaccuracies. Future research must further develop these tools.

CFD solvers and experimental tests will be highly beneficial for an implementation of the hydrodynamic particulars that are not captured by BEMs. In this work two important aspects of the broaching behaviour of the vessel were not investigated experimentally

and thus no numerical validations are available: the effect of the wave steepness on the manoeuvrability loads and the yaw rate induced loads. Since the high complexity of these investigations, dedicated studies are required.

7.2.2. EXPERIMENTAL TECHNIQUES

Model tests were carried out in three different experimental campaigns throughout this research. Experiments have the objective to model the physical reality; the information collected are used to assess directly the motions of the ship at sea, or to correct and validate the numerical tools. Future efforts will be directed towards the empirical prediction of the loads acting on the vessel in waves: an attempt in this direction was developed in Chapter 4, Section 4.2. The model, completely captive and rigidly connected to the Hexapod (see Chapter 3, Section 3.2) could perform different oscillations in wave thus measuring the forces and moments in every direction. This could be very important for manoeuvrability as well as seakeeping applications. The restrictions towards this towing tank testing developments are purely of technical nature.

Another issue only marginally treated in this research is the determination of the loads induced by yaw velocity in waves. The resistance that the vessel opposes to the broaching yawing motion can be significant in the dynamic instability event. However, these terms are difficult to obtain experimentally: no published research is available on this subject, neither numerical investigations. Dedicated studies must be still carried out, and this is an important aspect for the final accurate prediction of the broaching behaviour.

7.2.3. BROACHING-TO NUMERICAL PREDICTION

Numerical and experimental data and techniques were coupled in Chapter 5 and 6 to investigate the behaviour of the high-speed craft in following and stern-quartering regular waves. The results of this investigation showed how to optimise a design with respect to the dynamic stability of a fast craft in following seas. Although useful for designers, this information is not completely true, because they are obtained through a non realistic description of the operative behaviour of the vessel in rough sea. This is important in single wave, rare and sudden events such as surf-riding and broaching-to that are highly sensitive to any decisions of the masters or the crew on board.

First, the only way that researchers and designers have to simulate the ship motions in waves is by means of an autopilot. A great amount of data are available in literature to set-up an autopilot and steering architecture; especially in the case of following seas, the smallest change in these settings can lead to great variations of behaviour of the vessel.

Second, an autopilot will never fully replicate the human behaviour: as already discussed in the Introduction of this thesis, humans can react in several different manners when facing risky situations in rough seas. For example, an experienced mariner might anticipate the possibility of a broaching to occur, and starts to react as soon as the stern is lifted by the wave action. An autopilot does not do that. Moreover, masters have their own knowledge of the sea and of the vessel, that can be different from the view of a designer and thus rather unpredictable. Such discrepancies seem impossible to bridge, at least in the short-medium period of time. The only meaningful step toward a convergence between design and operability of a vessel would be a closer collaboration be-

tween research institutions and marine operators.

The latter considerations are particularly true for the operability of small, fast craft. The great amount of power that the high-speed craft have at disposal, typically provided by waterjets, allows the masters to avoid dangerous situations by enacting corrective manoeuvres, that would be not possible with less powerful ships. From the point of view of the dynamic stability problem, high-speed craft are less attractive than semi-displacement vessels that cannot reach the planing regime velocities, or equipped with more common and less effective propeller/rudder steering configurations. For the complexity and a lack of significant knowledge of this problem, high-speed craft builders and operators confide in the experience and judgement of the masters who know well the risks at sea. This does not exclude the improvements that can be applied to a design that can be agreed also with the operators and the masters, in order to give them a better reliance on the vessel.

7.2.4. BROACHING-TO IN A REALISTIC SEA STATE

This work examined the behaviour of the high-speed craft in regular waves. The dynamics of the vessel in realistic, irregular sea state can be significantly different. In the future, researchers can make use of the results of this study in order to assess the broaching behaviour in different sea states with respect to the ship manoeuvrability features. Information on the ship state in a *local* wave within a realization of a sea spectrum can be retrieved using empirical data as presented in Chapter 5, i.e. applying deterministic modelling of the ship dynamical behaviour on a wide range of combinations of ship speeds and wave characteristics.

Currently a great amount of work is being carried out on the topic of dynamic stability of ships. As mentioned in the Introduction of this work, the main aim of IMO is to draw guidelines and regulations concerning the safety of ship in the sea waves, substituting the static stability formulations of the IS Code 2008 [28]. This thesis does not deal with the important question that is central in the IMO debate on the dynamic stability. Concerning following seas problems: how to estimate the vulnerability of a vessel to broaching? The most feasible way to quantify the dynamic stability of a vessel seems only the direct assessment by means of numerical simulations or free running model tests. However, such direct assessments will only quantify the inclination of a vessel to be unstable in a seaway but they will not give any appropriate information about the evaluation of the vessel dynamics in dangerous following sea situations. Future investigations, concerning the quantification of the dynamic stability, the design improvements and the numerical tools validation, will be aimed to the realisation of principles, methods and comparative terms suitable to judge the vulnerability of a ship to dynamic instability phenomena.

7.2.5. RECOMMENDATIONS TO DESIGNERS

As already discussed in this thesis, the ship controllability is considered only in a rather late design phase, and mostly in calm water. Studies in waves are too complex and not normally carried out; moreover, not many design guidelines aimed to avoid instability events in waves are available in literature, since this is a relatively new topic.

Predicting earlier a certain behaviour of the ship in complex scenarios can be ex-

tremely useful in a design process: great improvements in a design can be achieved with better targeted variations of the vessel characteristics. Especially considering that in a final phase of the project the possible modifications of the ship controllability are limited by other design constraints.

Designers could already mitigate the vessel broaching behaviour applying some modifications to the directional stability and the steering effectiveness of the vessel: this work shows the effects that such characteristics have in an inception of a following sea dynamic instability. But most importantly they can also assess the effect of these aspects in calm water, that is a relatively easy task, in order not to compromise the performance that a fast vessel must possess in milder sea conditions.

A

UNCERTAINTY ANALYSIS

In the work of this thesis three experimental campaigns were carried out on the model of the SAR NH-1816 high-speed rescue craft; the results are presented in Chapter 3 and 4:

- captive model tests in calm water performed at the towing tank of TU Delft. The sway velocity and static heel induced loads were measured;
- captive model tests in following regular waves performed at TU Delft. The heel induced loads were measured at different forward speed and wave conditions;
- captive model tests in following and stern-quartering waves performed at the Seakeeping and Manoeuvring Basin of MARIN. The sway velocity, wave incidence angle and steering device induced loads were measured.

For each of the experimental campaign an uncertainty analysis was carried out, in order to estimate the confidence on the values measured. The uncertainty of the measured experimental values was estimated following the ITTC Recommended Procedures and Guidelines no. 7.5-02 06-04 (Force and Moments Uncertainty Analysis, Example for Planar Motion Mechanism Test) [77].

The total uncertainty is composed by the two terms: the elemental bias that represents the systematic instrumentation error present in each run; the precision limits of the 95% confidence of the measured value, calculated by means of 10 repetitions of the same run. For the experimental tests carried out at MARIN, only the precision limits were taken into account.

The uncertainty of the hydrodynamic coefficients was evaluated according to Equation A.1. The total uncertainty of a certain coefficient is calculated by the square root of the sum of the i-th load points total uncertainty and the 95% confidence band of the fitted linear curve. N is the number of data points used for the curve fitting; the parameter t is the coverage factor of the Student distribution for N data points.

$$U_{Rf_\phi} = \sqrt{\sum_i U_{Rf_i}^2 + t\sum_i \frac{(f_i^2 - f_\phi^2\phi^2)}{N-2}} \tag{A.1}$$

A.1. MODEL TESTS IN CALM WATER

The elemental bias considered were related to inaccuracies in the determination of model length L, model draft at zero speed T_m, water density ρ, carriage speed U, model alignment with respect to the towing tank and strain gauge calibration factors. The uncertainty results are presented in Figures A.1 and A.2.

Precision limits P_R, and the bias of draft B_{T_m}, carriage speed B_U, and model alignment bias $B_{F,align}$, are expressed in terms of percentage of the total uncertainty. Model length, water density and sensor calibration factors bias are omitted in Figure A.1 because their contributions to the total uncertainty are negligible with respect to the other components. The model alignment is the largest bias component for the sway force and the roll moment. The mean draft bias is rather large for the yaw moment. The precision limit is a large source of uncertainty of the measurements, especially for the sway force,: the sway force uncertainty was around 20% of the total estimation. In Figure A.1, the values are presented for sway force and roll, yaw moments for a single run used as example; the results shown apply both for the heeled and drifting model tests.

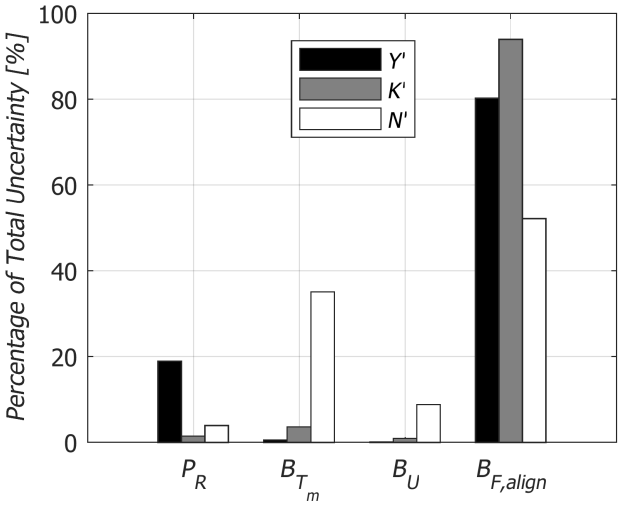

Figure A.1: Percentage contributions of total uncertainty (Stage A, $Fr = 1.05$, $\phi = 12$ degrees).

Since the model alignment was the largest bias component, it means that alignment was of particular importance at lower speeds, when the loads measured were smaller and the model was more immersed in the water. In fact, Figure A.2 shows that the total uncertainty of heel-sway, roll and heel-yaw hydrodynamic coefficients depicted as a

function of Froude number decreases with increasing forward speed. The same trend was observed for the sway velocity induced coefficients.

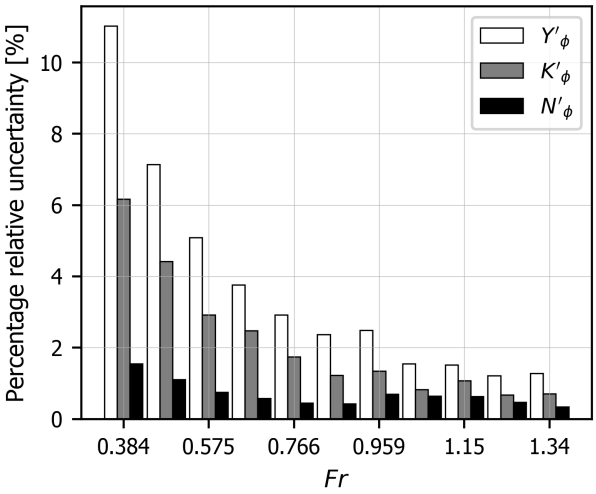

Figure A.2: Percentage uncertainty of the obtained heel induced hydrodynamic coefficients. Values are relative to the coefficients absolute values.

A.2. MODEL TESTS IN REGULAR WAVES

The same elemental bias of uncertainty of the experiments in calm water are taken into account in the case of following waves. In addition to those, also the wave probe position x_P, the wave elevation ζ and the wave frequency ω are considered. The main contributions to the total uncertainty are the wave amplitude bias and the repeatability of the measured loads.

The contribution to the total uncertainty of the synchronization procedure (see Chapter 4, Section 4.2) is implicitly estimated by the confidence limits of the forces and wave elevation, calculated after 10 measurement repetitions. This method was the only feasible one to assess the uncertainty of the wave-carriage-oscillator synchronization. The most accurate way would be the measure of the wave elevation at the instant at which the measurement starts, to assess the relative position wave-model and hence the synchronization between them. However, this measurement is disturbed by the presence of the model and by the flow on the probe due to the forward motion. At this stage, it is considered that the repeatability of the runs is the most reasonable way to estimate the quality of the synchronization methods.

The results of the total uncertainty of the heel-sway and heel-yaw coupling coefficients are shown in Figure A.3.

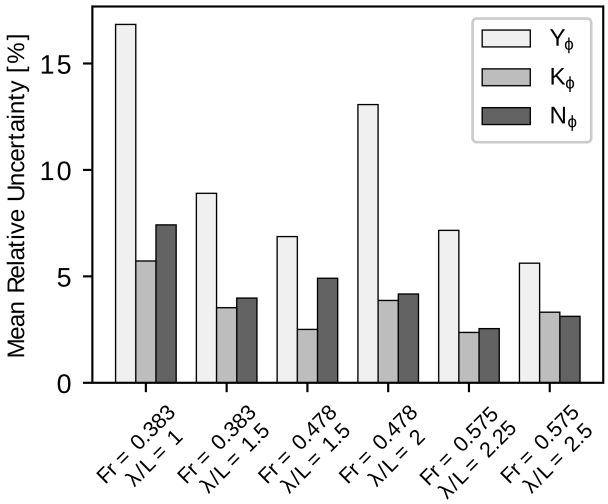

Figure A.3: Percentage uncertainty of the measured manoeuvring coefficients for the six conditions considered. The values are averaged along the positions on the wave, and relative to the coefficient maximum absolute value.

B

DATA OF THE EMPIRICAL AND NUMERICAL DESCRIPTION OF THE MANOEUVRABILITY LOADS IN WAVES

This Appendix contains the comparison between the measured and the predicted captive tests results. The numerical captive tests were carried out over a number of conditions different than the cases tested in the experiments. This is aimed to highlight a trend of the manoeuvring forces and moments on a wider domain of ship speed and wave combinations investigated in the simulations. A summary of the conditions investigated is reported in Table B.1.

Fr	λ/L	H/λ	β, ϕ and δ [deg]
0.32	0.75, 1, 1.25,1.75		
0.38	1, 1.25, 1.5, 2		
0.43	1.25, 1.5, 1.75, 2.25		
0.48	1.5, 1.75, 2, 2.5	0.06	β=0,5,10; ϕ =0,6,12; μ =0,5,10
0.53	2.0, 2.25, 2.5, 3		
0.575	2.25, 2.5, 2.75, 3.25		
0.59	2.5, 2.75, 3, 3.5		

Table B.1: Summary of the conditions of the numerical captive model tests. For each of the 7 Froude numbers, 4 wave length were simulated. The wave steepness H/λ, the wave incidence angles μ, the heel angles ϕ and the drift angles β are the same tested in the experimental campaigns (see Chapter 4).

The figures included in this Appendix show the comparison between measurements and prediction of the following quantities: the amplitude a, the phase φ, the mean value $\bar{\eta}$ of:

- the wave surging force X'_W in Figure B.1 and B.2;
- the sway velocity induced coefficients Y'_v, K'_v and N'_v in Figure B.3 and B.4;
- the heel induced coefficients Y'_ϕ, K'_ϕ and N'_ϕ in Figure B.5 and B.6;
- the wave coefficients Y'_μ, K'_μ and N'_μ in Figure B.7 and B.8;

These terms are depicted alternatively as functions of Froude number Fr and non-dimensional wave length λ/L. The wave surging force and the wave coefficients computed by the 3D BEM were not corrected; instead the numerical sway velocity and the heel induced coefficients were corrected keeping into account the empirical results. The wave surging force terms reported in the plots refer to a zero wave incidence angle ($\mu = 0$). The measurements are denoted with white squares; the numerical prediction with black dots.

The numerical results were obtained correcting the computations using the empirical description explained in Chapter 5, Section 5.2. The procedure consisted in the fit of the coefficients amplitude, phase and mean value through a plane function of Fr and λ/L. The polynomial coefficients of the planar fit are reported in Table B.2, B.3 and B.4 for the sway velocity induced coefficients; Table B.5, B.6 and B.7 for the heel induced coefficients. The terms included in these tables refer to Equation 5.2, Chapter 5.

	a'_{Y_v}	φ'_{Y_v}	$\bar{\eta}'_{Y_v}$
p_0	-3.32E-02	-3.05E-01	-4.77E-02
p_1	7.27E-04	1.49E-01	4.73E-03
p_2	1.95E-02	-1.01E+00	-1.62E-02

Table B.2: Coefficients of the plane polynomials for amplitude, phase and mean value of Y'_v (see Equation 5.2, Chapter 5).

	a'_{K_v}	φ'_{K_v}	$\bar{\eta}'_{K_v}$
p_0	-4.48E-03	1.18E+00	4.37E-03
p_1	1.77E-04	7.94E-02	-7.25E-04
p_2	3.02E-03	-8.93E-01	-1.19E-03

Table B.3: Coefficients of the plane polynomials for amplitude, phase and mean value of K'_v (see Equation 5.2, Chapter 5).

	a'_{N_v}	φ'_{N_v}	$\bar{\eta}'_{N_v}$
p_0	1.74E-02	5.48E-02	-8.16E-03
p_1	-1.08E-04	7.89E-02	6.50E-04
p_2	-4.08E-03	-2.26E-01	-7.99E-03

Table B.4: Coefficients of the plane polynomials for amplitude, phase and mean value of N'_v (see Equation 5.2, Chapter 5).

	a'_{Y_ϕ}	φ'_{Y_ϕ}	$\bar{\eta}'_{Y_\phi}$
p_0	-4.07E-02	2.19E+00	-3.83E-03
p_1	1.18E-02	-6.93E-01	1.31E-02
p_2	4.81E-03	-2.32E-01	-2.50E-02

Table B.5: Coefficients of the plane polynomials for amplitude, phase and mean value of Y'_ϕ (see Equation 5.2, Chapter 5).

	a'_{K_ϕ}	φ'_{K_ϕ}	$\bar{\eta}'_{K_\phi}$
p_0	4.03E-03	4.83E+00	1.80E-02
p_1	-6.58E-04	-1.03E+00	7.60E-04
p_2	-1.48E-04	-9.96E-01	-1.39E-02

Table B.6: Coefficients of the plane polynomials for amplitude, phase and mean value of K'_ϕ (see Equation 5.2, Chapter 5).

	a'_{N_ϕ}	φ'_{N_ϕ}	$\bar{\eta}'_{N_\phi}$
p_0	1.19E-02	-1.75E+00	-2.52E-02
p_1	-1.28E-03	2.29E-01	1.18E-03
p_2	-8.02E-04	-1.61E-01	1.21E-02

Table B.7: Coefficients of the plane polynomials for amplitude, phase and mean value of N'_ϕ (see Equation 5.2, Chapter 5).

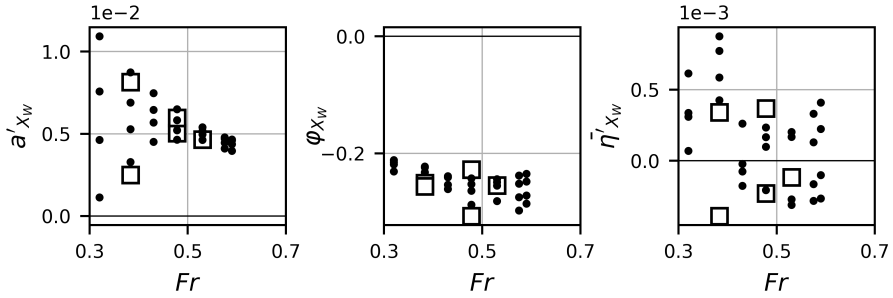

Figure B.1: Comparison of the experimental (white squares) and numerical (black dots) captive tests results for the wave surging force X'_W. In the columns, starting from the left: amplitude, phase and mean values of the sinusoidal signal function of the location in the wave ξ_G/λ. The terms are plotted as function of Froude number Fr.

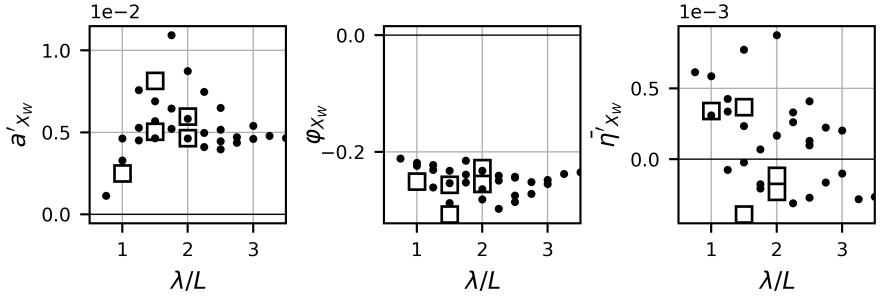

Figure B.2: Comparison of the experimental (white squares) and numerical (black dots) captive tests results for the wave surging force X'_W. In the columns, starting from the left: amplitude, phase and mean values of the sinusoidal signal function of the location in the wave ξ_G/λ. The terms are plotted as function of the non-dimensional wave length λ/L.

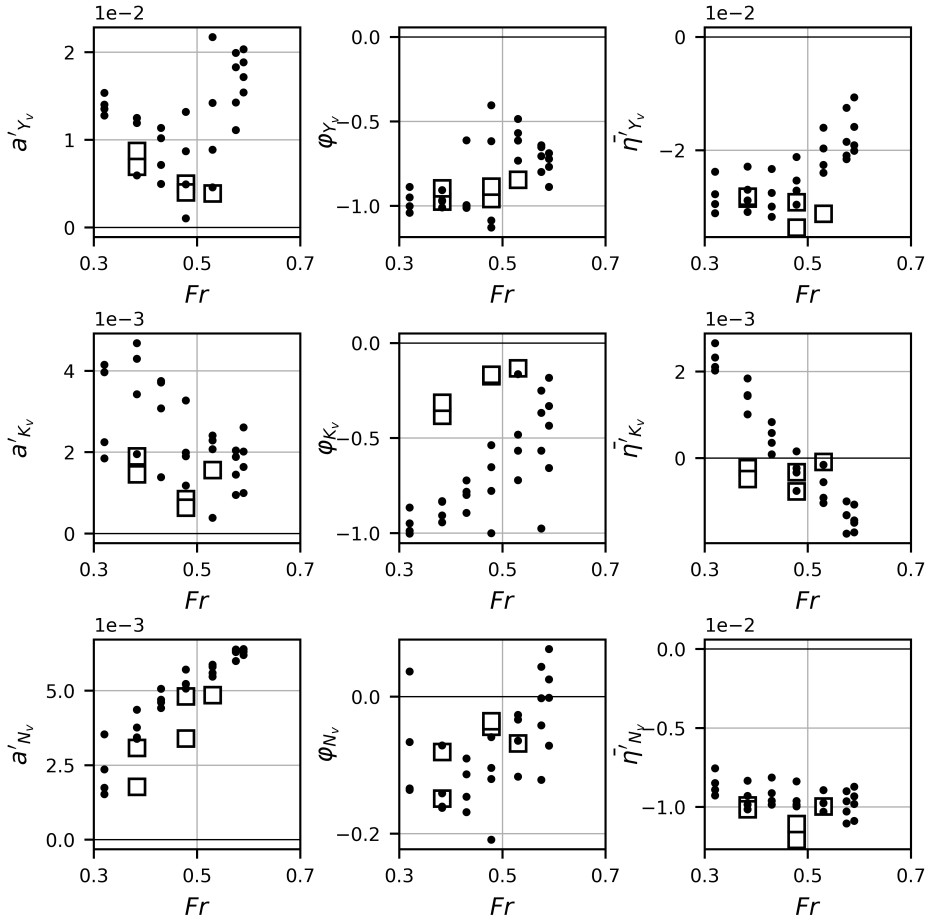

Figure B.3: Comparison of the experimental (white squares) and numerical (black dots) captive tests results for the sway velocity induced coefficients. In the rows, starting from the top: Y'_v, K'_v and N'_v; in the columns, starting from the left: amplitude, phase and mean values of the sinusoidal signal function of the location in the wave ξ_G/λ. The terms are plotted as function of Froude number Fr.

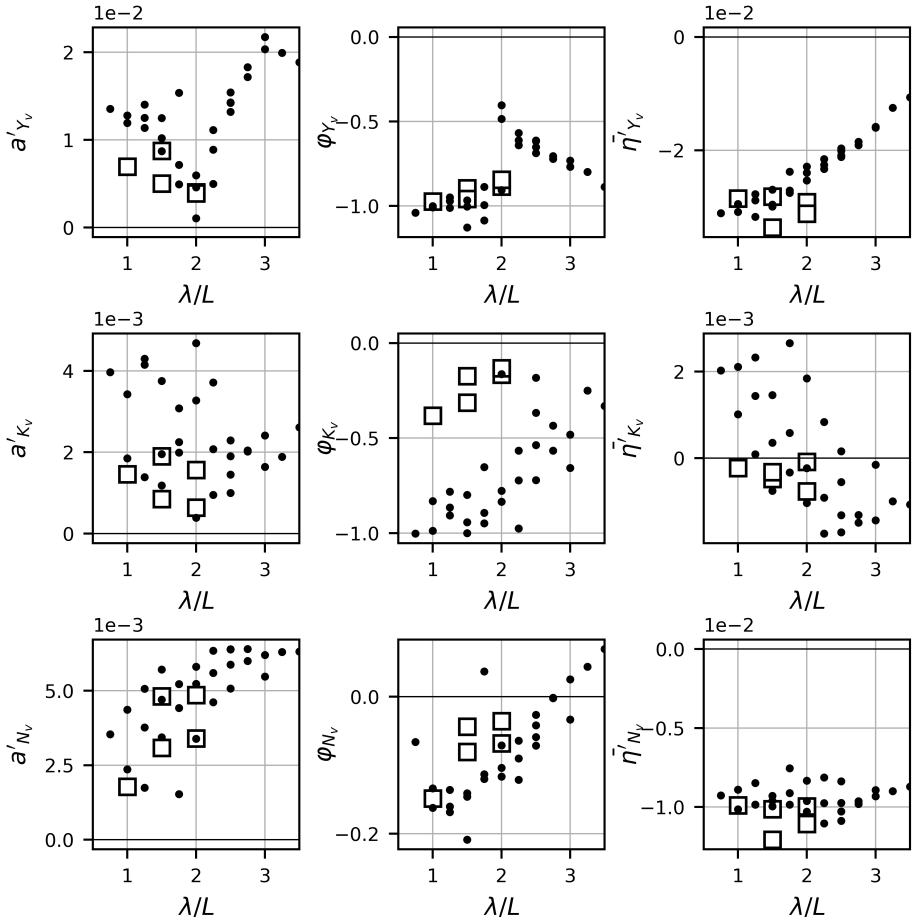

Figure B.4: Comparison of the experimental (white squares) and numerical (black dots) captive tests results for the sway velocity induced coefficients. In the rows, starting from the top: Y'_v, K'_v and N'_v; in the columns, starting from the left: amplitude, phase and mean values of the sinusoidal signal function of the location in the wave ξ_G/λ. The terms are plotted as function of the non-dimensional wave length λ/L.

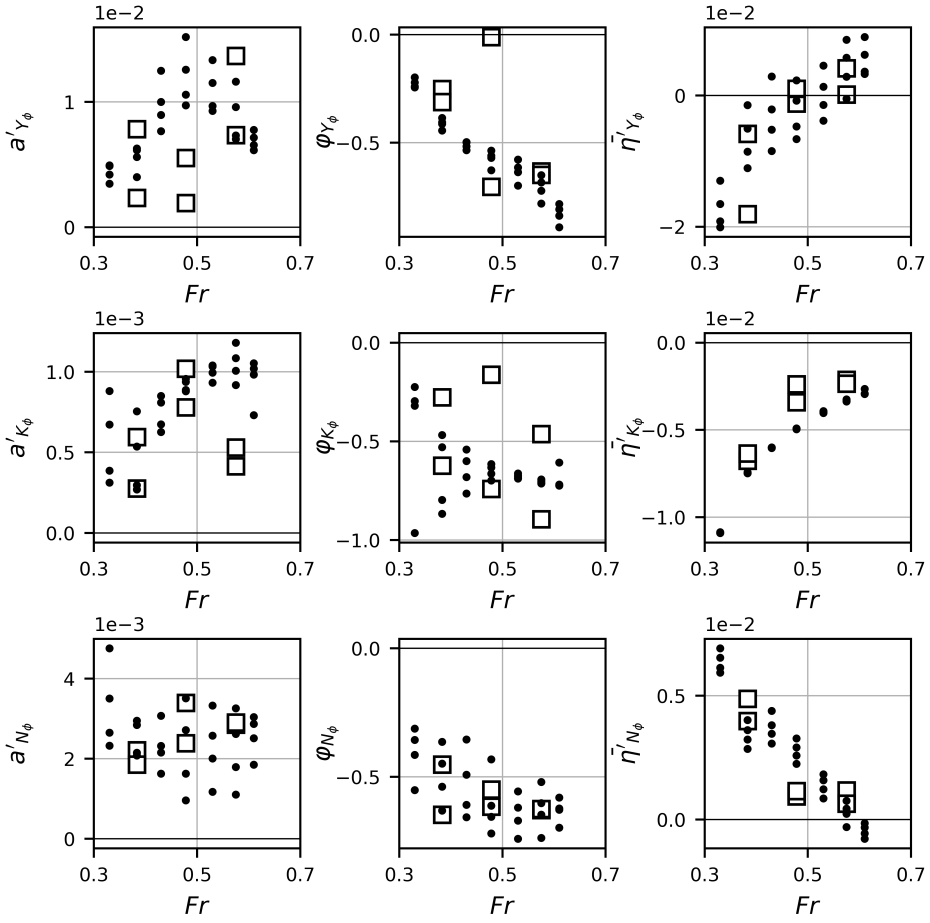

Figure B.5: Comparison of the experimental (white squares) and numerical (black dots) captive tests results for the static heel induced coefficients. In the rows, starting from the top: Y'_ϕ, K'_ϕ and N'_ϕ; in the columns, starting from the left: amplitude, phase and mean values of the sinusoidal signal function of the location in the wave ξ_G/λ. The terms are plotted as function of Froude number Fr.

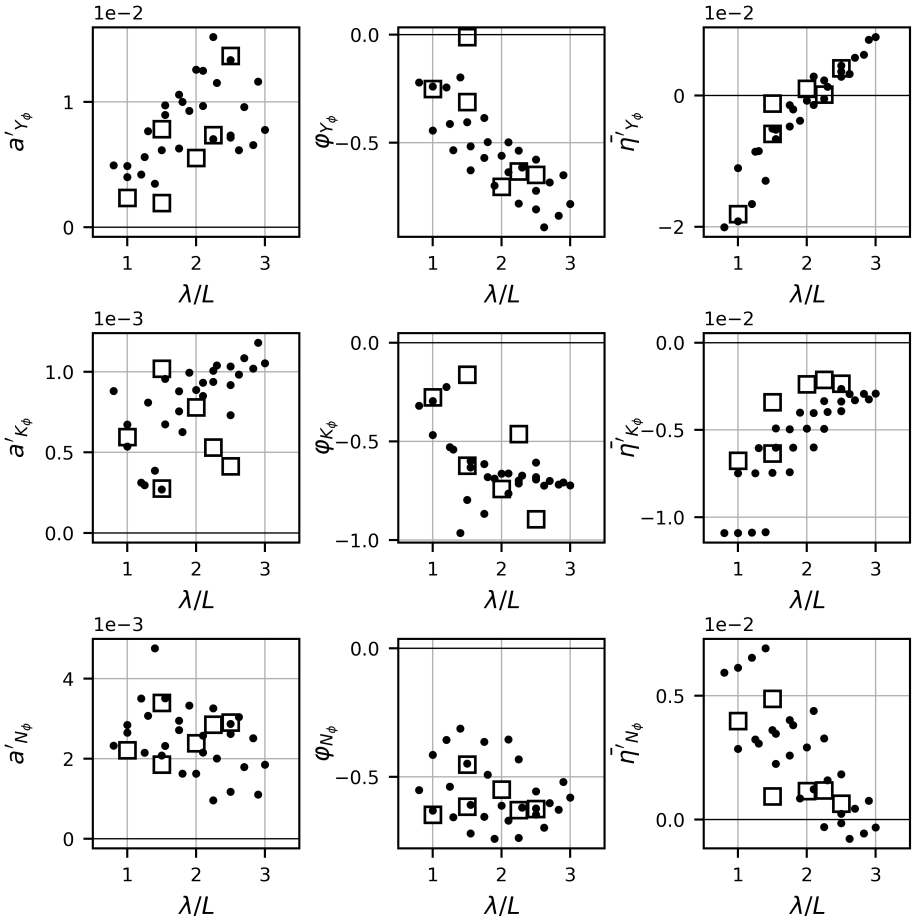

Figure B.6: Comparison of the experimental (white squares) and numerical (black dots) captive tests results for the static heel induced coefficients. In the rows, starting from the top: Y'_ϕ, K'_ϕ and N'_ϕ; in the columns, starting from the left: amplitude, phase and mean values of the sinusoidal signal function of the location in the wave ξ_G/λ. The terms are plotted as function of the non-dimensional wave length λ/L.

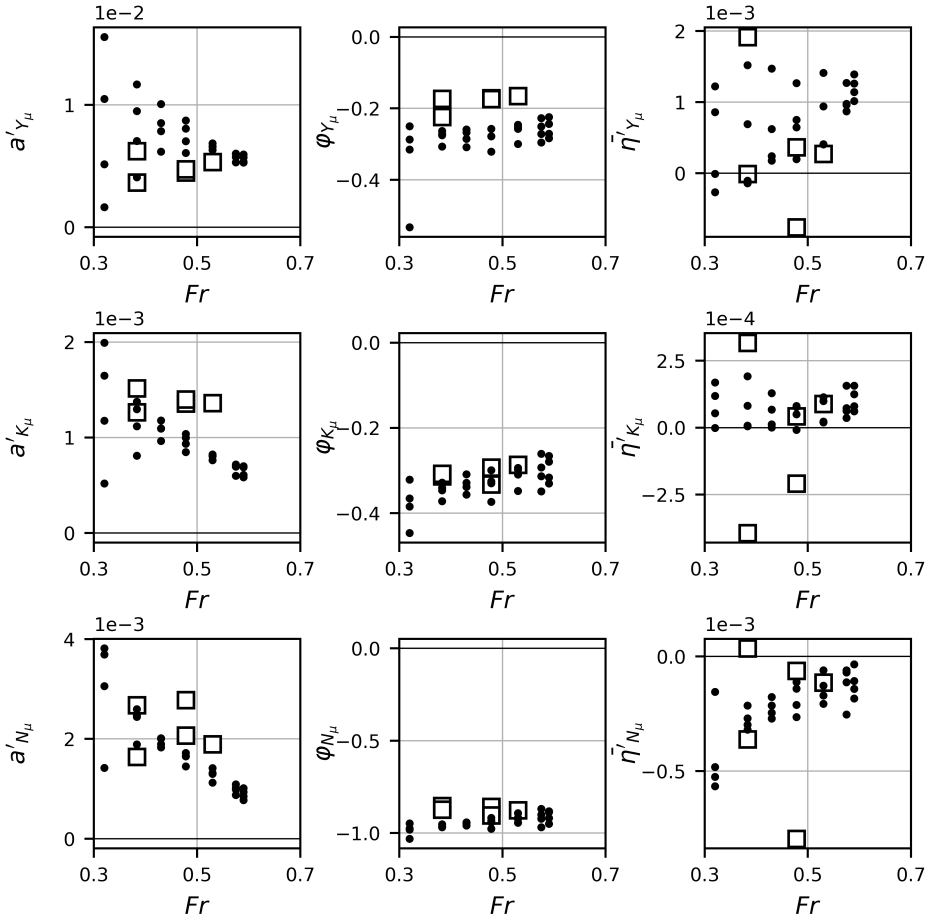

Figure B.7: Comparison of the experimental (white squares) and numerical (black dots) captive tests results for the wave incidence angle induced coefficients. In the rows, starting from the top: Y'_ϕ, K'_ϕ and N'_ϕ; in the columns, starting from the left: amplitude, phase and mean values of the sinusoidal signal function of the location in the wave ξ_G/λ. The terms are plotted as function of Froude number Fr.

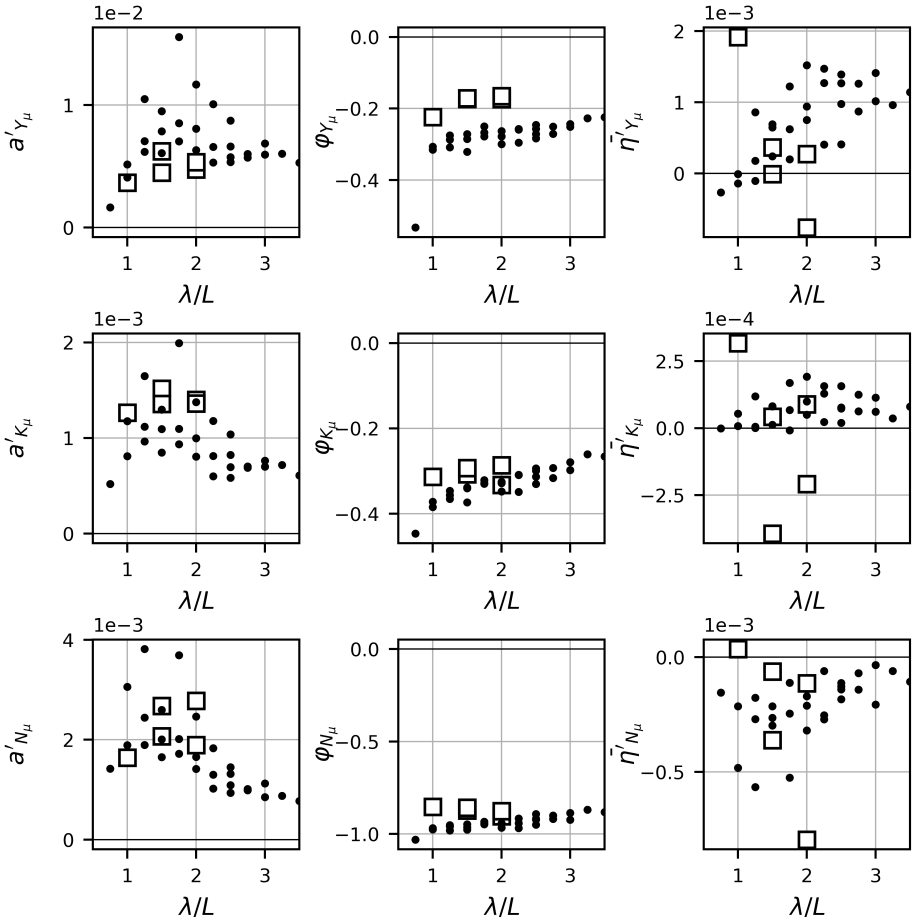

Figure B.8: Comparison of the experimental (white squares) and numerical (black dots) captive tests results for the wave incidence angle induced coefficients. In the rows, starting from the top: Y'_μ, K'_μ and N'_μ; in the columns, starting from the left: amplitude, phase and mean values of the sinusoidal signal function of the location in the wave ξ_G/λ. The terms are plotted as function of the non-dimensional wave length λ/L.

REFERENCES

[1] J. E. Conolly. “Stability and control in waves: a survey of the Problems”. In: *Journal of Mechanical Engineering Science* 14.7 (1972), pp. 186–193.

[2] *"broach". Merriam-Webster Dictionary. https://www.merriam-webster.com*. 2019.

[3] W. Falconer. *The Shipwreck*. 1762.

[4] K. J. Spyrou. “Perceptions of Broaching-To: Discovering the Past”. In: *Contemporary Ideas On Ship Stability and Capsizing in Waves*. Springer, 2011, pp. 399–411.

[5] R. Anderson. *The Works of the British Poets. With Prefaces, Biographical and Critical*. Printed for John & Arthur Arch, 1795.

[6] M. Renilson. “The Broaching of Ships in following Seas”. PhD thesis. University of Glasgow, 1981.

[7] K. S. M. Davidson. “A note on the Steering of Ships in Following Seas”. In: 7^{th} *International Congress of Applied Mechanics*. 1948.

[8] P. Du Cane. “Model Evaluation of 4 High Speed Hull Forms in Following and Head Sea Conditions”. In: *Proceedings Symposium on the Behaviour of Ships in a Seaway*. 1957.

[9] L.F. Rydill. “A Linear Theory for Steered Motion of Ships in Waves”. In: *Transactions RINA* (1959).

[10] H. Eda and C.L. Crane. “Steering characteristics of ships in calm water and waves”. In: *Transactions SNAME* 73 (1965).

[11] P. Boese. *Steering a Ship in a Heavy Following seaway*. Tech. rep. Institut fur Schiffbau, Hamburg University, 1970.

[12] H. Eda. “Directional Stability and Control of Ships in Waves”. In: *Journal of Ship Research* 16.3 (1972), pp. 205–218.

[13] H. Eda. “Yaw control in Waves”. In: *Proceedings of International Symposium on Directional Stability and Control of Bodies moving in water*. 1972.

[14] M. Hamamoto. “On the Hydrodyamic Derivatives for the Directional Stability of Ships in Following Seas (Part 1 and 2)”. In: *Journal of Society of Naval Architecture of Japan* (1973).

[15] K. Nicholson. “Some parametric Model Experiments to Investigate Broaching-to”. In: *International Symposium on the Dynamics of Marine Vehicles and Structures in Waves*. London, 1974.

[16] M. Renilson and A. Driscoll. “Broaching - An investigation into the loss of directional control in severe following seas”. In: *Transactions RINA*. Vol. 124. 1982, pp. 253–273.

[17] N. Umeda. “Nonlinear dynamics of ship capsizing due to broaching in following and stern-quartering seas”. In: *Journal Of Marine Science and Technology* 4.1 (1999), pp. 16–26.

[18] N. Umeda, A. Matsuda, M. Hamamoto, and S. Suzuki. “Stability assessment for intact ships in the light of model experiments”. In: *Journal of Marine Science and Technology* 4.2 (1999), pp. 45–57.

[19] N. Umeda and A. Matsuda. “Broaching in following and quartering seas - Theoretical attempts and new prevention device”. In: 7^{th} *International Conference on the Stability of Ships and Ocean Vehicles (STAB2000)*. Vol. A. Launceston, Tasmania, Australia, 2000, pp. 460–70.

[20] N. Umeda and M. Hamamoto. “Capsize of ship models in following/quartering waves: physical experiments and nonlinear dynamics”. In: *Philosophical Transactions of the Royal Society of London. Series A: Mathematical, Physical and Engineering Sciences* 358 (2000), p. 1771.

[21] N. Umeda, S. Yamamura, A. Matsuda, A. Maki, and H. Hashimoto. “Model Experiments on Extreme Motions of a Wave-Piercing Tumblehome Vessel in Following and Quartering Waves”. In: *Journal of the Japan Society of Naval Architects and Ocean Engineers* 8 (2008), pp. 123–129.

[22] J. De Kat. “The numerical modelling of ship motions and capsizing in severe seas”. In: *Journal of Ship Research* 34.4 (1990), pp. 289–302.

[23] Z. Ayaz, D. Vassalos, and K. J. Spyrou. “Manoeuvring behaviour of ships in extreme astern seas”. In: *Ocean Engineering* 33.17-18 (2006), pp. 2381–2434.

[24] F. Van Walree and P. De Jong. “Validation of a time domain panel code for high speed craft operating in stern and quartering seas”. In: 11^{th} *International Conference on Fast Sea Transportation (FAST2011)*. Honolulu, USA, 2011.

[25] O. Rutgersson and P. Ottosson. “Model Tests and Computer Simulations - An Effective Combination for Investigation of Broaching Phenomena”. In: *SNAME Transactions* 95 (1987), pp. 263–281.

[26] P. De Jong, F. Van Walree, and M. Renilson. “The broaching of a fast rescue craft in following seas”. In: 12^{th} *International Conference on Fast Sea Transportation (FAST2013)*. Amsterdam, The Netherlands, 2013.

[27] N. Umeda, S. Usada, K. Mizumoto, and A. Matsuda. “Broaching probability for a ship in irregular stern-quartering waves: theoretical prediction and experimental validation”. In: *Journal of Marine Science and Technology* 21.1 (2016), pp. 23–37.

[28] *Code On Intact Stability (IS)*. International Maritime Organization (IMO), 2008.

[29] V. Belenky, K. J. Spyrou, K.M. Weems, and W.M. Lin. “Split-time method for the probabilistic characterization of stability failures in quartering seas”. In: *International Shipbuilding Progress* 60.1 - 4 (2013), pp. 579–612.

[30] M. Bonci, M. Renilson, F. Van Walree, J. A. Keuning, and R. Van’t Veer. “On the direct assessment of broaching-to vulnerability of a high-speed craft”. In: 13^{th} *International Conference on the Stability of Ships and Ocean Vehicles (STAB2018)*. Kobe, Japan, 2018.

[31] K. J. Spyrou. “Dynamic Instability in Quartering Seas: The Behavior of a Ship During Broaching”. In: *Journal of Ship Research* 40.1 (1996), pp. 46–59.

[32] M. Renilson. “Behaviour of high speed craft in following sea”. In: 10^{th} *Symposium on High Speed Marine Vehicles (HSMV2014)*. Naples, Italy, 2014.

[33] Steven H. Cohen and D. L. Blount. “Research Plan for the Investigation of Dynamic Instability of Small High-Speed Craft”. In: *SNAME Transactions* 94 (1986), pp. 197–214.

[34] P. De Jong, M. Renilson, and F. van Walree. “The effect of ship speed, heading angle and wave steepness on the likelihood of broaching-to in astern quartering seas”. In: 12^{th} *International Conference on the Stability of Ships and Ocean Vehicles (STAB2015)*. Glasgow, United Kingdom, 2015.

[35] K. J. Spyrou. “Asymmetric Surging of Ships in Following Seas and its Repercussions for Safety”. In: *Nonlinear Dynamics* 43.1-2 (2006), pp. 149–172.

[36] A. Maki, N. Umeda, M. Renilson, and T. Ueta. “Analytical formulae for predicting the surf-riding threshold for a ship in following Seas”. In: *Journal of Marine Science and Technology* 15 (2010), pp. 218–229.

[37] J.A. Keuning. “Non linear behaviour of fast monohulls in head waves”. PhD thesis. Delft University of Technology, 1994.

[38] P. De Jong. “Seakeeping behaviour of high speed ships - An experimental and numerical study”. PhD thesis. Technical University of Delft, 2011.

[39] A. Van Deyzen. “Improving the operability of planing monohulls using proactive control - From idea to proof of concept”. PhD thesis. Delft University of Technology, 2014.

[40] A. Rijkens. “Proactive control of fast ships - Improving the seakeeping behaviour in head waves”. PhD thesis. Delft University of Technology, 2016.

[41] S.L. Toxopeus, J.A. Keuning, and J.P. Hooft. “Dynamic stability of planing ships”. In: *International Symposium on the safety of high-speed craft*. 1997.

[42] H. Yasukawa, N. Hirata, and Y. Nakayama. “High-Speed Ship Maneuverability”. In: *Journal of Ship Research* 60.4 (2016), pp. 239–258.

[43] J. A. Keuning, G. L. Visch, J. L. Gelling, W. de Vries Lentsch, and G. Burema. “Development of a new SAR boat for the Royal Netherlands Sea Rescue Institution”. In: *Proceedings of the* 11^{th} *International Conference on Fast Sea Transportation (FAST2011)*. Hawaii, USA, 2011.

[44] J.A. Keuning. “Grinding the bow”. In: *International Shipbuilding Progress* (2006), pp. 281–310.

[45] G.L. Visch and J. A. Keuning. *KNRM1816 Project: Comparison of the Resistance in Calm Water and the Seakeeping Behaviour of the Arie Visser, Concept 1 and Concept 2*. Tech. rep. Delft University of Technology, 2011.

[46] G.L. Visch and J. A.f Keuning. *KNRM1816 Project: Resistance in Calm Water and the Seakeeping Behaviour of Concept 3*. Tech. rep. Delft University of Technology, 2011.

[47] G.L. Visch. *NH1816 SAR open Water Skeg Variations Turning Circles and Zig-Zag Model Tests Data Report*. Tech. rep. Delft University of Technology, 2013.

[48] Edward V. Lewis, ed. *Principles Of Naval Architecture*. Vol. Vol III - Seakeeping and Manoeuvrability. The Society of Naval Architects and Marine Engineers, 1988.

[49] P. Oltmann. "Roll - An Often Neglected Element of Manoeuvring". In: *MARSIM 93, International Conference on Marine Simulation and Ship Manoeuvrability*. Vol. 2. St. John's, Newfoundland, Canada, 1993.

[50] H. Hashimoto, N. Umeda, and A. Matsuda. "Model Experiment on Heel-Induced Hydrodynamic Forces in Waves for Realising Quantitative Prediction of Broaching". In: *Contemporary Ideas on Ship Stability and Capsizing in Waves*. 2011.

[51] M. Bonci, P. De Jong, F. Van Walree, M. Renilson, J. A. Keuning, and R. Van't Veer. "The heel-induced sway force and yaw moment of a high-speed craft in following regular waves". In: *Journal of Marine Science and Technology* (2019). ISSN: 10.1007/s00773-019-00637-0.

[52] H. Yasukawa and Y. Yoshimura. "Roll-Coupling Effect on Ship Maneuverability". In: *Ship Technology Research* 61.1 (2014), pp. 16–32.

[53] M. Bonci, M. Renilson, P. De Jong, Keuning J. A. Van Walree F., and R. H. M. Huijsmans. "Experimental and numerical investigation on the heel and drift induced hydrodynamic loads of a high-speed vessel". In: 14^{th} *Conference on Fast Sea Transportation (FAST2017)*. Nantes, France, 2017.

[54] M. Bonci, M. Renilson, P. De Jong, F. Van Walree, J. A. Keuning, and R. H. M. Huijsmans. "Heel-sway-yaw coupling hydrodynamic loads on a high speed vessel". In: 11^{th} *Symposium on High-Speed Marine Vehicles (HSMV2017)*. Naples, Italy, 2017.

[55] M. Bonci, M. Renilson, P. De Jong, F. Van Walree, J. A. Keuning, and R. H. M. Huijsmans. "The heel-sway-yaw coupling on a high-speed craft in calm water". In: *The Transaction of the Royal Institution of Naval Architects, Part B - International Journal of High-Speed Craft Technology* 160 (2018), pp. 121–129.

[56] C. Bird, F. Van Walree, D. Sgarioto, L. Thomas, and T. Turner. "Validation of a time domain panel code for predicting the seakeeping behaviour of a rigid hull inflatable Boats". In: 14^{th} *Conference on Fast Sea Transportation (FAST2017)*. 2017.

[57] A. Matsuda and N. Umeda. "New experimental procedure for identifying manoeuvring coefficients of a ship suffering broaching in following and quartering seas". In: *Fourth Osaka colloquium on seakeeping performance of ships*. 2000.

[58] H. Hashimoto, S. Yoneda, Y. Tahare, and E. Kobayashi. "CFD-based study on the prediction of wave-induced surge force". In: *Ocean Engineering* 120 (2016), pp. 389–397.

[59] K. Mizumoto, M. Araki, F. Stern, H. Hashimoto, and N. Umeda. "Improvement of broaching prediction method by system identification using CFD". In: 13^{th} *International Conference on the Stability of Ships and Ocean Vehicles (STAB2018)*. Kobe, Japan, 2018.

[60] S. Toxopeus. "Practical application of viscous-flow calculations for the simulation of manoeuvring ships". PhD thesis. Delft University of Technology, 2011.

[61] F. Quadvlieg, F. van Van Walree, and V. Barthelemy. “Manoeuvring of fast monohulls”. In: 13^{th} *International Conference on Fast Sea Transportation (FAST2015)*. Washington, USA, 2015.

[62] P. A. Bailey, W. Price, and P. Temarel. “A Unified Mathematical Model Describing the Maneuvering of a Ship Travelling in a Seaway”. In: *Transactions of the Royal Institution of Naval Architects* 140 (1997), pp. 131–149.

[63] T. Fossen. “A nonlinear unified state-space model for ship maneuvering and control in a seaway”. In: *Journal of Bifurcation and Chaos* 15.9 (2003), pp. 2717–2746.

[64] R. Skejic and O. M. Faltinsen. “A unified seakeeping and maneuvering analysis of ships in regular waves”. In: *Journal of Marine Science and Technology* 13.4 (2008), pp. 371–394.

[65] Ernest Zarnick. *A non linear Mathematical model of motions of a planing boat in irregular waves*. Tech. rep. David W. Taylor Naval Ship Research and Development Center, 1979.

[66] Odd M. Faltinsen. *Hydrodynamics of high speed vehicles*. Cambridge University Press, 2005.

[67] A. Papanikolaou. “Hydrodynamische Koeffizienten fur die linearen Schwinguingen von schwimmenden Zylindern”. In: *Schiffstechnik* 41.3 (1980).

[68] B. Hunt. “The mathematical basis and numerical principles of the boundary integral method for incompressible potential flow over 3-D aerodynamic configurations”. In: *Numerical Methods in Applied Fluid Dynamics* 1 (1980). Ed. by London Academic Press, pp. 49–135.

[69] A. Reed and R. Beck. “Mathematical Models of Maneuvering in Waves: Historical Perspectives and the State of the Art”. In: 13^{th} *International Conference on the Stability of Ships and Ocean Vehicles (STAB2018)*. 2018.

[70] Frans Van Walree. “Computational methods for hydrofoil craft in steady and unsteady flow”. PhD thesis. Technical University of Delft, 1999.

[71] P. De Jong, F. Van Walree, J. A. Keuning, and R. Huijsmans. “Evaluation of the free surface elevation in a time-domain panel method for the seakeeping of high speed ships”. In: 17^{th} *International Offshore and Polar Engineering*. Lisbon, Portugal, 2007.

[72] F. Van Walree. “Development, validation and application of a time domain seakeeping method for high speed crafts with a ride control system”. In: 24^{th} *Symposium on Naval Hydrodynamics*. Fukoka, Japan, 2002.

[73] P. De Jong and F. Van Walree. “Hydrodynamic lift in a time-domain panel method for the seakeeping on high speed ships”. In: 6^{th} *International Conference on High-Performance Marine Vehicles (HSMV2008)*. Naples, Italy, 2008.

[74] P. De Jong and F. Van Walree. “The development and validation of a time-domain panel method for the seakeeping of high speed ships.” In: 10^{th} *International Conference on Fast Sea Transportation*. Athens, Greece, 2009.

[75] John V. Wehausen and Edmund V. Laitone. “Surface Waves”. In: *Encyclopedia of Physics*. Ed. by S. Flugge. University of California, 1960, pp. 446–778.

[76] D. Stewart. “A Platform with Six Degrees of Freedom”. In: *Proc. Institution of Mechanical Engineers*. Vol. 1. 15. United Kingdom, 1966.

[77] ITTC. *Uncertainty Analysis for manoeuvring predictions based on captive manoeuvring tests*. Tech. rep. 7.5-02 06-04. ITTC, 2014.

[78] M. Bonci, P. De Jong, F. Van Walree, M. Renilson, and R. H. M. Huijsmans. “The steering and course keeping qualities of high-speed craft and the inception of dynamic instabilities in the following sea”. In: *Ocean Engineering (Manuscript under review)* (2019).

[79] M.R. Renilson and T. Manwarring. “An investigation into roll-yaw coupling and its effect on vessel motions in following and quartering seas”. In: 7^{th} *International Conference on the Stability of Ships and Ocean Vehicles*. Vol. Vol. A. Launceston, Tasmania, Australia, 2000, pp. 452–459.

[80] M. Renilson and A.J. Tuite. “Broaching-to - a proposed definition and analysis method”. In: *Twenty-Fifth American Towing Tank Conference*. Iowa City, USA, 1998.

[81] K. Garme. “Improved time domain simulation of planing hulls in waves by correction of the near-transom lift”. In: *International Shipbuilding Progress* 52.3 (2005), pp. 201–230.

TABLE OF SYMBOLS

Greek letters

α_X, α_Z	Longitudinal and vertical locations of the centre of effort of the sway added mass, with respect to the ship body frame	$[m]$
β	Ship drift angle	$[deg]$
β_D	Hull deadrise angle	$[deg]$
β_R	Relative drift angle at the control devices of the ship	$[deg]$
δ	Steering angle	$[deg]$
δ_M	Maximum steering angle	$[deg]$
$\dot{\delta}$	Steering speed	$[deg/s]$
Δ	Ship displacement	$[N]$
∇	Ship displaced volume	$[m^3]$
$\bar{\eta}$	Mean value of the loads acting on the ship in waves	$[N, Nm]$
ϕ	Roll angle	$[deg]$
φ	Phase of the loads acting on the ship in waves	[-]
φ_P	Phase between the wave generator motion and the actual wave elevation measured at the model centre of gravity	[-]
λ	Wave length	$[m]$
λ	Wave length	[-]
μ	Wave incidence angle on the ship sailing direction	$[deg]$
ψ	Ship heading	$[deg]$
ρ	Water density	$[kg/m^3]$
σ	Ship sink/rise	$[m]$
θ	Pitch angle	$[deg]$
ξ_G	Longitudinal location of the ship centre of gravity with respect to the closest approaching stern wave crest	$[m]$
ξ_G/λ	Non-dimensional ship location in the wave	[-]
ζ	Wave elevation	$[m]$
ω	Wave frequency	$[rad/s]$

Latin letters

a	Wave amplitude	$[m]$
B	Ship breadth	$[m]$
$b_{\delta\psi}$	Autopilot damping coefficient	$[deg/(deg/s)]$
c	Wave crest celerity	$[m/s]$
C'	Directional stability index	[-]
c_M	Waterjet inflow momentum coefficient	[-]
$c_{\delta\psi}$	Autopilot proportional coefficient	$[deg/deg]$
D	Ship draught at zero speed	$[m]$
F	Generic force	$[N]$
Fr	Froude number, defined as $U/\sqrt{gL}$	[-]
Fr_∇	Volumetric Froude number, defined as $U/\sqrt{g\nabla^{1/3}}$	[-]
g	Gravity acceleration	$[m/s^2]$
G	Ship centre of gravity	[-]
GM_T	Metacentric height	$[m]$
H	Wave height	$[m]$
H/λ	Wave steepness	[-]
I_X, I_Y, I_Z	Ship inertia	$[kgm^2]$
J_X, J_Y, J_Z	Added inertia	$[kgm^2]$
k	Wave number	$[1/m]$
L_{PP}	Length between perpendicular	$[m]$
L	Ship reference length	$[m]$
LCG	Longitudinal location of the ship centre of gravity	$[m]$
m	Ship mass	$[kg]$
m_X, m_Y, m_Z	Ship added mass	$[kg]$
m_X, m_Y, m_Z	Ship added mass	$[kg]$
p_0, p_1, p_2	Plane equation coefficients	[-]
Q	Waterjet flow	$[m^3/s]$
R_T	Total resistance	$[N]$
S_W	Ship wetted area at zero speed	$[m^2]$
t	time	$[s]$
t_{EXE}	Steering execution time	$[s]$
U	Ship total speed, $U = \sqrt{u^2 + v^2}$	$[m/s]$
x_T	Distance traveled by the carriage	$[m]$
u_{NOZ}	Waterjet nozzle flow speed	$[m/s]$
x_{NOZ}, z_{NOZ}	Longitudinal and vertical location of the waterjet nozzle	$[m/s]$
x, y, z	Coordinates of the ship body moving frame	$[m]$
x_0, y_0, z_0	Coordinates of the earth fixed frame	$[m]$
u	Surge velocity with respect to the ship body moving frame	$[m/s]$
v	Sway velocity with respect to the ship body moving frame	$[m/s]$

w	Heave velocity with respect to the ship body moving frame	$[m/s]$
p	Roll velocity with respect to the ship body moving frame	$[rad/s]$
q	Pitch velocity with respect to the ship body moving frame	$[rad/s]$
r	Yaw velocity with respect to the ship body moving frame	$[rad/s]$
$\dot{u}$	Surge acceleration with respect to the ship body moving frame	$[m/s^2]$
$\dot{v}$	Sway acceleration with respect to the ship body moving frame	$[m/s^2]$
$\dot{w}$	Heave acceleration with respect to the ship body moving frame	$[m/s^2]$
$\dot{p}$	Roll acceleration with respect to the ship body moving frame	$[rad/s^2]$
$\dot{q}$	Pitch acceleration with respect to the ship body moving frame	$[rad/s^2]$
$\dot{r}$	Yaw acceleration with respect to the ship body moving frame	$[rad/s^2]$
X	Surge force	$[N]$
Y	Sway force	$[N]$
Z	Heave force	$[N]$
K	Roll moment	$[Nm]$
M	Pitch moment	$[Nm]$
N	Yaw moment	$[Nm]$
X_W	Wave surging force	$[N]$
Y_v, K_v, N_v	Linear derivatives in sway, roll and yaw with respect to the sway velocity	$[Kg/s, Kgm/s]$
Y_ϕ, K_ϕ, N_ϕ	Linear derivatives in sway, roll and yaw with respect to the roll angle	$[N, Nm]$
Y_r, K_r, N_r	Linear derivatives in sway, roll and yaw with respect to the yaw velocity	$[Kgm/s, kgm^2/s]$
Y_μ, K_μ, N_μ	Linear derivatives in sway, roll and yaw with respect to the wave incidence angle	$[N, Nm]$
Y_δ, K_δ, N_δ	Linear derivatives in sway, roll and yaw with respect to the steering angle	$[N, Nm]$
Z_σ, M_σ	Linear derivatives in heave and pitch with respect to the ship sink/rise	$[N/m, N]$
Z_θ, M_θ	Linear derivatives in heave and pitch with respect to the pitch angle	$[N, Nm]$

The non-dimensional quantities in the text are denoted with the superscript $'$.

ACKNOWLEDGEMENTS

More than four years have passed since I arrived in the Netherlands. At that moment, obtaining a Ph.D. was a vague, far goal, and I did not have any idea on what to expect trying to complete this research. Now that I am writing these lines at the end of this book, I am more secure than ever that it would not have been possible without the people who gave a help in this work and all the friends which shared many pleasant moments with me.

First, I would like to express my gratitude to my promotor Prof. **Rene Huijsmans**, for his guidance during the initial phase of the Ph.D., and the help for the finalization of the book and the defense; to my co-promotor, Prof. **Ido Akkerman**, for his great dedication in the very last period of the Ph.D.; to **Riaan Van't Veer**, who guided me during a very important phase of the Ph.D.; to Prof. **Lex Keuning**, whose knowledge and practical view of the Naval Architecture made me a better researcher and helped me taking many important decisions. I must thank also Dr. **Pepijn De Jong**, who initially proposed this extremely interesting research and gave me an invaluable help throughout the development of this work, and Dr. **Frans Van Walree**, for his insights into the mathematical modelling of the ship, and his help in the translation of the summary and the propositions in Dutch. Finally, Prof. **Martin Renilson** deserves my most sincere gratitude: his enthusiasm and interest for my research contributed significantly to the realization of this project, I will be always grateful for that.

I also would like to acknowledge the project committe members and their organisations that funded this research. Dr. **Richard Nievaart** of NWO, Dr. **Jochem De Jong** of DAMEN, Dr. **Frans Verbaas** of LR, Dr. **Bastian Van Der Sluijs** and Dr. **Dimitra Damala** of BV, Dr. **Sietske Hendriks** of DMO, and Dr. **Hans Van Der Molen** of KNRM.

I spent most of my office-hours at the towing tank, definitively the best facility of the entire TU Delft. Also because populated by beautiful people who played an important role in this work and which I would like to thank: **Hans** and **Frits** for their help in setting up the model and the carriage for the experiments; **Pascal** for his friendship in the very last part of the Ph.D.; **Sebastian** for his help and late-afternoon-almost-evening discussions; **Jasper** for his help on the carriage; **Bongjun** for his precious fitness sessions in front of the coffe machine; **Jennifer** for her help in the experiments and for the unique on-the-carriage Dutch lessons: *sorry, ik ben een slechte student geweest, stom van mij!*; **Piet** for his help in finding some necessary publications, and for his coffee-break pepernoten and motivational chocolate; **Peter P.**, whose great knowledge of the facilities have been essential in the success of my experiments; **Cornel** for his support during this project; **Gunnar** my office-mate: it was a pleasure share the office with you and to share our ideas with each other; **Nico**, for his friendship and his American attitude, a bit less for the never-ending discussions on uncertainty; **Giovanni** even for a little time, it was

good to have another Italian buddy in the towing tank; the bloody Indians **Raghu** and **Swaraj** for all our long discussions at lunch and in the coffe-breaks; **Wick** for his help in the experiments and for all the beers we drank together; **Peter N.**, I will always appreciate your effort in learning the most genuine Italian gestures. Finally I must thank **Bono** and **Freddie**, for having improved the quality of my work at the office and the for all the fun during the coffee-breaks.

I must also thank the other colleagues of the TU: although I spent less time with them, they have been an important part of my life at the TU. To **Joost**, my very first office-mate, who gave me a great help to settle in the university environment; to **Reinier**, aka the Lider Maximo, my companion in the SHS weekly meeting; to **Gabriele**, the guardian of the Beast; and **Peter W.**, **Arthur**, **Henk**, **Paula**, **Menno**, **Marco**, **Vittorio**, **Matin**, **Jack**, **Erik**, **Gem**, **Sören**, and to the secretaries **Monique**, **Patty**, and **Dineke**.

Beyond the work at the TU, I must begin thanking my closest group of friends in Delft, the **AlFeZeMa & Co.**; as the name suggests, I start with **Alessandro**, aka Gennà or Sasy: I admire your ability in building stuff and in messing things up around, thank you for all the *Nino D'Angelo* in the morning and the great work on the boat together; **Federico**, my neighbour, flat-mate, *ommemmè*, it is great to have such a honest person as a friend: you can consider me for any philosophical discussion; **Zeno**, the Almighty, your sensibility is a very important source of inspiration for me; I am looking forward for the next Pernod, the next Hemingway book, the next song of Nada, the next aperitif in your truest style; **Costanza**, my personal trainer and motivator, I know that I can always count on your help because you are an amazing friend (thank you for the blinds!). We spent an amazing time together, on the boat, during the *Giovedì con Zeno*, on every single dinner together. I have been very lucky to meet you at the beginning of the Ph.D.

A particular mention must go to the **Pickwick Club**. Not long ago, a member of this poetry club, **Chris**, defined us as a bunch of pretentious people who want to be poets. I definitively agree, and I would also add: we are the ones who consider important what is not. This means that we have been avant-garde, I am sure of that. Thank you for this rewarding experience, hope it will continue. Thank you **Federico**, **Zeno** and **Alessandro** (the *original* Pickwick Club), and to **Anthony**, the Voice of our souls, to **Paola**, **Mehran**, **Alberto**, **Sonja**, **Fede**, **Sam**.

I also owe to acknowledge all the people I met during this four years: your friendship means a lot to me. The Italian crew, **Anna** (*O Vecia!*), **Elly**, **Giulia**, **Alessandro**, **Caterina**, **Tonino**, **Saskia**, **Nicola**; a big thanks to **Christian**, who helped me setting-up the experiments at MARIN, is good to be colleague now!

Heartily thanks also to whom I spent a little time with, you are nonetheless amazing friends: **Helena**, **Becca**, **Wayne**, **Mathia**, **Kuba**, **Dirk**, **Skadi**, **Albert**, **Benedetta**, **Enrico**, **Sara**, **Giovanni**, **Lorenzo**.

And thank you, **Martina**, you made me become a better person.

Ancora, voglio ringraziare tutte le persone alle quali, seppur lontane, devo la mia più profonda amicizia e gratitudine.

La *Falsa Amicizia* dell'UniGe, alla base del risultato di questo dottorato, non mi ha

mai abbandonato. Saremo sempre amici (falsi) come Δ sarà sempre uguale a W. Grazie a **Satta**, **Pana**, **Maro**, **Demma**, **Tuz**, **Gigi** e **Giulio**, il preferito di mia madre: è una fortuna esserci ritrovati in Nederlaaand in mezzo a tutti questi Dutchini, come li chiami tu. Non posso non ringraziare i *Vianò*, gli amici di sempre, **Marco**, **Walter**, **Giulio**, **Fra** e **Luca**, il mio compagno di banco e confidente; e **Ilenia**, nonostante la lontananza e le pochissime volte che riusciamo a incontrarci, sei sempre la mia migliore amica.

Infine, grazie alla mia famiglia. A mia sorella **Manuela**, a cui voglio bene, ma a cui non sono mai riuscito davvero a dirlo. Sei la mia vera guida su cui potrò sempre contare, e io proverò ad esserci sempre per te, anche da lontano. Grazie anche a **Francesco**, per tutte le volte che mi siete venuti a trovare. Grazie a **Olga**, che non chiamo mai quanto dovrei, e a chi non c'è più, **Maria** e **Sergio**. E grazie ai miei genitori: ancora una volta, tutto questo è merito loro.

Matteo Bonci, Utrecht 26 September 2019

CURRICULUM VITÆ

Matteo BONCI

Matteo Bonci was born in 1989 in Genoa, Italy. In 2011 he obtained the Bachelor Degree in Naval Architecture and Maritime Engineering at the University of Genoa. He continued the studies at the University of Genoa achieving, in 2014, the Master Degree. His master thesis, entitled *"Methods for estimating parameters of practical ship manoeuvring models based on the combinations of RANSE computations and System Identification"*, was the result of a research partially carried out at the Italian Towing Tank CNR-INSEAN in Rome.

After his graduation in 2014, he started working at Palumbo Shipyards of Naples, as technical superintendent during the construction of two motor-yachts. One year later, in May 2015, he was appointed as Ph.D. Promovendus at Delft University of Technology, in the faculty of Mechanical, Maritime and Materials Engineering, department of Ship Hydromechanics and Structures. During this appointment, he took part to several International Conference and Symposia, in Washington, Nantes, Naples and Kobe, Japan. Since June 2019, he works at the Maritime Research Institute of the Netherlands (MARIN) in quality of Project Manager.

His interests include the manoeuvrability and seakeeping of ships and high-speed craft, the dynamic stability and the design of the vessel.

LIST OF PUBLICATIONS

6. **Bonci M.**, De Jong P., Van Walree F., Renilson M., Huijsmans R. H. M., *The steering and course keeping qualities of high-speed craft and the inception of dynamic instabilities in the following sea*, Manuscript under review at Ocean Engineering, (2019).

5. **Bonci M.**, De Jong P., Van Walree F., Renilson M., Keuning J. A., Van't Veer R., *The heel-induced sway force and yaw moment of a high-speed craft in following regular waves*, Journal of Marine Science and Technology, (2019).

4. **Bonci M.**, Renilson M., De Jong P., Van Walree F., Keuning J. A., Huijsmans R. H. M., *The heel-sway-yaw coupling on a high-speed craft in calm water*, The Transaction of The Royal Institution of Naval Architects, Part B - International Journal of High-Speed Craft Technology, 160, 121-129, (2018).

3. **Bonci M.**, Renilson M., De Jong P., Van Walree F., Van't Veer R. *On the direct assessment of broaching-to vulnerability of a high speed craft*, 13^{th} International Conference on the Stability of Ships and Ocean Vehicles (STAB 2018), Kobe, Japan, (2018).

2. **Bonci M.**, Renilson M., De Jong P., Van Walree F., Keuning J. A., Huijsmans R. H. M., *Heel-sway-yaw coupling hydrodynamic loads on a high speed vessel.* 11^{th} Symposium on High-Speed Marine Vehicles (HSMV 2017), 25-27 October, Naples, Italy, (2017).

1. **Bonci M.**, Renilson M., De Jong P., Van Walree F., Keuning A. J., Huijsmans R. H. M., *Experimental and numerical investigation on the heel and drift induced hydrodynamic loads of a high-speed vessel*, 14^{th} International Conference on Fast Sea Transportation (FAST 2017), Nantes, France, (2017).

Other publications:

Bonci M., Viviani M., Broglia R., Dubbioso G., *Method for estimating parameters of practical ship manoeuvring models based on the combination of RANSE computations and System Identification*, Applied Ocean Research, 52, 274-294, (2015)